Development Of A Cell Free System For Analysis Of The Mechanisms Of Exocytosis Using Total Internal Reflectance Microscopy

Andrew Craig Don-Wauchope

Doctor of Medicine

The University of Edinburgh

2004

I hereby declare and affirm that the thesis is entirely my own work and composition. The work recorded in the thesis is largely my own but includes work that was performed by other members of the membrane biology research group of the University of Edinburgh. All the work was performed while I was employed in South East Scotland, initially as a research fellow and subsequently as a specialist registrar.

The thesis has not been submitted for any other degree, postgraduate diploma or professional qualification.

Date: ..... Signature of Candidate: .....

Acknowledgements

Dr David Apps for guidance and supervision during the writing of the thesis.

Dr Bob Chow for the opportunity to undertake this challenging project

Dr Georg Bodammer for instruction in the use and maintenance of the TIRF microscope

Dr Rolly Wiegand for continuing where I left the project and confirming my findings.

Dr Rory Duncan for the outstanding molecular biology producing the EGFP constructs.

Dr Ioulia Matskevich for her work on the TIRF microscope.

Ms Jenny Greaves for the cell culture preparations in the later years of the project.

Dr Sompol Tapechum for the capacitance and cell culture work early in the project.

Dr Martin Oheim for the basic dish design and the preparation of the TIRF microscope.

Mr Peter Frew and Mr John Lissemore for all the assistance they provided in the workshop.

Ms Linda Wilson for performing the confocal imaging.

Louise, Alexander, Rachel and Sarah who had to put up with me while I completed the thesis.

Funding for the research was provided by a Sir Henry Welcome Commemorative Award for Innovative Research awarded to Robert H. Chow.

Abstract

Regulated exocytosis occurs in a number of cell types and has been studied in many of these. There appears to be a commonality of function in the cells that exhibit regulated exocytosis. Many proteins have been implicated in the process of regulated exocytosis and a number of trigger signals have been identified. There are various means of investigating regulated exocytosis and these include capacitance measurements, amperometry and single-cell imaging. Reconstitution from defined components of the steps leading to exocytosis has not yet been achieved, whereas the investigation of the actual exocytotic event is well described. Access to the cytosolic components of the cell is a requirement of any assay that attempts to investigate the process leading to the final 'fusion event' of regulated exocytosis.

The aim of this research was to develop an in-vitro assay that would allow investigation of the steps leading to regulated exocytosis on a plasma membrane. The method was based on the use of ‘unroofed’ bovine adrenal chromaffin cells, viewed by total internal reflection fluorescence microscopy. Development of the assay posed a number of challenges, not all of which were overcome during the study. The basic platform for the assay, a cell membrane patch with adhering secretory vesicles, was produced with some degree of success. However the imaging method had a number of limitations and this frustrated the method’s development.

The results, although encouraging, were judged not to be robust enough to permit development of a reconstituted system and a more reliable imaging procedure is recommended for further study.

List of abbreviations

BoNT	botulinum neurotoxin
CAPS	Calcium Activator Protein for Secretion
CNT	Clostridial neurotoxins
Csp	Cysteine String Proteins
DIC	differential interference contrast microscopy
EPP	End Plate Potential
ER	endoplasmic reticulum
GAP	GTPase activating protein
GDF	GDI dissociation factor
GDI	GDP-dissociation inhibitor
GEF	guanidine nucleotide exchange factor
LDCV	Large dense core vesicle
NEM	N-ethyl maleimide
NSF	N-ethyl maleimide Sensitive Fusion protein
PKA	protein kinase A
PKC	protein kinase C
PKG	Guanylate Cylcase
PMA	phorbol myristate acetate
SM	Sec1/Munc18 homologs
SNAPs	soluble NSF attachment proteins
SNARE	Soluble N-ethyl maleimide Sensitive Factor receptors
SOP	standard operating procedures
TeNT	Tetanus neurotoxin
TIR	Total internal reflection
TIRFM	total internal reflectance fluorescence microscopy
TMR	transmembrane region
TPM	Two photon microscopy

List of Figures

List of Tables

1.1 Introduction to membrane fusion

Membranes compartmentalise the cell into multiple functional units (organelles), maintaining the integrity of the cell. Membrane fusion and budding is essential to the compartmentalisation and traffic of cellular compartments within a cell and the ability of a cell to share its content with other cells. Traffic of macromolecules between cellular compartments is essential to eukaryocte cell survival. The ability of membranes surrounding compartments to fuse with each other and to bud off smaller compartments (vesicles) from a larger compartment makes traffic of macromolecules possible. Membrane fusion also allows cells to communicate with each other by sharing their secretory products with other cells, in the surrounding tissue (paracrine) or with others at a greater distance away (endocrine) and also by release of neurotransmitter substances. In this context membrane fusion is termed exocytosis. There are two fundamental types of exocytosis: constitutive, as in the secretion of protein products by some cell types, or regulated, as in neurotransmission and release of hormones by neuroendocrine cells.

Research on regulated exocytosis has demonstrated that the fusion process can be highly regulated in time and be very tightly controlled within localised areas, thereby allowing release of products to occur in precisely timed spatial patterns. Products released in such temporo-spatial patterns include many of the peptide hormones, digestive enzymes, a vast array of mediators, cytokines, growth factors and neurotransmitters.

Before discussing synaptic and neurosecretory vesicles a short review of the history (Katz, 1996; Eccles, 1990; Shepherd and Erulkar, 1997) of synaptic transmission and the important findings leading to our current knowledge is included. Sherington, a neurophysiologist who was working on the spinal reflexes, introduced the term ‘synaptic transmission’ in a textbook of physiology edited by Foster (Sherington 1897). He was referring to the junction between adjacent nerve cells, which had been alluded to in 1856 by Bernard. Visualisation of the neuromuscular junction by microscopy was greatly

assisted by the development of the Golgi stain in about 1886 and this led to the improved understanding of the anatomy of nerve endings. The debate around the nature of the synapse resulted in intense study over many years (Shepherd and Erulkar, 1997).

In the mid-twentieth century physiologists began to define the synapse. Fatt and Katz (1950; 1951), working on the frog neuromuscular junction introduced the concept of End Plate Potential (EPP), a change in the post-synaptic membrane potential induced by the action potential reaching the nerve terminal. They used intracellular recording electrodes that had recently been developed. The action of acetylcholine as a neurotransmitter was characterised at the neuromuscular junction, which then became a model system for studying the mechanism of the synapse. Eccles and his colleagues applied the same technology to the spinal cord reflexes and soon characterised the neurone to neurone synapse. Katz and Fatt (1952) introduced the idea that neurotransmitters are released in quanta that represented packages of the neurotransmitter released in an all-or-nothing fashion. This was inferred from their observation and recording of miniature End Plate Potentials (MEPPs), spontaneous transient potential changes of low amplitude (~0.5 mV) that are now known to be brought about by the random exocytotic fusion of individual synaptic vesicles. Del Castillo and Katz (1954) demonstrated that MEPPs were aboloshised by curare, and that quantal frequency was controlled by the presynaptic membrane potential while quantal amplitude was controlled by the postsynaptic receptors. A full-blown EPP was produced by large depolarisation of the presynaptic membrane resulting in rapid increase in the rate of quantal secretion.

Simultaneously, anatomists began to unravel the structure of the synapse by use of the electron microscope. Palay (1954;1956) described the components of the neuromuscular junction and these included the collection of small vesicles near the presynaptic membrane. The possibility that the synaptic vesicles were the morphological correlate of physiological quanta was immediately obvious but remained controversial for some

time. The best evidence for the vesicles being the source of the physiological quanta has come from neuroendocrine cells and this evidence is discussed in section 1.2 that covers single vesicle exocytosis.

Vesicles are small membrane-bounded organelles that act as transporters by moving between compartments within the cell, and can potentially excrete cell content/product to the extracellular environment. A variety of different kinds of vesicles travel through the cytoplasm, executing a complex pattern of secretory, biosynthetic and endocytotic protein traffic to deliver distinct groups of proteins and lipids to the different organelles they target for fusion. Biosynthetic transport of many newly-synthesised proteins occurs from their site of synthesis in the endoplasmic reticulum (ER) via the Golgi stack to the various intracellular compartments in which they function. Vesicle transport originating at the plasma membrane, a process called endocytosis, is responsible for internalizing and distributing macromolecules and key nutrients such as vitamins, iron, and cholesterol. Endocytosis also allows the sensitivity of cells to external signals to be dynamically regulated by providing means to control the turnover of signalling receptors.

To achieve these movements and interactions the membranes of organelles fuse and split. As the two lipid bilayers merge into one, the lumen of the vesicle becomes continuous with the lumen of the target compartment, resulting in sharing of the stored content. There seems to be a common pathway for all trafficking reactions, with some means of identifying specific pathways for the appropriate molecules. Likewise the events of exocytosis and endocytosis that allow cells to exchange products with other cells also require membrane fusion and budding. The dynamics of membrane fusion are an essential part of exocytosis of vesicles.

Intracellular membrane fusion

The fusion of membranes within cells has been well studied but there are still many gaps in our knowledge. Studies of enveloped viral membrane fusion have demonstrated

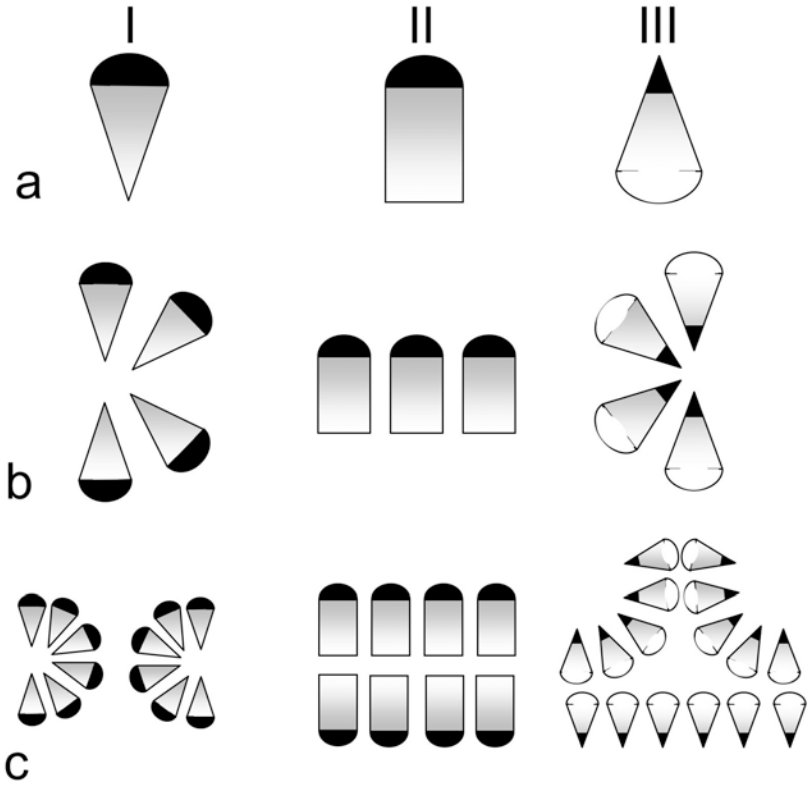

Figure 1.1.1 . The Shapes of lipid molecules
(a), energetically favourable structures formed in a monolayer by lipids of different shapes (b), and typical defects in a bilayer membrane (c) .
(Ia) represents a lipid with a polar head exceeding the hydrophobic tail in cross-section - cone. (Ib) A monloayer of spontaneous curvature. (Ic) A hydrophilic pore in a bilayer.
(IIa) Cylindrical shaped lipid. (IIb) Planar monolayer. (IIb) Bilayer.
(IIIa)Inverted-cone, with hydrophobic tail greater than the polar head in cross-section. (IIIb) Monolayer of negative spontaneous curvature. (IIIc) Local bulging defect.

striking similarities to membrane fusion in eukaryotic cells. The best described processes in eukaryocytes are those involving secretory vesicles and the plasma membrane. Other techniques that have helped our understanding of the mechanisms of membrane fusion include the *in vitro* use of Golgi stacks and other intracellular compartments, while mutant yeast cells have provided insight into vesicular transport from the endoplasmic reticulum to the Golgi, and of vacuolar fusion.

The process that is central to the fusion of membrane is the ability of two phospholipid bilayers to fuse under certain conditions. Biological membranes are composed predominantly of phospholipids and these membrane phospholipids have head and tail groups of similar diameter resulting in a planar structure. Other formations are possible and these include amphiphilic lipids (large head group and small tail diameter) that form micelles and when present in a phospholipid monolayer will cause a positive (outside of a sphere) curvature of the membrane. Conversely, phospholipids with a small head group and large tail diameter will support a negative curvature. These can form "inverted" micelles as shown in figure 1.1.1 adapted from (Chernomordik *et al*., 1985).

The fusion of two phospholipid bilayers is a process with a large activation energy, needed to overcome the repulsive force that exists between two phospholipid bilayers. Under experimental conditions the required energy is provided by one of the following mechanisms; 1) thermal fluctuation, 2) abstraction of hydration water, 3) charge shielding or 4) mechanical energy. This experimental fusion must also take place within an aqueous environment that enhances the repulsive force between two phospholipids bilayers. If the repulsive force is overcome the two phospholipid bilayers will either dissociate into monolayers or the two proximal monolayers ('hemifusion') will merge as demonstrated by cartoon in figure 1.1.2 (Chernomordik *et al*., 1995; Jahn and Sudhof, 1999). This implies that the phospholipid bilayers must be rearranged during fusion into monolayers that are highly curved. It is this formation of the transitional state that requires large amounts of energy (the lowest energy state of a phospholipid bilayer is planar). Figure 1.1.2 demonstrates in cartoon the steps involved in the formation of a fusion pore. The primary stage is the local reorganisation of the interacting membranes, followed by the formation of a stalk between two bilayers (Chernomordik *et al*., 1985; Chernomordik *et al*., 1995). The two opposing bilayers (A) have the opposing forces reduced. This results in the merging of the proximal monolayers producing a stalk (B). The stalk may consist of either one or two monolayers from a bilayer. Monolayer stalks result in a trilaminar structures, while bilayer stalks result in immediate fusion. The stalk then either produces a fusion pore or a hemifusion diaphragm (C). The stalk may also

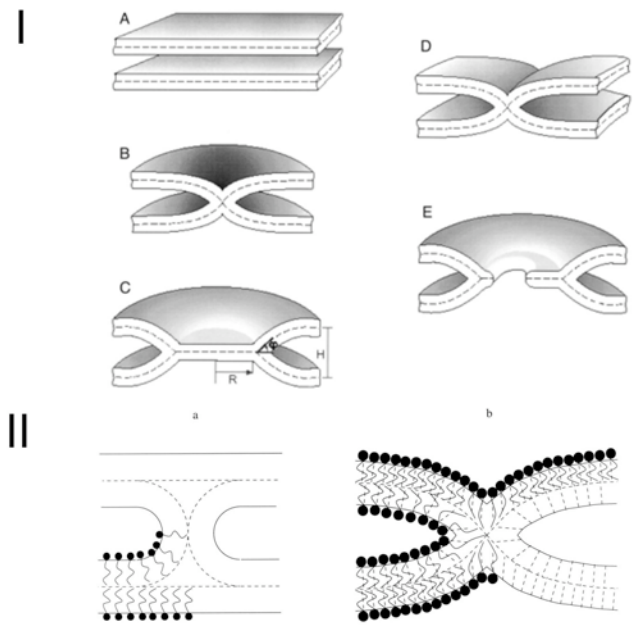

Figure 1.1.2
I Pathway of membrane fusion. (A) Initial flat membranes (B) Fusion stalk. (C) Circular hemifusion diaphragm. (D) Elongated connection. (E) Fusion
II Structure of a fusion stalk. (a) First model with empty interstices. (b) Current model with interstices filled by tilting the hydrocarbon chains.

Formation of a stalk can be presented as a two-step process. First, the contacting monolayers of the two membranes undergo strong bending and form an intramembrane connection, illustrated in Fig. 1.1.2 II*a*, which represents the first model of a fusion stalk [Chernomordik et al., 1995]. A void, referred to as a hydrophobic interstice, is formed inside this structure in the region between the apposing differently curved portions of the monolayers (Fig. 1.1.2 II *a*). Filling this void by hydrocarbon chains requires a second step of deformation, which consists in the tilt of the hydrocarbon chains facing the interstice with respect to the monolayer surface (Fig. 1.1.2 II *b*). This tilt model of the hydrophobic interstice, first suggested in the context of the inverted hexagonal (*HII*) phases of phospholipids (Hamm and Kozlov, 1998, 2000) constitutes the essence of the new approach to the analysis of the stalk intermediate. The chain tilt decays from the center towards the periphery of the stalk and gives rise to splay of the hydrocarbon chains, which interferes with the splay induced initially by the bending of the monolayer (Hamm and Kozlov, 1998, 2000). As a result of the combined deformations of bending and tilt, the profiles of the monolayers form sharp corners in front of the stalk center (Fig. 1.1.2 IIb). While unusual in the context of the earlier models, this stalk structure proved to be self-consistent, exhibiting moderate local deformations of splay and tilt of the hydrocarbon chains and possessing energy much lower than that predicted previously, thus, solving the "energy crisis" of the stalk model (Kozlovsky and Kozlov, 2002).

Figure copied from Biophys J, November 2002, p. 2634-2651, Vol. 83, No. 5

elongate or grow ansiotropically rather than radially (D) and finally fusion takes place (E). Recently more work has been performed on the mechansims of lipid bilayer fusion in model systems. This has shown that the pore may elongate linearly and that the fusion pore may not be round (Kozlovsky *et al.*, 2002). This work has also demonstrated that

the lipid arrangements may be slightly different to that proposed earlier by Chernomodik and others, in that the void between the lipid bilayers may actually be filled by tilting of the hydrocarbon chains. The bending and tilt of the monolayers results in sharp corners in the fusion pore. This structure possesses less energy than that proposed previously and may solve the "energy crisis" of membrane fusion. Figure 1.1.2 IIb demonstrates this change in conformation.

For fusion between membranes to occur within cells specialised processes have been developed to overcome the inherent repulsive energy. Many cytoplasmic and membrane associated proteins have been identified and implicated in membrane fusion. However their roles have not yet been fully characterised. An overview of our current knowledge of regulated exocytosis will follow in section 1.1.1. Two different proposals have been put forward with respect to the mechanism of fusion; (1) a proteinaceous ring spans the two membranes bringing them into close proximity and allowing a protein-containing fusion pore to form (Almers, 1990; Lindau and Almers, 1995) and (2) a mainly lipidic fusion pore forms, with proteins helping to lower the energy requirement of pore formation (Monck *et al*., 1995). Whichever proposal proves to be correct there is a requirement for specialised protein components in membrane fusion to assist in overcoming the repulsive force between two lipid bilayers.

Exocytosis is the fusion of secretory vesicles with the plasma membrane. Certain cells such as Mast cells and the adrenal chromaffin cells have relatively large secretory vesicles, and the large vesicle size has allowed optical and electophysiological study of exocytosis (see section 1.2). These studies have enhanced our knowledge about some of the mechanisms of exocytosis. Studies of fusion pores have demonstrated that lipid passes between the donor and the acceptor plasma membrane during fusion demonstrating that the pores are not entirely composed of a protein ring inserted through the membranes (Chizmadzhev *et al*., 1999). In vesicle studies using a lipid mixing assay (Weber *et al.*, 1998) the membrane bilayers are shown to merge. If the pore was composed entirely of proteins then the lipids would not mix (Chizmadzhev *et al*., 1999). The studies performed in different cell types indicate that the membrane fusion observed

in exocytosis is similar to that observed in *in vitro* lipidic experiments and also similar to viral fusion reactions. It has been postulated that other membrane fusion reactions will be similar even though these have not been observed. These observations also lead to the tentative conclusion that the biophysical processes and transition states regulating fusion of phospholipid membrane, viral membranes and cellular membranes are similar.

Proteins have an essential role in the process of membrane fusion. Some of these proteins appear to be universal, in that homologous proteins have been described in yeast and mammalian cells. These proteins include the soluble N-ethylmaleimide sensitive fusion protein (NSF) receptors (SNARE) proteins, soluble NSF attachment proteins (SNAPs) and Sec1/Munc18 homologs (SM) proteins. Other proteins apparently play an indirect or regulatory role and this includes the Rab proteins, rabphillin and cysteine string protein. Proteins are also involved in the formation of vesicles: recently the importance in secretory vesicle biogenesis of ‘cargo’ proteins, such as the chromograinins/secretograninis, has come to light (Tooze *et al.*, 2001) . Other proteins, such as the vesicle coat proteins, play a role in vesicular traffic within the ER-Golgi complex, and in the targeting of vesicles to their receptor membranes.

1.1.1 Proteins involved in regulated exocytosis

Background

Early biochemical work in the study of vesicle transport was performed *in vitro*, using Golgi stack preparations. This 'cell-free' biochemical assay established the principles and opened the way for studying the molecular mechanisms underlying protein transport. Membranes isolated from VSV-infected, ^{35}S-labelled CHO cells were incubated with cytosol and ATP, this allowing for vesicles to transport packaged proteins from ER to Golgi and between Golgi cisternae. Transport was detected by SDS-PAGE analysis of a model protein, VSV-G, using ‘donor’ membranes from cells with a mutational defect in oligosaccharide processing, and ‘acceptor” membranes from wild-type cells.

This early *in vitro* work demonstrated that a non-specific alkyalting agent, N-ethyl maleimide (NEM) blocked vesicle transport indicating that a NEM-sensitive fusion

Table 1.1.1 Number of members of vesicle-trafficking families

	S. cerevisiae	*C. elegans*	*D. melanogaster*	*H. sapiens*
Coat complexes (subunit)	6 (31)	6 (29)	6 (29)	7 (53)
Rabs	11	29	26	60
SNAREs	21	23	20	35
Qa-SNAREs/syntaxins	7	9	7	12
Qb-SNAREs/SNAP Ns	5	7	5	9
Qc-SNAREs/ SNAP Cs	6	4	5	8
R-SNAREs/VAMPs	5	6	5	9
Sec1s	4	6	5	7
Total predicted genes	6,241	18,242	13,601	30,000-50,000

For a more extensive ananlysis of these protein families, including accession numbers and searching methodology, see Supplementary Information on Nature website (JB Bock et al, A genomic perspective on membrane compartment organization. Nature 409:839-41 (2001)). SNARE helical definitions were determined by protein profiling. Some proteins (SNAP-25) contain two SNARE-coil domains and thus are counted twice in the coil subdivisions. Table 1 from JB Bock et al, A genomic perspective on membrane compartment organization. Nature 409:839-41 (2001).

protein (NSF) must play a role in fusion. The factor was cytosolic as transport could be restored by the addition of fresh cytosol. Subsequently NSF was purified. Its sequence was homologous to that of a yeast protein Sec18p, that was known to be required for secretion in the yeast. NSF is an ATPase with two homologous domains containing ATP binding sites. It does not bind directly to Golgi membranes but requires the presence of other cytosolic molecules for it to facilitate transport. This allowed the development of an assay to purify the soluble NSF attachment proteins (SNAPs), which are also necessary for vesicle fusion (Sollner *et al.*, 1993b). Yeast homologues to SNAPs (e.g. sec17p, analagous to a-SNAP) have also been demonstrated to have a role in vesicle fusion. SNAPs can bind to Golgi membranes in the absence of NSF indicating the presence of an integral membrane receptor. These receptor proteins are called SNAP receptors (SNARE). To purify SNAREs, recombinant SNAPs and epitope-tagged NSF were used (Sollner *et al.*, 1993b). Pull-down experiments revealed the formation of stoichiometric complexes of NSF, SNAPs and SNAREs, and these complexes were also isolated from solubilized brain membranes by velocity centrifugation through sucrose gradients (Sollner *et al.*, 1993a). The study of the genome of many eukaryotic organisms from yeast to man has enabled further comparison of the protein families involved in

vesicle trafficking. Table 1.1.1 (Bock *et al*., 2001) demonstrates the number of members of the important proteins for vesicle traffic in 4 eukaryotic species. From this table we can see that the number of members of each group increases with complexity of each organism. The variety of proteins is thought to play a very important role in localising and directing membrane traffic (Bock *et al*., 2001).

1.1.1.1 SNAREs

Classification

SNARE proteins were identified independently in yeast and neurones (Review by (Bennett and Scheller, 1993)). The initial classification was based on their localisation, either on the target membrane (t-SNAREs) or on the vesicular membrane (v-SNAREs) (Sollner *et al*., 1993a). Syntaxin and SNAP-25 were the first groups of t-SNAREs to be described, while synaptobrevin/VAMPs were the first v-SNAREs. Many other SNARE proteins have been described subsequently and more recently new classifications have evolved dependent on the binding characteristics of the SNAREs as not all the new SNAREs can be allocated easily to the v-/t-SNARE classification.

The basis of the SNARE action is the formation of a heterotrimeric complex, known as the core complex, that was originally postulated to confer specificity on vesicle tethering and docking, but is now thought to have a fundamental role in the fusion process itself. A complex formed between SNAREs on different membranes (i.e. vesicular and plasma membranes is called a *trans*-complex; after fusion, all the SNAREs are in the same membrane (the *cis*-complex).

Profile-based sequencing of the SNARE proteins has demonstrated that all these proteins have a highly conserved homologous domain of ~60 amino acids dubbed the SNARE motif (Weimbs *et al*., 1997). The SNARE motif, apart from defining the family, is functional in that it is the domain that mediates the formation of SNARE complexes. SNAREs are divided into subfamilies on the basis of the number of SNARE motifs (1 or 2), the sequences of SNARE motifs and on the type and sequence of the flanking domains.

The SNARE motif has recently been further divided into tN and tC domains for the t-SNAREs and vN and vC domains for v-SNARES. The vN or tN domain is membrane-distal and pair before the vC and tC domains that are membrane-proximal. This structural independence is important for the conformational patterns in SNARE complex formation. It potentially enables the concept of a tC fusion switch to regulate the final step of fusion (Melia *et al*., 2002).

Another classification based on crystal structure is also in use. In the middle of the four-helix bundle is a highly conserved layer of interacting aminoacids, known as the zero-layer. SNAREs are defined as the R-SNAREs, which have an arginine in this central position and Q-SNAREs, with a glutamine (Fasshauer *et al*., 1998). The arginine and glutamine interact to produce the central ionic layer within the SNARE core complex.

The SNARE motif classification shown in table 1.1.1 is based on the SNARE motifs of VAMP, syntaxin and the C and N terminal motifs of SNAP-25. This divides Q-SNAREs into 3 groups; a) Qa-SNAREs/syntaxins; b) Q-b SNAREs/SNAP Ns and Q-c SNAREs /SNAP Cs; c) with R-SNAREs/VAMPs.

As described there are a number of different classifications for SNAREs in use. Preference for use varies with author and context. The SNAREs are found in different isoforms in all cellular compartments and probably function in all cellular fusion reactions. The membrane-associated SNAREs are inserted into the membrane of the endoplasmic reticulum and then transported to other cell compartments. It appears that SNAREs are essential for membrane fusion at all intracellular trafficking sites, from endoplasmic reticulum to synaptic vesicles.

VAMP, syntaxin and SNAP-25

These are the neuronal SNAREs that were first described and on which much of the classification is based. The initial identification work was done on crude brain membrane preparations using functional assays of complex formation based on NSF and SNAPs (Baumert *et al*., 1989; Trimble *et al*., 1988). These assays resulted in the purification of three SNAREs, all proteins that turned out to have been cloned and

sequenced previously. SNAP-25 is a lipid-anchored target membrane protein; VAMP (synaptobrevin-2) is inserted into synaptic vesicles by a single hydrophobic C-terminal segment, the remainder being cytoplasmic; and syntaxin is an integral protein of the plasma membrane, that appears to be concentrated in the active zones of the target membrane (Sollner *et al.*, 1993b). Syntaxin can be present in either an 'open' or 'closed' formation: in the closed formation its SNARE motif is complexed with a three-helix bundle formed by the N-terminal H_{abc} domain, and therefore unavailable for complex formation, while in the open conformation the SNARE motif is exposed and able to interact with cognate SNARE proteins (Misura *et al*., 2000).

Elucidation of the molecular action of the clostridial neurotoxins provided important evidence of the essential function of SNARE proteins in neurotransmission (see (Burgoyne and Morgan, 2003)). Tetanus toxin and the seven types of botulinum toxin are heterodimers, each containing a heavy chain (H) that targets the toxin to a particular neuronal type, and a light chain (L) that is a metalloproteinase. After entry into the cytoplasm, these endoproteinases specifically cleave VAMP (tetanus toxin or botulinum toxins B,D,F and G), SNAP-25 (botulinum toxins A and E) or syntaxin 1 (botulinum toxin C). Even in neuroendocrine cells, which have no receptors for the toxins, exocytosis is blocked if the toxins are introduced into the cytoplasm by permeabilization of the plasma membrane or expression within the cell itself. In some cell types exocytosis is resistant to these toxins through expression of toxin-resistant SNARE isoforms.

SNAREs and the core complex

SNAREpins (*trans* SNARE complexes) are formed when v-SNAREs on a vesicle membrane pair with their cognate t-SNAREs on the target membrane (Sollner *et al.*, 1993b). Figure 1.1.1.1.1 taken from Weber (Weber *et al.*, 1998) shows the SNAREpin complex.

A SNARE complex is formed by 3 Q-SNAREs binding 1 R-SNARE. The 3 SNAREs involved in the core complex have 4 SNARE motifs between them, one contributed by

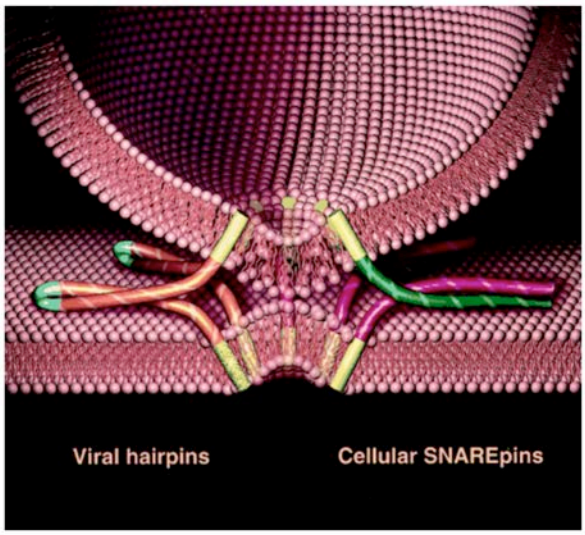

Figure 1.1.1.1.1 Cellular SNAREpins and Viral Hairpins
v-t SNAREpins (at right) are complexes of cognate v-SNAREs (in green, in the transport vesicle above) and t-SNAREs (in red, in the planar target membrane below) bridging two membranes. Analogous t-t SNAREpins may also be possible. Membrane anchors are highlighted in yellow. The core of certain viral fusion proteins (at left, in orange) is diagrammed in a simplified fashion. The membrane anchor of the fusion protein (in yellow) is inserted into the viral membrane, represented by the spherical lipid bilayer. The fusion peptide (textured yellow) is inserted into the planar target membrane below. Viral fusion proteins generally consist of continuous polypeptides (indicated conceptually by the blue polypeptide loop), within which oppositely oriented (i.e., antiparallel) helical hairpin-like structures assemble in a helical bundle and are proposed to link up the two membranes for fusion (Lu et al. 1995; Chan et al. 1997; Weissenhorn et al. 1997). A SNAREpin (whose precise internal structure is not yet known) consists of a 13–14 nm long helix-rich core rod of 2 nm width, which most likely contains the membrane-proximal helices of VAMP and syntaxin oriented parallel to each other (Hanson et al. 1997; Lin and Scheller 1997). In contrast to viral hairpins, cellular SNAREpins are formed from separate polypeptides that reside in different membranes before fusion. It is likely that multiple copies of viral hairpins or SNAREpins are needed to trigger fusion, and these are likely arranged in a ring-like structure at a contact point along the lines illustrated. The striking similarity between SNAREpins and viral hairpins suggests that extracellular and lumenally oriented viral fusion proteins, as well as intracellular membrane fusion proteins, all employ a fundamentally similar mechanism to coalesce lipid bilayers.
Figure copied from figure 5: T Weber et al. Cell, 92:759-772 (1998)

each of syntaxin and VAMP (synaptobrevin-2) and two by SNAP-25. The complex is formed with four parallel chains in a helical bundle with an ionic layer formed within the complex and the interactions in the core mainly between hydrophobic layers (Sutton *et al*., 1998).

Subsequent to this stepwise SNARE assembly, the ‘zippering up’ of the helices in the *trans* core complex brings the two membranes into close apposition, a process called “loose’ to ‘tight’ transition. The formation of the tight SNARE complex, which is

extremely stable, may release enough energy to overcome the thermodynamic barrier to membrane fusion. The surface of the core complex includes four shallow grooves that contain charged and hydrophobic regions. Although the formation of the core complex is an essential step in membrane fusion its precise function in the fusion process is not yet clearly defined (reviewed by (Jahn and Sudhof, 1999)). One of its functions may be the energy-releasing step that allows membrane fusion. As mentioned in section 1.1 the fusion of two lipid bilayers requires a large amount of activation energy to overcome the repulsive force. The individual v- and t- SNAREs exist in a thermodynamically metastable state but when combined to form a SNAREpin they exist in a lower energy state. The large free energy change accompanying complex formation is thought to be able to overcome the activation energy required to allow disruption of a lipid bilayer (Weber *et al.*, 1998).

Figure 1.1.1.1.2 (Rizo and Sudhof, 2002) illustrates a model of neuronal SNAREs in complex formation. The SNARE complex is stable, unusually resistant to denaturation by heat or, resistant to detergent (SDS) and resistant to proteolysis by Clostridial neurotoxins (botulinum and tetanus). Although monomeric VAMP, syntaxin 1 and SNAP 25 are very sensitive to proteolytic cleavage by neurotoxins, it is only once the SNAREs form the core complex they become resistant to the proteolytic effect of the neurotoxins (Jahn and Niemann, 1994; Schiavo *et al.*, 1992).

The cytoplasmic domains of SNAREs can be expressed as soluble proteins, and readily form core complexes when in solution. However it has been claimed that the transmembrane domains are also functional in complex formation (Hu *et al.*, 2003). Partial complexes may be formed in solution but the ternary complex is the most stable (Lang *et al.*, 2002). The SNARE motif undergoes a structural change to form a helix on assembly of a core complex. The SNAREs have little specificity and will form complexes with a number of other SNAREs. Transmembrane domains of synaptobrevin and syntaxin allow the formation of homo and hetero-oligomeric complexes. This contributes further to stability and allows association into larger entities that may play role in membrane fusion.

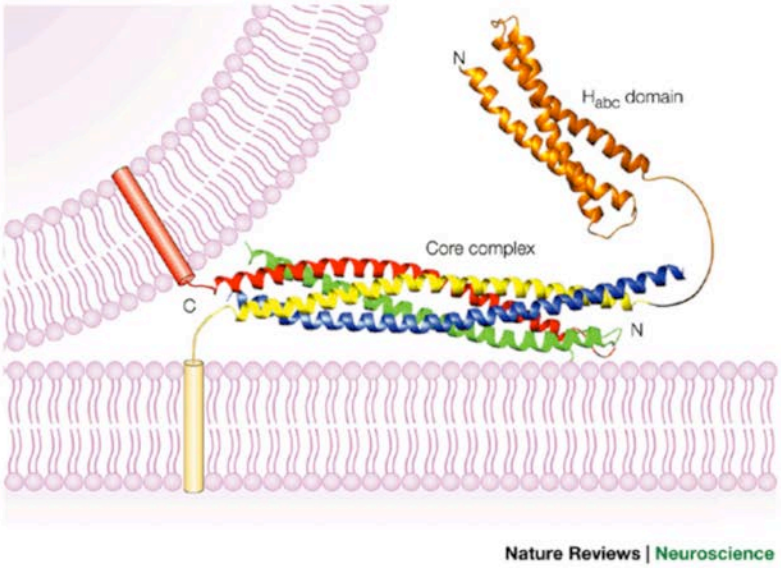

Figure 1.1.1.1.2| Model of the neuronal SNAREs assembled into the core complex.

The ribbon diagrams represent the crystal structure of the core complex41 and the NMR structure of the amino-terminal Habc domain of syntaxin 1 (Ref. 101). The Habc domain is coloured in orange and the SNARE (SNAP receptor) motifs are colour coded as follows: synaptobrevin, red; syntaxin 1, yellow; synaptosomal-associated protein of 25 kDa (SNAP25) amino terminus, blue; SNAP25 carboxyl terminus, green. The cylinders represent the transmembrane regions of synaptobrevin and syntaxin 1, which are inserted into the synaptic vesicle and plasma membranes, respectively. The curved lines represent short sequences that connect the SNARE motifs and the transmembrane regions, as well as the linker region between the Habc domain and the SNARE motif of syntaxin 1. All ribbon diagrams were prepared with the program MOLMOL157
Figure copied from J Rizo and R Jahn. Nature Reviews, 3: 641-653 (2002)

In vitro assays have shown that the SNARE proteins alone are sufficient for membrane fusion, as they permit the slow fusion of proteoliposomes containing them (Weber *et al.*, 1998). However the very slow speed of fusion of SNARE-containing proteoliposomes suggests that other as yet unidentified factors must act to accelerate the fusion process to speeds required for neurotransmission.

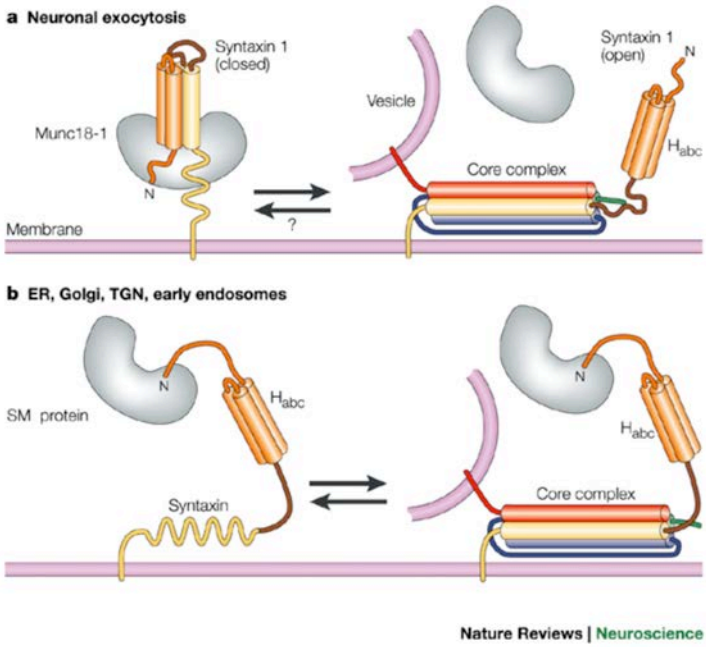

Figure 1.1.1.2 Different modes of coupling between syntaxins and SM proteins.

a | In neuronal exocytosis, the interaction between Munc18-1 (grey) and the closed conformation of syntaxin 1 (yellow and orange)39, 102 is incompatible with formation of the core complex by the SNARE (SNAP receptor) motifs of syntaxin, synaptobrevin and synaptosomal-associated protein of 25 kDa (SNAP25)123 (same colour scheme as that in Fig. 2). b | The interaction of syntaxin amino-terminal peptide motifs with Sec1/Munc18 homologues (SM proteins) that occurs in the endoplasmic reticulum (ER), the Golgi apparatus, the trans-Golgi network (TGN) and the early endosomes is fully compatible with core-complex formation.
Figure copied from J Rizo and R Jahn. Nature Reviews, 3: 641-653 (2002)

The disassembly of the very stable core complex requires an input of energy provided by soluble NSF attachment proteins (SNAPs) and N-ethyl maleimide sensitive factor (NSF). NSF and SNAPs act as core complex chaperones in almost all intracellular transport steps. They also appear to be conserved between species. NSF is an ATPase and is activated by the binding of a SNAP to the core complex. Not much is yet known about the conformation of the SNAREs after dissociation from a core complex by NSF.

1.1.1.2 Sec1/Munc18 Family of Proteins

Sec1/Munc18 (SM) proteins are a family of proteins that have been found in yeasts, *Caenorhabditis elegans* and vertebrates. They are hydrophilic proteins that share homology throughout their sequences and appear to be devoid of subdomains. In vertebrates at least seven SM proteins have been associated with action at the plasma membrane (Bock *et al*., 2001). (See table 1.1.1) The function of SM proteins is still not entirely clear although they must have an essential role in membrane fusion as mutations in SM proteins completely block membrane fusion (Rizo and Sudhof, 2002). The most probable role seems to be binding to syntaxin-like Q-SNAREs and an undefined role downstream from docking (Verhage *et al*., 2000; Voets *et al*., 2001b; Rizo and Sudhof, 2002), but there may well be other functions. The binding of Munc18 to syntaxin

Table 1.1.1.2 Sec1/Munc18 Family of proteins: localisation and proposed interactions

SM protein	Site of membrane fusion activity	Proteins that may interact with the SM protein
Yeast		
Sly1p	endoplasmic reticulum and golgi	
Sec1p	plasma membrane	Mso1p
S1p1/Vps33p/Vam5p	endosomal and vacuolar traffic	Vps16p (RING-type zinc finger), Vam3 (Q-SNARE)
Vps45p/Stt10-p	endosomal and vacuolar traffic	Pep12p (Q-SNARE), Vac1p/Vps8p (RING-type zinc finger)
Vertebrates		
munc-18-1	plasma membrane	syntaxins, mints and DOC2
munc-18-2	plasma membrane	syntaxins
munc-18c	plasma membrane	syntaxins
Sly1	endoplasmic reticulum	syntaxin 5 and 18
Vps45	golgi	syntaxin 16
Vps33a	endosomal and vacuolar traffic	
Vps33b	endosomal and vacuolar traffic	

appears to prevent the SNARE motif of syntaxin from interacting with the other SNARE motifs, that is it seems to lock syntaxin in its closed formation (Yang *et al.*, 2000). Figure 1.1.1.2 illustrates the postulated interactions of Munc18 and Syntaxin (Rizo and Sudhof, 2002).

SM proteins also interact functionally with other proteins, but the functions of these interactions are not yet well established and the association with exocytosis is unclear. Table 1.1.1.2 highlights some of the known functional interactions with SM proteins.

1.1.1.3 Rab Proteins

These are a family of low molecular weight GTPases, that are highly conserved across species. There are many isoforms (~40), each specific to a membrane compartment. Rab proteins undergo an intricate cycle of membrane and protein interactions. There are three ways in which Rab interactions are likely to regulate vesicle targeting and membrane fusion: (1) they may facilitate vesicle targeting to the appropriate destination; (2) they may regulate trafficking at the vesicle docking step; (3) Rabs potentially facilitate the correct pairing of SNAREs by selectively activating the SNARE fusion machinery (Gonzalez and Scheller, 1999). Figure 1.1.1.3, taken from (Gonzalez and Scheller, 1999) illustrates the cycle of a Rab protein from the membrane to a vesicle and back to the membrane. The addition of two geranylgeranyl groups at the C-terminal cysteines mediates membrane association when the Rab is in a GTP-bound state. Next GTP hydrolysis occurs, resulting in Rab forming a complex with GDP-dissociation inhibitor (GDI) and extracting itself from the membrane. GDI, a cytosolic intermediate, is recycled to a newly forming vesicle, probably through displacement by a secondary factor termed GDI dissociation factor (GDF). The rab protein then becomes membrane-bound (to the new vesicle). A guanidine nucleotide exchange factor (GEF) then promotes release of GDP and the subsequent loading of GTP. In the GTP-bound form the Rab protein can then associate with a specific set of effectors. These effectors may lead to the eventual fusion of the vesicle with the target membrane. To complete the cycle, a GTPase activating protein (GAP) accelerates nucleotide hydrolysis, switching

off the GTPase. The remaining GDP-bound Rab can participate in another round of fusion (Gonzalez and Scheller, 1999).

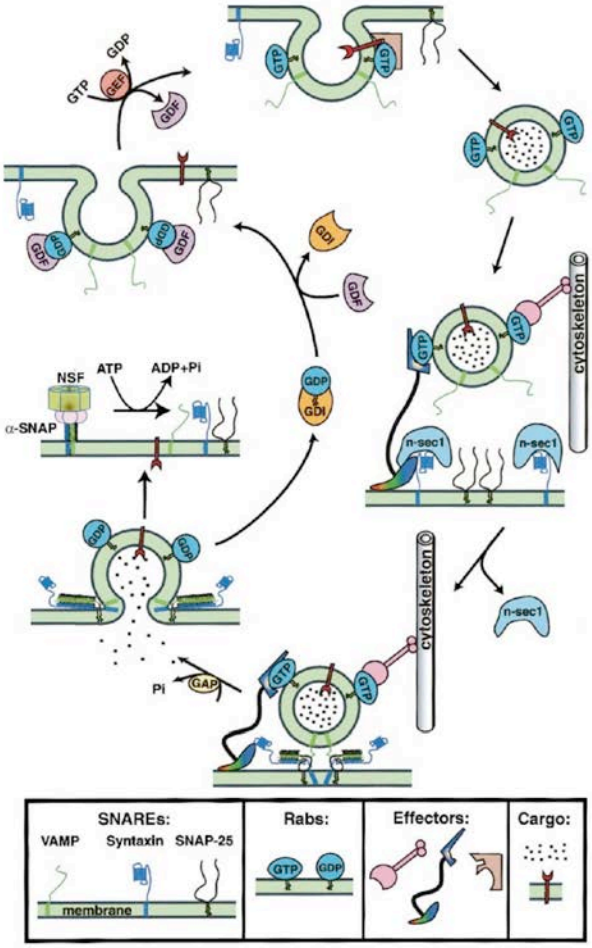

Figure 1.1.1.3 Composite Model of the Rab and SNARE Functional Cycles
A description of the Rab cycle is included in the text. Once recruited to a newly formed vesicle and activated by binding GTP, a Rab protein can interact with a select set of effectors (illustrated as generic effectors) and implement various activities in the membrane trafficking process. For example, an effector, such as TIP47 (Díaz and Pfeffer 1998), might facilitate cargo selection by linking specific cargo molecules to a specific Rab protein (top panel, brown effector). Next, Rabs may function through effector proteins that translocate and dock the vesicle to a target membrane (central right panel). Once docked, Rab effectors may activate the fusion machinery through interactions with SNARE regulatory proteins, such as n-sec1 (also termed munc-18), freeing SNAREs to associate into elongated -helical bundles, leading to membrane fusion (bottom and lower left panels). At each of these steps, Rab proteins may impart specificity to the overall process of membrane trafficking. Following fusion, the SNARE complex is disassembled into individual components through the actions of the ATPase NSF and -SNAP (central left panel). For vesicle SNAREs to function in an additional cycle, they must be returned to a donor membrane via retrograde transport.
Figure copied from L Gonzalez et al. Cell 96, 755-758 (1999)

1.1.1.4 Synaptotagmins

The synaptotagmins constitute a family of membrane-trafficking proteins that are characterised by an N-terminal glycosylated domain, a single transmembrane region (TMR), a central linker and two C-terminal C2 domains, sequentially numbered C2A and C2B. There are 13 vertebrate synaptotagmins described, and table 1.1.1.4 provides the details of each including a class stratification. The two C2-domains represent the only homologous domains of the synaptotagmin sequences. These C2A- and C2B-domains are structurally similar to the C2 regulatory domain on protein kinase C and have been shown to be functional Ca^{2+} binding modules and are functionally conserved in all synaptotagmins suggesting a specialised role. The C2A-domains generally bind three Ca^{2+} ions while the C2B-domains bind only two Ca^{2+} ions, however the Ca^{2+} affinities of the different synaptotagmins vary greatly. Synaptotagmins also interact

Table 1.1.1.4 Properties of synaptotagmins

Form	Expression pattern and localization	Function	Special properties
Class 1, Syts 1 and 2	Brain and endocranium; localized to synaptic vesicles and secretory granules	Ca^{2+} sensor for fast exocytosis	N-Glycosylated N terminus
Class 2, Syt 7	Brain >>ubiquitous; localized to active zone and plasma membrane	Ca^{2+} sensor for fast exocytosis?	>12 splice forms
Class 3, Syts 3,5,6 and 10	Brain >>ubiquitous; localized to active zone and plasma membrane	Ca^{2+} sensor for fast exocytosis?	Disulfide bonds at N terminus
Class 4, Syts 4 and 11	Brain>>ubiquitous; localisation controversial	Unknown	Asp - Ser substitution in C2A-domain
Class 5, Syt 9	Brain>ubiquitous; localised to synaptic vesicles?	Unknown	Also named Syt5
Class 6, Syts 8,12 and 13	Brain>>ubiquitous	Unknown	No consensus Ca2+-binding sites

Table modified from T Sudhof. J.Biol.Chem. 277, 7629-3 (2003)

with other ligands: for example Synaptotagmin I binds syntaxin, phospholipids, phosphoinositides, the synaptic vesicle membrane protein SV2, the clatherin adaptor AP2 and the synprint sequence of Ca^{2+} Channels. There are a number of other proteins with two C2-domains including some that have been implicated in the regulation of synaptic function; rabphilin, DOC2 and munc13-1, but these are not classified as

synaptotagmins as they do not have a TMR. Figure 1.1.1.4 illustrates some of the proposed roles of the different synaptotagmins associated with membranes. The presence of C2-domains suggest that most synaptotagmins are membrane bound Ca^{2+} signalling machines. Different classes of synaptotagmins are found on different membrane compartments, notably synaptic vesicles and plasma membrane/active zone membrane. The model in figure 1.1.1.4 proposes that at least synaptotagmins 1,2,3,6 and 7 perform complementary functions in Ca^{2+} triggered exocytosis. It is proposed the Ca^{2+} binding to each synaptotagmin contributes differently to the process of exocytosis: vesicular synaptotagmins have a lower Ca^{2+} affinity and are more important in fast

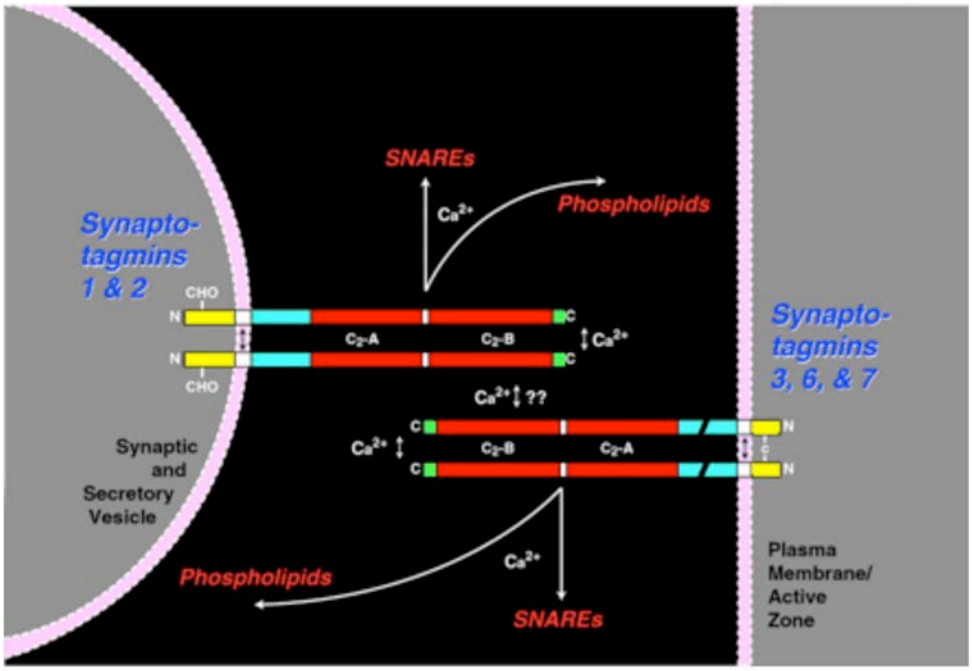

Fig. 1.1.1.4 Geometry of synaptotagmins during exocytosis.
One class of synaptotagmins (Syts 1 and 2 and possibly Syts 4, 9, and 11) are located on synaptic vesicles or secretory granules, whereas a second set (Syts 3, 6, and 7 and possibly others) are targeted to the plasma membrane, creating a symmetrical arrangement of opposing Ca2+-sensors. All synaptotagmins are probably dimers via interactions in the TMR and/or disulfide bonds between the extracytoplasmic N-terminal regions (for Syts 3, 5, 6, and 10). In addition to Ca2+-dependent interactions of the C2-domains of synaptotagmins with phospholipids, at least some synaptotagmins also bind to themselves and each other via Ca2+-dependent interactions that may be mediated by the C2B-domains (modified from Ref. 22).
Figure copied from TC Sudhof. The Journal of Biological Chemistry. 277: 7629-7632 (2002).

synaptic exocytosis; while plasma membrane synaptotagmins have a higher Ca^{2+} affinity and may be more important for endocrine exocytosis. The different properties of the synaptotagmins and their relative abundance could contribute to modulating the Ca^{2+} response of different neuroendocrine cells (Sudhof, 2002).

1.1.1.5 Cysteine String Proteins (Csp)

These soluble proteins have a central palmitoylated cysteine-rich string that facilitates membrane attachment and an N-terminal "J" domain that is found in molecular chaperone proteins that interact with and regulate members of the Hsc-70/Hsp-70 chaperone family. There is also a highly conserved linker region between the cys-string and the J domain (Chamberlain and Burgoyne, 2000). Csp is found in many tissues and is particularly associated with synaptic vesicles. It forms about 1% of the neuronal synaptic vesicle protein and 0.45% of the adrenal chromaffin cell protein (Chamberlain and Burgoyne, 2000), and is also found on other secretory granules in cells. It has been shown to be essential for neurotransmission in Drosophila. There is evidence for two roles in of Csp in regulating exocytosis. The first is as a modulator of Ca^{2+} channels (Umbach *et al*., 1998; Graham and Burgoyne, 2000) and the second as modulator of vesicle fusion machinery (Chamberlain and Burgoyne, 1998; Graham and Burgoyne, 2000). When Csp is phosphorylated it releases syntaxin from its closed formation making it available to form SNAREpins with SNAP25 and synaptobrevin. Over-expression of Csp in chromaffin cells changes the amperometric measurements of exocytosis in an opposite way to that produced by protein kinase C (PKC) activation by phorbol myristate acetate(PMA) (Graham *et al*., 2000). Recently it has been shown that phosphorylation of Csp by protein kinase A (PKA) will modify the release kinetics and quantal size, which may suggest that Csp acts as a syntaxin chaperone. Phosphorylation of Csp releases syntaxin allowing it to engage with other proteins that then act to slow the late stages of exocytosis. Phosphorylation of Csp may also act by affecting Ca^{2+} signalling through reduced binding to syntaxin (Evans *et al*., 2001). Further work in this area is still required to finally define the role of Csp in exocytosis.

1.1.1.6 Complexins

Complexins are small (~17kDa) cytoplasmic proteins that bind specifically to the ternary SNARE complex, though not to monomeric SNAREs. Complexin I and II are conserved between species and particularly found in brain where they co-localise with neuronal SNAREs. Complexin II is found more widely and has been isolated from adrenal chromaffin cells, although complexin I is also present in adrenal chromaffin cells

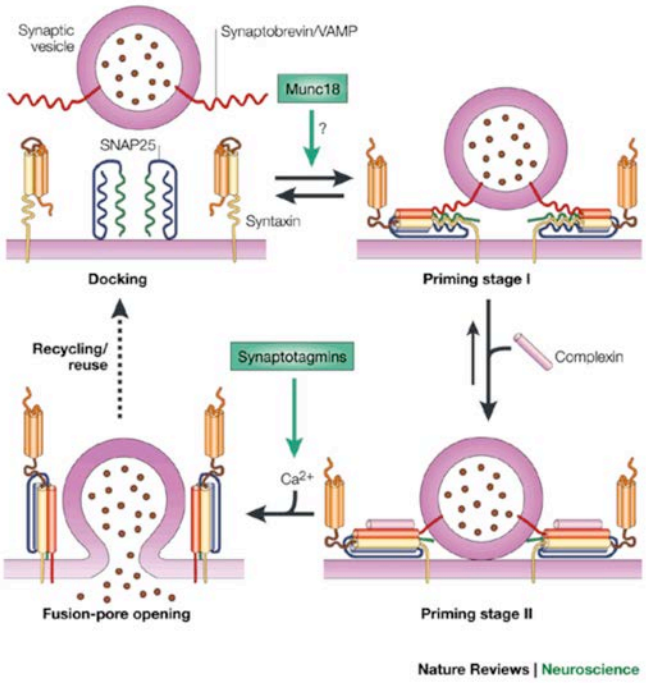

Figure 1.1.1.6 Model of complexin function.

The crucial aspect of this model is that priming might occur in two steps that involve partial and full assembly of the core complex. Only the fully assembled state, which is stabilized by complexin, can support fast, Ca2+-triggered neurotransmitter release. SNAP25, synaptosomal-associated protein of 25 kDa.
Figure copied from J Rizo and R Jahn. Nature Reviews, 3: 641-653 (2002)

(Archer *et al*., 2002). They have been shown to function in the Ca^{2+}-dependent step of exocytosis. Complexins bind in an anti-parallel a-helical conformation to the central region of the core complex, at the interface between synaptobrevin and syntaxin, without substantially altering the structure of the core complex (Pabst *et al*., 2002). Complexin

seems to act as a stabilising agent acting not only at the contact region but also towards the carboxy-terminal, membrane proximal region of the core complex. This suggests that complexins may freeze a primed state with a fully assemble core complex that is crucial to fast exocytosis. Figure 1.1.1.6 (Rizo and Sudhof, 2002) illustrates a model proposing that priming occurs in more than one step. Complexin possibly acts after the release of syntaxin by Munc-18 and then holds the SNARE complex in a release ready state. Archer et al (Archer *et al.*, 2002) have proposed that complexin II may regulate kiss-and-run recycling of exocytosis. There are potentially other roles for complexins and the proposed role here has yet to be confirmed. (Rizo and Sudhof, 2002).

1.1.2 Current Models of Exocytosis by regulated secretion

The SNARE hypothesis

The SNARE hypothesis (Sollner *et al.*, 1993b) postulates that for vesicle targeting each transport vesicle bears a unique address marker of one or more v-SNAREs obtained from its parental membrane during budding, while the target membrane is identified by one or more t-SNAREs. Targeting specificity is thus achieved by v-SNAREs binding to matching t-SNAREs. If the interaction between the cognate SNAREs were strong enough then docking could be achieved by SNAREs alone without the additional binding energy provided by interactions with SNAPs and NSF. The SNARE hypothesis postulated that the assembly of SNAREs mediates the attachment of membranes before fusion and that NSF-driven disassembly would lead to fusion completion. Although it is clear that ATP hydrolysis by NSF is required for the overall process of exocytosis, it is now appears that this reaction is part of the vesicle 'priming' process, and that ATP hydrolysis is not required for the membrane fusion event itself.

Zipper model of SNARE function

This model hypothesises that SNARE proteins "zip" together from their membrane distant amino terminal end toward the membrane-proximal carboxy termini (Bruns and Jahn, 2002). The energy to overcome the repulsive electrostatic forces may come from

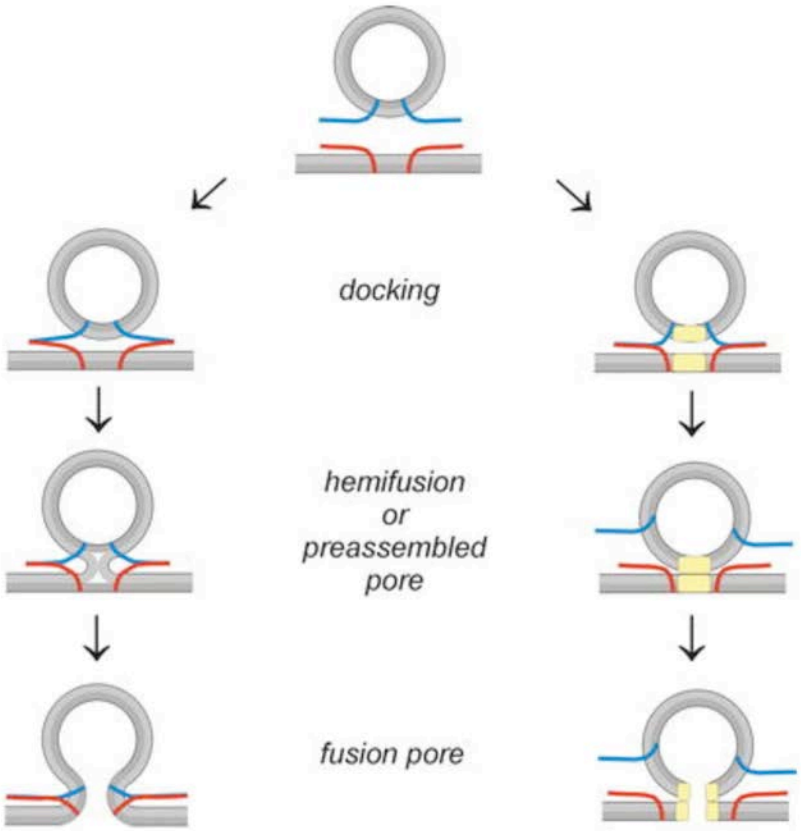

Fig. 1.1.2.1. Hypothetical models for protein-mediated membrane fusion. Vesicular SNAREs (blue) interact with the accepting SNARE protein (red) on the target membrane. SNARE proteins partially zipper to transfer the vesicle into a readily releasable state leading to hemifusion between both membranes (left side). Further assembly triggered by a calcium-dependent step may lead to the completion of fusion. Alternatively, membrane fusion is promoted by a proteinaceous pore as suggested by studies in yeast (right side). Trans-SNARE pairing is an intermediate step followed by pairing of V0 units (yellow) of the vacuolar V-ATPase present in both membranes. Opening of the channel-like pore that enlarges upon invasion of lipids between dispersing subunits leads to membrane merger. Figure taken from D Bruns and R Jahn. Euro.J.Physiol. 443: 333-338 (2002)

the conformational changes that occur as this happens. The hemifusion state may be achieved by the protein -protein interactions in the form of amino-termini of the SNAREs locating each other and then "zipping". This may also be equivalent to the

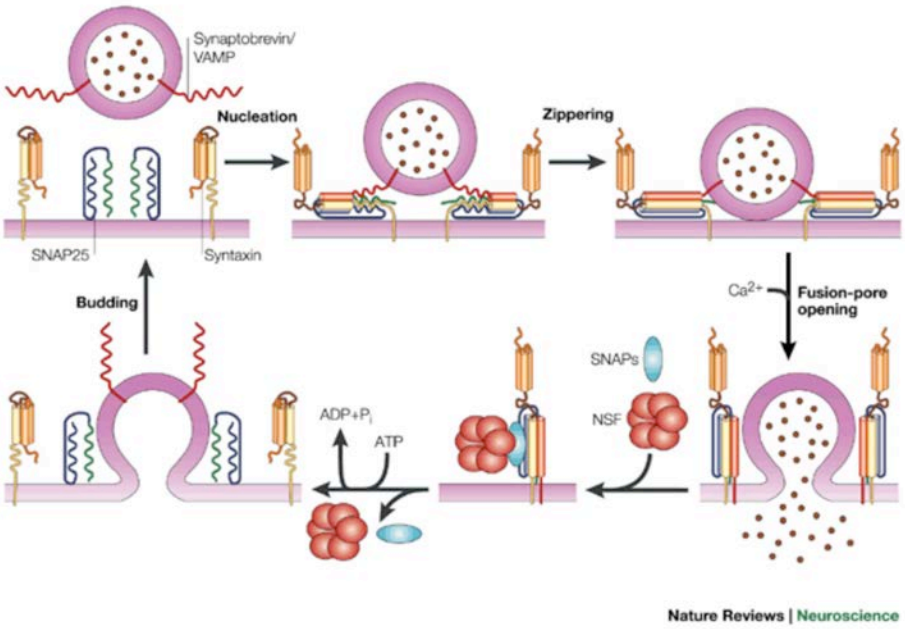

Figure 1.1.2.2 Cycle of assembly and disassembly of the SNARE complex in synaptic vesicle exocytosis.

Syntaxin exists in a closed conformation that needs to open to initiate core-complex assembly (nucleation). 'Zippering' of the four-helix bundle towards the carboxyl terminus brings the synaptic vesicle and plasma membranes towards each other, which might lead to membrane fusion. After fusion, N-ethylmaleimide-sensitive fusion protein (NSF) and soluble NSF-attachment proteins (SNAPs) disassemble the cis-core complexes that remain on the same membrane to recycle them for another round of fusion. SNAP25, synaptosomal-associated protein of 25 kDa; SNARE, SNAP receptor.
Figure copied from J Rizo and R Jahn. Nature Reviews, 3: 641-653 (2002)

docked state. Figure 1.1.2.1 (Bruns and Jahn, 2002) presents the docking step as the step prior to hemifusion. Much of this hypothesis is based on viral fusion pore proteins, which have some properties in common suggesting that SNARE proteins work in a similar way. The important unanswered questions are: which molecule completes the fusion step and does this step require Ca^{2+}?

Current thinking tends to favour the zipper model for SNARE function. With NSF playing a role in SNARE complex disassembly but without being directly involved in

membrane fusion as was originally suggested by the SNARE hypothesis. Syntaxin is held in its closed formation by Munc 18 and this acts as a clamp preventing fusion. Once Syntaxin is released by Munc 18 it unfolds allowing interactions with VAMP and SNAP-25 to form the SNARE complex resulting in fusion of the membrane (Misura *et al.*, 2000). Figure 1.1.2.2 from Rizo (Rizo and Sudhof, 2002) demonstrates recent thinking in the assembly and disassembly of the core complex. In this model the disassembly of the core complex requires energy from NSF-mediated ATP hydrolysis that returns the SNAREs to their initial high energy state and makes them available for further fusion events. Clearly membrane fusion is initiated by SNARE proteins, but the gradual expansion of the fusion pores after fusion suggest that the pore formation involves lipids. Even though amperometry and capacitance measurements have yielded a great deal of information about the kinetic characteristics of the fusion pore, its molecular structure remains unresolved. None of the proteins discussed has been shown to form pores in membrane and it has not been shown that at the onset the pore is constructed entirely of protein components. A further radical proposal, derived from work on vacuolar fusion in yeast, is that the fusion pore is formed by the H^+-conducting sector, called V_o, of the vacuolar H^+-ATPase (Bayer *et al.*, 2003). This enzyme also occurs in secretory vesicles, where its function is luminal acidification, but there is no evidence that it has a direct role in exocytosis in mammalian cells.

Quantal release during vesicle fusion

Until recently it was assumed that neurotransmission was determined by quantal release of neurotransmitter, the quantal size being constant. This assumption presumes the release of a constant amount of neurotransmitter per vesicle (probably the entire content). To change the stimulus of neurotransmission it was assumed that the number of vesicles released would be increased or decreased. This concept was modified as more details of the regulation of controlled exocytosis were elucidated. Amperometry with carbon fibre electrodes has demonstrated that catecholamines can be released from adrenal chromaffin cells in variable proportions, figure 1.1.2.3, this seems to be

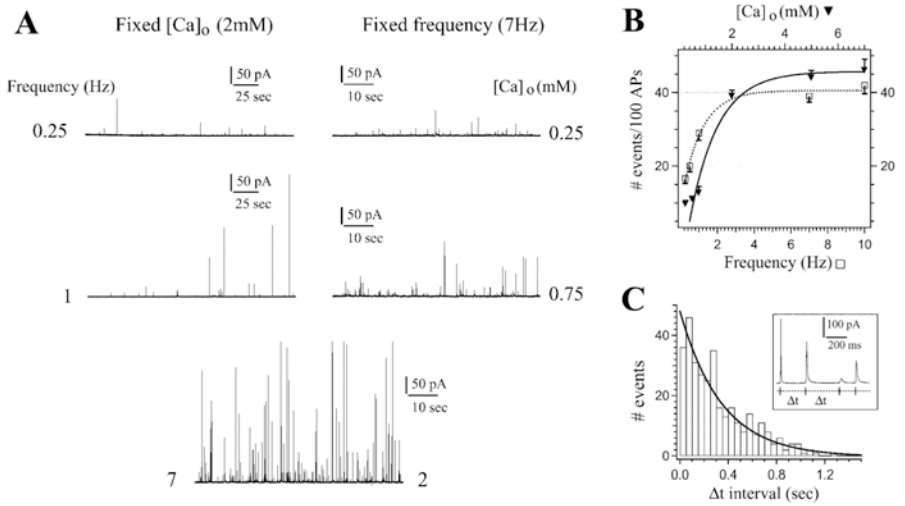

Figure 1.1.2.3 Exponential Increase in Secretory Events as a Function of Increasing Stimulation Frequency of [Ca^{2+}].
A) Representative amperometirc traces at different frequencies or [Ca2+],as indicated. Note the different time base for the 0.25,1, and 7 Hz traces and the increased probability of secretion with the higher stimulation conditions.
B) Secretory efficiency (expressed as number of Ass/AP) increases as a function of stimulation frequency or [Ca2+]. Both parameters raised the probability of release to plateau value of ~0.45 events per AP.
C) Distribution of latency times (Δt) between successive secretory events recorded at 7 Hz, 2mM [Ca2+], is determined as shown in inset (bin width of 50ms). Solid line is an exponential fit of the data; the corresponding τ = 0.395 was used to calculate the probability of overlapping events ($P = 1-et/\tau$) (see text in reference)
Figure copied from A Elhamdani et al. Neuron, 31, 819-830 (2001)

controlled by variations in [Ca^{2+}] (Elhamdani *et al*., 2001). The concept of 'kiss-and-run' exocytosis, in which the connection through the fusion pore is transient, resulting in incomplete release of vesicle content, has been described as a means to limit the amount of transmitter released at any one fusion event. As 40ms is long enough to allow full release of the contents of a chromaffin granule the opening and closing of the fusion pore to allow partial release of transmitter must be faster than 40ms. This has been described as flickering between open and closed states. This mechanism has been described in adrenal chromaffin cells but not yet in neuronal synapses as it remains difficult to measure single exocytotic events in a synapse with current techniques (Burgoyne and Barclay, 2002).

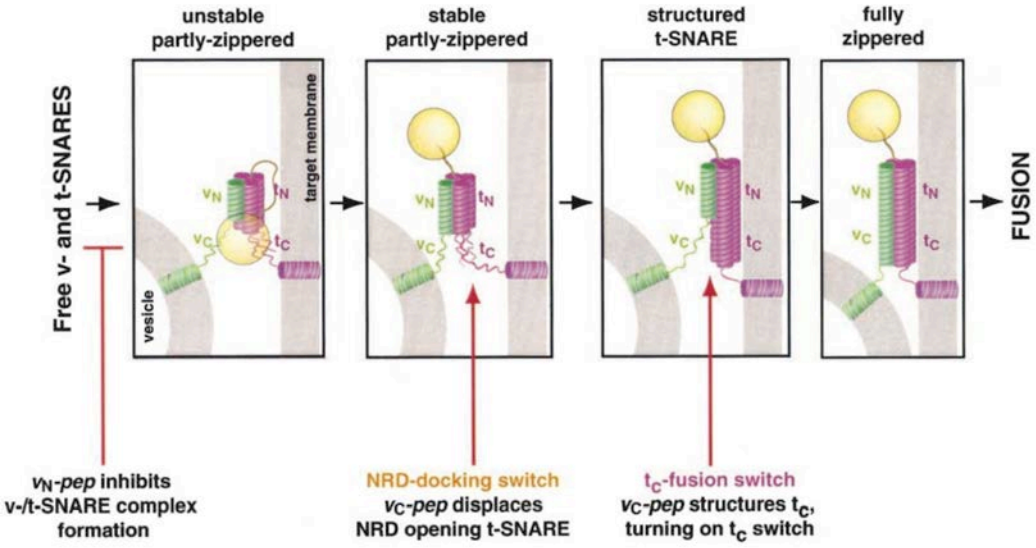

Figure 1.1.2.4. Polarized assembly of SNAREpins and membrane fusion. SNAREpin assembly proceeds in at least three successive stages: unstable SNAREpins; stable, partly zippered SNAREpins; and fully zippered SNAREpins. (unstable SNAREpins) SNAREpins assemble between liposomes via their membrane distal NH2-terminal ends, but are only partly zipped. This can occur rapidly, even when the t-SNARE is closed by NRD autoinhibition. (stable, partly-zippered SNAREpins) When the t-SNARE opens, further zippering-up occurs to produce stable SNAREpins that indicate irreversible docking between bilayers that are not yet fused. (structured t-SNARE) vc-pep structures, removing the impediment to the completion of zippering. (fully zippered SNAREpins) Zippering is completed and fusion occurs. This takes 4 min in the presence of bound vC-pep that needs to dissociate as part of this step, and could therefore be intrinsically faster than this.
Figure copied from TM Melia et al. The Journal of Cell Biology, 158, 929-40 (2002)

Regulation of core fusion machinery

As would be expected for a system that both directs and regulates traffic between membrane compartments, there are a number of sites at which control may take place, these sites are demonstrated in figure 1.1.2.4 (Melia *et al*., 2002). Regulation of SNARE proteins can be performed at a number of stages:

(i) Prior to SNAREpin assembly, regulation of the movement of the v- and t-SNAREs toward each other;

(ii) During SNAREpin assembly, controlling the rate of membrane fusion;

(iii) After SNARE complex assembly, regulating and fusion pore opening, disassembly of the complex and recycling of the proteins.

The role of NSF and SNAP proteins in disassembly has been discussed in section 1.1.1, as was the role of Munc-18 in keeping syntaxin folded in it closed conformation, and thus unavailable for SNARE complex formation. These switches will work at stages (iii) and (i) respectively. The switch at stage (ii) could be controlled by one of or a combination of synaptotagmin, complexin, or the tC fusion switch. The tC fusion switch is part of the t-SNARE SNARE motif that has been divided into tN and tC domains as discussed in section 1.1.1.1.

Other molecules could well be involved in regulation by controlling the proximity of vesicles to target membranes, by affecting the conformation or availability of free SNARE proteins and the insertion of specific SNAREs and other proteins in the vesicle membrane in the trans-Golgi network.

1.1.3 The role of Calcium in exocytosis

Calcium (Ca^{2+}) is an essential component for membrane fusion in regulated exocytosis. Ca^{2+} has been best characterised in its role as the trigger of regulated exocytosis in a number of neuronal and neuroendocrine cell models (for reviews see (Zucker, 1996; Bennett, 1997)). Increases in Ca^{2+} concentration ($[Ca^{2+}]$) in the microdomains surrounding docked vesicles induce neurotransmission by regulated exocytosis in a very rapid period of time (0.2-0.5 ms). The rate of exocytosis is a non-linear one, dependent on the $[Ca^{2+}]$ raised to the power of between 3 and 4 and experiments with caged Ca^{2+} compounds have demonstrated that there is a gradient of response to $[Ca^{2+}]$. Exocytosis has been demonstrated in the $[Ca^{2+}]$ range of 3 to 600 mMol (Heinemann *et al.*, 1994) and it would be expected that any $[Ca^{2+}]$ in excess of 50 mMol would induce rapid exocytosis. Detailed analysis of the dependence of the fast and slow phases of exocytosis on $[Ca^{2+}]$ (Voets *et al.*, 2001a) indicate that, as well as acting as the trigger for fusion, Ca^{2+} is required for vesicle priming. In addition it may be involved in steps upstream even of vesicle tethering: in chromaffin cells the Ca^{2+}-dependent acting

severing protein scinderin has been implicated in dissolution of the cortical actin network, allowing LDCVs to move to the cell periphery (Vitale *et al.*, 1995).

The mechanism by which Ca^{2+} triggers regulated exocytosis is yet to be finalised. Current knowledge suggests that exocytosis requires that Ca^{2+} enters through voltage-gated Ca^{2+} channels, although intracellular Ca^{2+} reservoirs may also play a role as empty stores may serve as a sink for external Ca^{2+} entering during depolarisation and thus blunt the exocytotic effect. In addition other receptors such as the muscarinic receptors activate pathways that provoke a rise in Ca^{2+} from intracellular stores and yet other receptors activate inositol phosphate pathways leading to Ca^{2+} rise (Aunis and Langley, 1999), however this is much less effective that Ca^{2+} that enters through channels in the plasma membrane, presumably because the local $[Ca^{2+}]$ at the sites of docked vesicles does not achieve such high levels. The molecules that function as Ca^{2+} regulated triggers of exocytosis must be located near the Ca^{2+} channels where local microdomains of high $[Ca^{2+}]$ are generated.

We know that a number of proteins involved in exocytosis have Ca^{2+} binding properties, in particular synaptotagmin (Bennett, 1997) and complexins. Synaptotagmin 1 is the prime candidate for the Ca^{2+} sensor in the central nervous system for fast synaptic exocytosis (Mahal *et al*., 2002; Yoshihara *et al*., 2003).The exact mechanism of action of synaptotagmin 1 remains unclear.

In *Drosphila* and *C.elegans*, genetic knockout of synaptotagmin 1 appears to have effects on vesicle docking and SNARE complex assembly, as well as abolishing fusion; but this was not seen in the mouse suggesting that synaptotagmins have multiple functions, some of which can be performed by other proteins, including synaptotagmin isoforms, in mammalian neurons. More acute knockout of synaptotagmin I in *Drosophila* suggests that only the fusion reaction is blocked (Marek and Davis 2002). Although synaptotagmin has been suggested to act as a fusion clamp, preventing fusion of docked vesicles until released by Ca^{2+}, acute knockout of synaptotagmin appears not to increase the rate of spontaneous fusion events, contradicting this theory. Recently some doubt has been thrown on the need for Ca^{2+} to induce the action of synaptotagmin

1 as Mahal *et al* have shown that synaptotagmin 1 on its own speeds up the process of SNAREpin assembly and membrane fusion in a reconstructed system (Mahal *et al*., 2002). This leads to the possibility of other Ca^{2+} dependent factors in membrane fusion. As discussed in section 1.1.2.5 the synaptotagmin family and other proteins exhibiting C2-domains may have roles in modulating membrane fusion in distinct ways (Sudhof, 2002)

It is interesting that in some systems, notably in the exocytosis of sea-urchin egg cortical granules and in vacuolar fusion in yeast, Ca^{2+}-triggered exocytosis seems to occur independently of the formation of the SNARE complex (Coorssen *et al.,* 1998). The role of Ca^{2+} is more clearly defined in membrane fusion of vesicles docked to the plasma membrane.

Further, the necessity of Ca^{2+} does not seem to be universal. Ca^{2+} has a critical role in all neurone and neuroendocrine cells that have been used as models for the study of regulated exocytosis but the requirement for Ca^{2+} has not been established in all other cells that have receptor based signalling leading to regulated exocytosis (Hille *et al.*, 1999).

1.1.4 Summary

Membrane fusion is essential to eukaryotic cell function. It requires a large amount of energy to overcome the repulsive force that exists between cell membranes and there are a number of proteins involved in the process of membrane fusion. There appears to be a degree of commonality in the process of membrane fusion for regulated exocytosis between species. Furthermore there is commonality in the different forms of membrane fusion within a cell type. The following steps are most likely common and they form the basis of membrane fusion in regulated exocytosis.

- Membrane attachment (docking); this occurs prior to fusion and is reversible. It is independent of the fusion process and may be regulated by rab GTPases.

- SNARE complex formation; the availability of SNAREs may be regulated by SM and other proteins.

- Priming; this is ATP-dependent and involves the Ca^{2+} dependent conversion of the SNARE core complex to a state in which Ca^{2+} can trigger fusion.

- Fusion pore formation; merging of proximal and distal lipid monolayers to open a fusion pore, in response to elevated [Ca^{2+}].

- Fusion pore dilation; expansion of the fusion pore.

- Disassembly of the SNARE complex by NSF and a- SNAP

The proposed models for the mechanisms of exocytosis and the control of regulated exocytosis have also been discussed. None of these models has been proven and the exact nature of regulated exocytosis remains to be determined. With current advances in the field we are moving toward a better understanding of the intricate details of regulated exocytosis. However it is important to note that even though a number of protein groups involved in regulated exocytosis have been described that not all of their actions have been proven in experiments and others remain postulated. There are still many unsolved questions relating to protein function and interaction, particularly in the process leading to the final steps of exocytosis.

1.2 Exocytosis Observed At Single Vesicle Resolution

Studying exocytosis at single vesicle resolution is important to allow interpretation of molecular events leading up to and occurring in relation to exocytosis. There have been a number of methods used to observe single vesicle exocytosis and the successful ones will be discussed in this section (Angleson and Betz, 1997; Henry *et al*., 1998)..

1.2.1 Methods used to study single vesicle exocytosis

Recently methods have been developed for measuring exocytosis, endocytosis and vesicle cycling in living cells in real time. This has resulted in a rapid expansion in the knowledge of these processes in secretory cells. The techniques covered in this section include electrical, electrochemical and optical methods. Each technique has on its own provided a share of our current knowledge of the kinetics of membrane fusion. However the combination of some of the techniques has added even more to our knowledge.

Other techniques used in monitoring exocytosis that are not appropriate to single vesicle resolution, for example postsynaptic current measurement, are not discussed.

1.2.2 Capacitance

Vesicles are surrounded by lipid bi-layer membrane and thus vesicle fusion with cell plasma membrane (lipid bi-layer) during exocytosis results in the cell plasma membrane surface area expanding and conversely endocytosis results in a decrease in cell plasma membrane surface area. Scientists have been able to use the electrical properties of the cell to monitor changes in cell surface area. Cell membrane electrical capacitance is proportional to cell surface area and thus changes in cell surface area can be measured as changes in electrical capacitance. The relationship between surface area and capacitance is the specific capacitance of biological membranes, which is typically in the order of 0.8-1.1 $\mu F/cm^2$. Cellular capacitance measurements have been used in many systems, the first description being from fertilisation studies of sea urchin eggs. The technique has

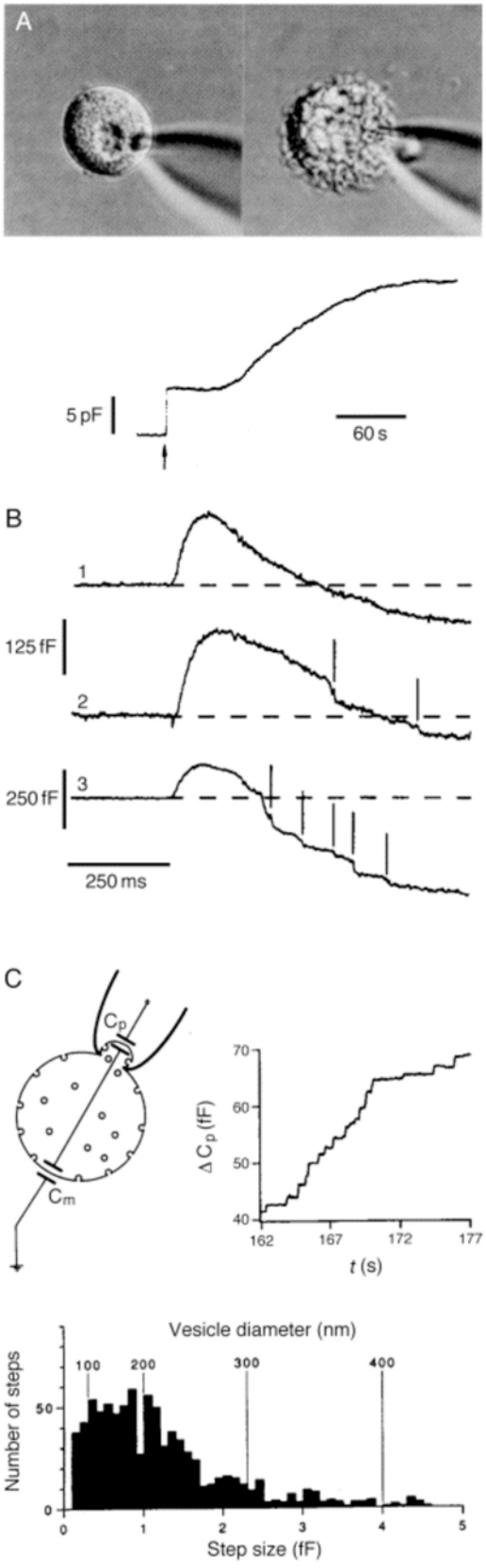

Fig. 1.2.2 The patch clamp capacitance technique monitors membrane surface area. (A) A patch clamped mast cell before (left image) and after (right image) dialysis with GTPS, which evoked massive exocytosis. The trace in the lower panel shows membrane capacitance, which increased after `break-in' with the patch pipette and start of GTPS dialysis (arrow). From Ref. [2]. (B) Three examples of capacitance changes in response to elevation of [Ca2+]i by flash photolysis of DM-nitrophen in pituitary melanotrophs. Vertical lines mark large endo-cytotic steps. From Ref. [3]. (C) Cell attached patch recordings of capacitance in a neutrophil resolve exocytosis of single granules; some steps reflect exocytosis of vesicles smaller than 100 n in diameter. From Ref. [4]. Figure copied from JK Angleson and WJ Betz. Trends in Neuroscience. 20, 281-287 (1997)

been refined and now measurements of single vesicle events are possible with millisecond temporal resolution (Chow *et al.*, 1996).Capacitance measurements can be performed in either conventional whole cell configuration or perforated patch configuration. Each method has distinct advantages for certain experiments. Whole cell dialysis allows for direct control of the ionic and second messenger composition of the cell by introduction of products, while a perforated patch is more suited to investigating the physiological context (Angleson and Betz, 1997).

To measure the time-resolved membrane capacitance of single cells in whole cell patch-clamp recordings, the cell and the cell-attached pipette are modelled as a linear three-element circuit with an access resistance, R_a, in series with the parallel membrane resistance, R_m, and membrane capacitance, C_m. In the frequency-domain method of measuring capacitance, a sinusoidal voltage command is superimposed on the holding potential, and the resulting current is analysed. This method allows for continuous recording of vesicle fusion and providing the secretory vesicles are large enough, fusion of individual vesicles can be detected as discrete events. The incorporation of a single vesicle, $C_{ves,}$ results in an increase in capacitance, ΔC, given by :

$$\Delta C = C_{ves}/(1+(\omega C_{ves} R_p)^2),$$

where ω is the frequency of the sine wave and R_p is the resistance of the fusion pore between the vesicle and the plasma membrane (von Gersdorff and Matthews, 1999). Figure 1.2.2 illustrates the features of capacitance changes that are observed during exocytosis.

There are limitations to this technique. Not all changes in capacitance are the direct result of vesicle exocytosis. For example gating charge movement in transmembrane proteins may bring about changes in capacitance. Other sources of artefact are non-exocytotic change in passive membrane electrical parameters, Ca2+-dependent conductance changes, access resistance changes and improperly compensated pipette capacitance. Further, the technique is based on linear voltage and the three-element

passive circuit model used to calculate capacitance is based on a spherical cell with equal electrical access to all parts of the cell surface. As capacitance detects net surface area change it is affected by both exocytosis and endocytosis and the one may reduce the effect of the other. For these reasons capacitance measurements have been combined with other techniques of the same time-resolution that detect other aspects of exocytosis, such as monitoring of catecholamine release by amperometry (Chow *et al.*, 1992).

1.2.3 Amperometry

Regulated exocytosis results in the secretion of neurotransmitters or hormones. The released transmitter molecule may be detected after oxidation or reduction with a change in current measured by amperometry or fast cyclic voltammetry. Fast cyclic voltammetry has an advantage in that it can give information about the chemical species whereas amperometry gives a higher time resolution. The most extensively studied secreted products are noradrenaline, adrenaline, dopamine and serotonin. Figure 1.2.3.1 shows oxidation of noradrenaline to its quinone product. The techniques have been miniaturised and only in the early 1990's was the technique applied to single cells (Wightman *et al.*, 1991). Since then there have been extensive studies of isolated cells, particularly mast cells and chromaffin cells because these cells have large vesicles with measurable amounts of exocytosed content.

The detection relies on an appropriate detector, which is a polarisable electrode. These electrodes when immersed in physiological solutions do not allow current to flow across the solid-liquid interface unless the electrode surface can undergo a rapid reaction with one of the dissolved species to covert ions to electrons and visa versa. The silver/silver chloride electrode immersed into a sodium chloride solution is such an electrode. When a voltage is applied to a polarisable electrode it will accumulate a charge on the surface facing the solution. The excess charge must be balanced by an equal and opposite charge in the solution. Mobile counter ions in the solution are attracted to the interface and form an aligned layer. The electroneutrality is achieved over a finite distance falling away with a space constant called Debye length. At equilibrium little or no current flows.

When oxidisable or reducable molecules diffuse to the surface of the electrode, electrons are transferred and current flows. The current generated may allow the calculation of the number of molecules released. This depends on the release of only one electro-active species and knowledge about the number of electrons transferred per molecule.

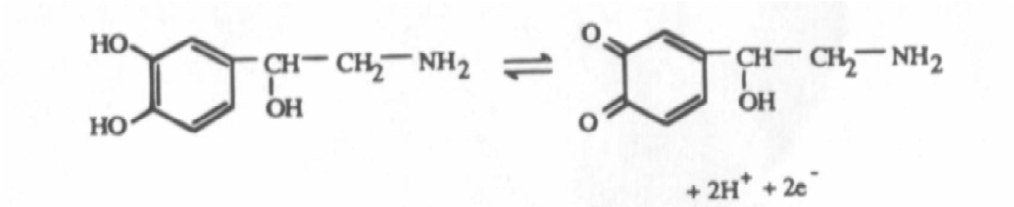

Figure 1.2.3.1 Oxidation of noradrenaline (left) to its quinone product (right) leads to the loss of two protons and two electrons.
Figure copied from RH Chow and L von Rüden. Single Channel Recording, 2nd edition (1995).

The relationship is known as Faraday's law:

$$Q = \int I dt = zFM/N_A = zeM$$

Q represents the total charge, obtained by integrating the current *(I)* transient; *M* represents the number of molecules reacted; z is the number of moles of electrons transferred per mole of compound reacted; *F* is Faraday's constant, N_A is Avogadro's number and *e* is the elementary charge (1.6×10^{-19} coul) (Chow *et al.*, 1996).

An example of such an electrode is a carbon fibre electrode. These can be placed near the cell can detect single exocytotic events by detecting the current generated by oxidation or reduction of the secreted molecule. The technique is limited to detectable secretory products, some of which are mentioned above. These electrochemical techniques are fast and sensitive, with a time resolution of milliseconds, and the ability to detect partial release of vesicle content (Chow and Von Ruden, 1995). As the method only measures events in the proximity of the electrode it also provides spatial information about secretion. For example single exocytotic events in isolated chromaffin cells have been temporally and spatially characterised through the relationships between voltage-gated Ca^{2+} influx and subsequent fusion events (Chow *et al.*, 1996). It is important to note that this measurement is not susceptible to interference from endocytosis. Figure 1.2.3.2 illustrates this technique.

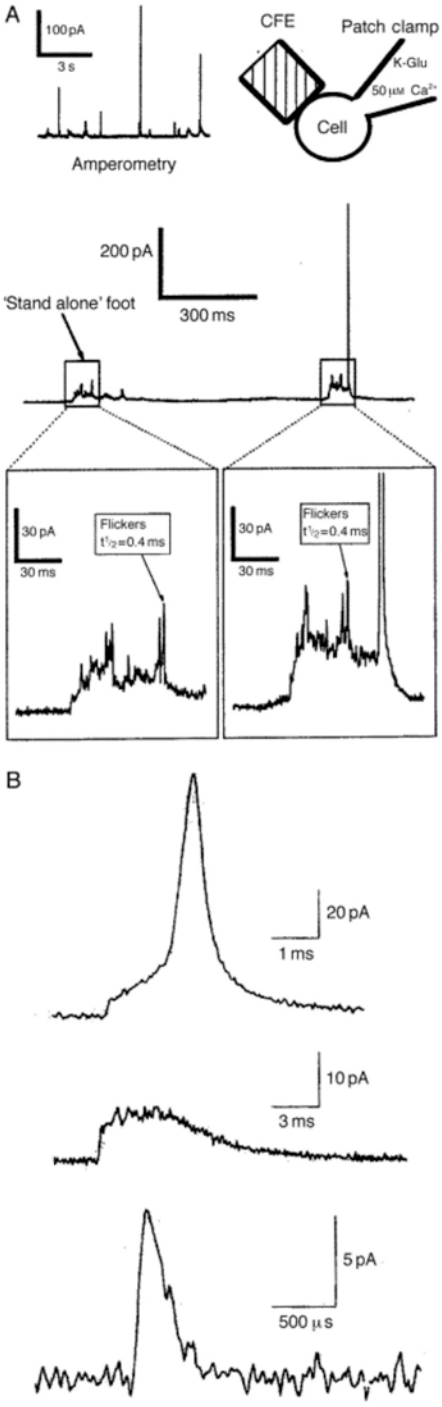

Fig. 1.2.3.2 Amperometry detects secretion from single granules. (A) Amperometric spikes recorded with a carbon fiber electrode (CFE) placed near a patch clamped cell. The spikes reflect the oxidation of catecholamines released from chromaffin cell granules. Many secretory events are preceded by `flickers' (lower panels) that probably reflect rapid fluctuations in fusion pore diameter. Usually these flickers are followed by full secretion (off-scale spike in lower right panel); sometimes `stand alone' flickers occur (lower left panel) that may reflect fusion pore closure. From Ref. [34]. (B) Similar phenomena were observed in recordings of serotonin secretion from isolated leech neurons. Evidence of full secretion from large granules (top trace) and `stand alone' feet (middle trace) were observed. In addition, much smaller, faster signals (bottom trace) may reflect secretion from small clear vesicles. Scales =5 pA and 1 ms. From Ref. [33]. Figure copied from JK Angleson and WJ Betz. Trends in Neuroscience. 20, 281-287 (1997)

Single exocytotic events appear as current spikes, allowing the recording of the frequency of fusion events from the area of the cell detected by the electrode. Detailed analysis of the height, half-width, rise and area of the individual current spikes gives information about the fusion pore opening and closing and information about the vesicle size (Chow and Von Ruden, 1995), thus providing insights into the kinetics of the last stage in exocytosis (Burgoyne and Barclay, 2002). Figure 1.2.3.3 demonstrates a model spike with measurements used for detailed analysis. Q represents total granule charge and $Q^{1/3}$ roughly indicates granule size, see paragraph 2 on page 38 (Wightman *et al.*, 1991). I_{max} is the maximum concentration of exocytosed content reaching the electrode tip. The half-width ($t_{1/2}$) and rise time (tP) may indicate the speed of exocytosis (Segura *et al.*, 2000). Figure 1.2.3.3. also demonstrates a foot, line *m* extrapololates the rising phase back to baseline to allow determination of the rise time (Chow *et al.*, 1992). The foot appears to be the escape of vesicle contents through the narrow initial opening of the fusion pore. Conceivably the fusion pore can flicker open and closed leading to 'stand alone' foot signals that do not result in a full amperometric spike (Chow and Von Ruden, 1995).

Amperometry has in particular provided knowledge about fusion pore dynamics and the ability of vesicles to release part of their content (Graham and Burgoyne, 2000, Elhamdani *et al.*, 2001). It has also provided knowledge about the time course of exocytosis (Chow *et al.*, 1992).

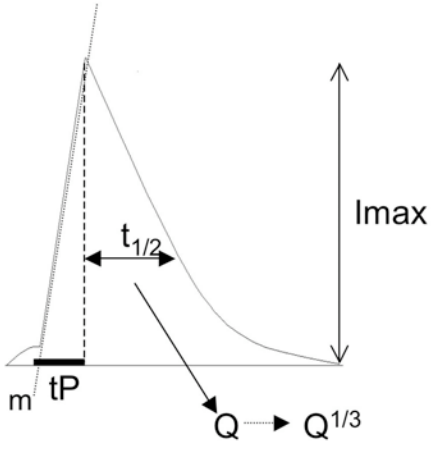

Figure 1.2.3.3 Spike parameters
Imax is the maximum recorded current, $t_{1/2}$ is the half width, tP is the rise time, Q and $Q^{1/3}$ are net granule charge and represent the amount of redox material in the granule

1.2.4 Optical Methods

A variety of microscopy techniques have been used to image single vesicle exocytosis in living cells. These include epi-fluoresence, confocal microscopy, differential interference contrast (DIC) microscopy, total internal reflectance fluorescence microscopy (TIRFM) and multi-photon microscopy. Of these only DIC does not rely on fluorescence. Total internal reflectance fluorescence microscopy, confocal and multi-photon microscopy will be discussed in detail in section 2.

Fluorescence microscopy is an important biophysical tool for studies in living cells and in reconstituted preparations *in vitro.* Fluorescent markers can be incorporated into living cells to measure a variety of functions, such as:

a. Physiological changes in cytosolic or organellar pH
b. Ca^{2+} fluxes into the cytoplasm or sub-cellular compartments
c. Membrane potentials
d. Sub-cellular locations and interactions of defined proteins
e. Lateral movement of lipids and proteins in membranes

With respect to imaging of single vesicle exocytosis, fluorescent markers can be used in the following ways:

i. labelling membrane proteins, by expressing them as fluorescent chimeras
ii. labelling contents of vesicles, with acidophillic dyes or targeted fluorescent proteins
iii. using dyes that change fluorescence depending on hydrogen ion concentration
iv. linking a released product to change in fluorescence of a marker dye

Imaging of vesicles has been challenging as the microscope spreads out the image so that the individual vesicle is not seen as a single spot of light but rather as a cone with the vesicle in focus as the point and the three-dimensional spread of light as the cone. Resolving two individual vesicles becomes difficult if they lie close to one another, and since the bovine chromaffin cell is packed with up to 20,000 secretory vesicles this is of

particular concern. It is possible to resolve vesicles that are separated by a distance equal to the wavelength of light but with the density and size of vesicle this can prove difficult in certain cell types.

The other limitations of optical methods depend critically upon the size of the secretory vesicle. Some cells, such as adrenal medulla chromaffin cells and mast cells, have relatively large secretory vesicles, which make them more suitable for these techniques. Technical limitations include auto-fluorescence (many endogenous molecules will fluoresce at certain wavelengths), photo-bleaching (destruction of fluorescence by light-induced conversion of the fluorophore to a non-fluorescent compound) and light scattering, from the object of interest and other specimen content. Quantitation of fluorescence intensity is directly proportional to its concentration only in very dilute concentrations that follow Beer's law. At higher concentrations the intensity can decrease through self-quenching. Further, saturation of the optical detector may occur if the emitted fluorescence is too intense (Lansing Taylor and Salmon, 1989).

Recently there have been huge advances in the ability to obtain video images from the fluorescence microscope. The computer software available to monitor and analyse the data has improved in the recent past. The combination of powerful computing and versatile new markers such as green fluorescent protein (and its variants) has added much to our knowledge of the mechanisms of vesicle cycling.

The main advantage of optical imaging is, apart from the fact that we can see what is happening, that information about vesicle function can be obtained at multiple spatial locations simultaneously (Murthy, 1999). With the fast acquisition rate of modern specialised digital cameras we can record events that we could not determine in the past. The ability to visualise single vesicle secretory events is possible with a number of the microscopy techniques. TIRFM (Steyer *et al*., 1997) and confocal laser scanning microscopy (Burke *et al.*, 1997) have provided a means of monitoring single vesicle events in living cells. There have been further improvements in the speed of confocal microscopy while and the application of multi-photon microscopy has assisted progress in imaging in recent years.

TIRFM has been used to image single vesicle events with some success since first described for this purpose in 1997 by Steyer and Lang (Steyer *et al*., 1997; Lang *et al*., 1997). Individual granules can be tracked as they approach the membrane, dock and fuse (Oheim *et al.*, 1998, Steyer and Almers, 1999). The use of TIRFM is still limited by the numbers of vesicles present in the intact cell at the glass cell interface. We observed in our confocal experiments that most vesicles appeared close to the base of the cell and this was also reported by Cuchillo-Ibanez (1999). As the number of vesicles in the region of excitation of TIRF is high, complicated de-convolution and thresholding steps are often required to resolve single vesicles. TIRFM has other theoretical advantages over confocal laser scanning microscopy and multi-photon microscopy and these are discussed in more detail in section 2.

1.2.5 Combinations

The combination of optical and electrical methods has only been successful with one approach thus far. The use of a fluorescent styrene dye, FM 1-43, that partitions into membranes adjacent to the solution containing it, have led to some interesting results in combination with capacitance measurements (Smith and Betz, 1996). These have not yet been translated into single vesicle events. In TIRFM optical monitoring of vesicles occurs in the excitation field adjacent to the cover slip, while the carbon fibre electrode is placed along side the cell; this complicates TIRFM when attempted in combination with amperometry. In effect different areas of the cell are monitored and it is difficult to make any one to one comparisons (Steyer *et al*., 1997). The combination of amperometry and capacitance has, however, been very informative and has improved our knowledge extensively (Chow *et al*., 1994; Chow *et al*., 1996).

1.2.6 Summary

In summary, each of these methods on its own can provide insight into the membrane fusion event of single vesicles. The findings from one method can be compared to the findings from another method and this enables a better understanding of the dynamics of

membrane fusion. As each method gets more developed we will begin to understand more fully the dynamics of the membrane fusion event associated with regulated exocytosis.

1.3 Cell-free models

As discussed previously regulated exocytosis involves the highly ordered fusion of a vesicle with the plasma membrane. The cell-free biochemical approach has established the principles and molecular mechanisms underlying protein transport from the endoplasmic reticulum (ER) through the Golgi to the plasma membrane (Alberts *et al*., 2002). These *in vitro* experiments have been based on isolated membrane compartments in combination with constituents of cytosol, including the appropriate energy source. The principle of these *in vitro* assays has been applied to vesicles and the plasma membrane to try to understand the interactions of the proteins and molecules described in section 1.2. The first successful assay was developed in sea urchin eggs (Vacquier, 1975), however this assay has proved difficult to extend to mammalian cells. Further work on developing a cell free plasma membrane model from which regulated exocytosis can be triggered is required. The development of an assay to investigate regulated exocytosis in a controlled environment will provide a powerful tool for elucidating the roles of the proteins that are known to be associated with the vesicles and the plasma membrane (Avery *et al*., 1999). Two recent papers that report promising systems have nevertheless not resulted in a flurry of new work (Edwardson, 1998; Avery *et al*., 2000).

In this section the two methods used for establishing a cell-free environment for monitoring exocytosis from plamsa membrane will be discussed. The design of our own method will be discussed in the methods section.

1.3.1 Cortical Lawns

The sea urchin egg is the basis of this system. Prior to fertilisation the sea urchin egg has a large number of large cortical secretory vesicles docked at the cytoplasmic face of the plasma membrane. As the sperm fertilises the egg the intracellular [Ca^{2+}] transiently increases triggering a number of events. One of these is exocytosis of the cortical secretory vesicles, their contents forming a fertilisation barrier around the egg (reviewed by(Zimmerberg *et al*., 1999)).

Vacquier was first to use sea urchin eggs in a cell-free system (Vacquier, 1975). They prepared a lawn of membrane by shearing the eggs attached to a polylysine-coated surface using a buffer of similar composition to the intracellular compartment of the cell. Once the cell contents had been washed away the egg plasma membrane and its attached secretory vesicles were left attached to the polylysine-coated surface. Addition of buffers with Ca^{2+} in micromolar concentrations triggered exocytosis of these attached vesicles.

Crabb and Jackson (1985) later were able to add exogenous vesicles to such a membrane lawn and achieve exocytosis (Crabb and Jackson, 1985). As these vesicles are large (1mm) in size the events could be monitored by light microscopy. Other methods have also been used to monitor these experiments, for example changes in turbidity. It has been concluded that the disappearance of granules is due to fusion and exocytosis rather than to vesicle lysis.

The ‘cortical lawn’ studies have been particularly helpful in characterising the requirements of ATP for priming and Ca^{2+} for triggering regulated exocytosis. Some progress in elucidating the fusion reaction has also been made but has not kept up with the characterisation of the proteins involved in fusion. Very briefly some of the findings include: (a) synaptobrevin, syntaxin, SNAP-25, synaptotagmin and rabs have been identified in sea urchin egg cortex using antibodies raised against the mammalian homologues; (b) incubation with tetanus toxin light chain cleaves the synaptobrevin immunoreactive protein and this partially inhibits Ca^{2+} dependent exocytosis (reviewed

by (Avery *et al*., 1999)); (c) Ca^{2+} disruption of the sea urchin SNARE complexes prior to membrane fusion suggests that VAMP is not an absolutely required protein for membrane fusion in this system (Tahara *et al*., 1998).

1.3.2 Permeabilised cells

Creating holes in the membrane of cells allows access to the intracellular cytoplasm. Cells with such holes in the plasma membrane are termed permeabilised cells. As in intact cells, exocytosis is measured by monitoring release of secretory product into the surrounding medium or lipid mixing with fluorescent probe. Permeabilised cells retain most of the cytoarchitecture involved in secretion and are at present the most useful *in vitro* model for vesicle to plasma membrane fusion. However, the model is limited by the size of the created pores.

There are a number of methods described for permeabilising cells (reviewed by (Avery *et al*., 1999)). These techniques render the membrane of the cell permeable to exogenous compounds. The techniques include the following:

1- high voltage discharges resulting in breakdown of plasma membrane

2- application of detergents (eg. digitonin & saponin);

3- pore-forming bacterial toxins (a-toxin, streptolysin-O); this utilises the bacterial toxin's ability to form a pore through the plasma membrane to allow entry of the bacteria to the cell.

4- amphotericin B or nystatin, polyene antibiotics that form channels in cholesterol or ergosterol containing membranes

5- ATP^{4-} ; utilises the ATP receptors on certain cell types (Mast cells) to create electrical access to the cell

6- Mechanical shearing forces (Klenchin *et al*., 1998)

   a) Cracked cells with a single pass through a precision ball homogeniser

b) Freeze-thawed cells, permeabilisation determined by the rates of freezing and thawing the cells.

c) Secretory granule-plasma membrane complexes; prepared from cell homogenates by centrifugation (Martin and Kowalchyk, 1997)

d) Sonication of cells attached to glass coverslips (Avery *et al*., 2000)

7- Patch clamp pipette with (as described in section 1.2.2)

a) whole cell dialysis

b) permeabilised membrane patch (using methods 2,3,4 and 5 above (Rae and Fernandez, 1991))

Once a cell has been permeabilised by one of these methods the study of small effector molecules and soluble proteins may take place. The different techniques described each have different characteristics and the most suitable for the planned experiment should be chosen. On the whole they are more suited to molecules that diffuse easily into the cytoplasm and are not suited to experiments where essential cytosolic components may wash out while the cell is permeabilised. However cell 'run down' after digitonin permeabilisation has been exploited to identify the soluble proteins involved in exocytosis (Morgan *et al*., 1993).

Cell permeabilisation techniques have been highly informative in the study of the mechanisms controlling regulated exocytosis. Definition of the stages of exocytosis has been one of the core findings from cell permeabilisation experiments. They have also been instrumental in identifying regulatory proteins in the exocytotic pathway. Further, other potential regulating factors have been investigated in permeabilised cells. The roles of all the factors involved in regulated exocytosis are still far from clear and this technique has several limitations. Washing out of cytosolic components occurs at variable rates in different experimental conditions and varies between components. This makes it difficult to control the depletion of certain proteins that rate-limit exocytosis (eg. NSF and a-SNAP). Another limitation is that only the final fusion event can be assayed. The intermediate steps cannot be accessed directly, thus the permeabilised cells

can offer a vast amount of information in the kinetics of the final stages of fusion but less in the priming, docking and triggering stages and offer no insight into the cytoskeletal movement of vesicles. Studies on individual proteins are limited to those where specific inhibitors or effectors are available (eg. SNARE cleaving neurotoxins). As the upstream regulatory events cannot be monitored the effect of an applied compound can only be interpreted at the membrane fusion stage. This may be obscured by events leading up to membrane fusion and has led to multiple interpretations.

A very brief review of some of the findings from permeabilised cells follows. Permeabilised cell studies were crucial in originally establishing that a rise in intracellular Ca^{2+} is required to trigger exocytosis. Likewise the need for MgATP was demonstrated. A number of cell types have been used in the experimental models, including adrenal chromaffin cells, platelets, pituitary tumour cells, insulin-secreting tumour cells and pancreatic b-cells. These studies have led to the definition of a number of Ca^{2+} dependent steps leading up to exocytosis. There is an apparent difference in the number of reported steps depending on the cell type and the method of permeabilisation (reviewed by (Avery *et al*., 1999)).

The steps characterised in the PC12 cell line are as follows. Firstly distinct cytosolic factors are responsible for mediating ATP dependent priming of Ca^{2+}-activated exocytosis, including phosphatidyl inositol-4-phosphate 5-kinase and phosphatidylinositol transfer proteins. Similar requirements have been demonstrated in chromaffin cells. The exact nature of the dependence on polyphosphinositides for exocytosis is not well understood. Their involvement has been demonstrated in mammalian cells and yeasts. They also play a role in other membrane trafficking steps.

Secondly, triggering of exocytosis has been documented. The SNAREs as previously discussed have an integral role in exocytosis although whether they participate in the fusion reaction *per se* is still controversial, but most evidence from animal systems suggests that they are involved in the fusion process itself. The SNAREs can be degraded by the use of Clostridial neurotoxins (tetanus and botulinum). The active light chains of these toxins can inhibit Ca^{2+} regulated secretion in a variety of cell types in

different permeabilised models. Work in Richard Scheller's laboratory has demonstrated some of these principles in secretory granule-plasma membrane complexes (Chen *et al*., 1999).

Thirdly, soluble Ca^{2+} binding proteins have been investigated with a degree of success in permeabilised models. The role of Ca^{2+} Activator Protein for Secretion (CAPS) in exocytosis was discovered, but remains to be fully determined (Martin and Kowalchyk, 1997). On the other hand it is far more difficult to investigate the membrane bound Ca^{2+} binding proteins, as these are not removed on cell breakage. Some experiments using antisense oligonucleotides, over expression of protein fragments (eg synaptotagmin fragments) and injection of peptides corresponding to domains of proteins have been performed, particularly for synaptotagmin (Shin *et al*., 2002). The results of these studies are difficult to interpret as high concentrations of the additive are required and this often results in loss of function.

1.3.3 Conclusion

Current methods allow investigation of the final steps of exocytosis. The steps leading up to the final event remain difficult to investigate with current cell-free methods. Speculative pathways have been proposed from current knowledge (section 1.1.1) but none of these has been fully documented experimentally and there are many large gaps in our knowledge. Thus there is a need to develop a cell-free model that allows better regulation of the pre-docking stages of vesicle transport as well as better access to monitoring of the stages of exocytosis. This method or a number of methods need to be able to investigate all the trafficking steps in vesicle movement from cytoskeleton to cell membrane and the final regulated exocytotic event. Permeabilised cells have proved very useful and will continue to provide insight into exocytosis but they do not offer the possibility to manipulate fully the machinery of regulated exocytosis. The membrane patch of the sea urchin egg is a good model but a mammalian cell membrane model requires development for investigation of regulated exocytosis. This mammalian model has thus far been fairly elusive to investigators.

1.4 Second Messenger (or Molecular) Manipulation of Exocytosis

A number of molecular agents including toxins and drugs have been used to manipulate exocytosis. These will be briefly described each and illustrated with a published example.

1.4.1.1 Neurotoxins that block exocytosis

The different Clostridial neurotoxins each cleave one or more of the SNARE proteins involved in exocytosis resulting in disruption of exocytosis. Tetanus neurotoxin (TeNT) and botulinum neurotoxin (BoNT) B/D/F and /G cleave synaptobrevin/VAMP, but each at a different point in the sequence. BoNT/A and /E cleave SNAP-25 at two different sites in the carboxy-terminal, while BoBT/C cleaves both syntaxin and SNAP-25. Figure 1.4.1.1 demonstrates the site of action of the BoNT's. Clostridial neurotoxins (CNT) has been shown to cleave synaptobrevin, SNAP-25 and syntaxin (Meunier *et al*., 2002).

1.4.1.2 Neurotoxins that stimulate exocytosis

a-Latrotoxin results in exocytosis by one of two mechanisms. Firstly it facilitates an a-latrotoxin induced cation channel in the plasma membrane, the subsequent influx of Ca^{2+} resulting in exocytosis. Secondly it enhances secretion by interacting with a Ca^{2+}-independent receptor for a-latrotoxin (latrophillin) and neurexin 1a (Bittner *et al*., 1998). This action seems to be mainly one of placing the toxin at the plasma membrane and allowing it to bind to the plasma membrane and form the cation pore. However, recent work has postulated that latrophillin may regulate secretion by slowing a discrete rate limiting step and if bound by a-latrotoxin that the inhibitory effect is removed (Bittner, 2000).

1.4.2 Molecules that interact with Ca2+

As described in section 1.1.3 Ca^{2+} is required for exocytosis. Ca^{2+} plays a role in recruiting vesicles to the plasma membrane, docking of vesicles, priming of vesicles and

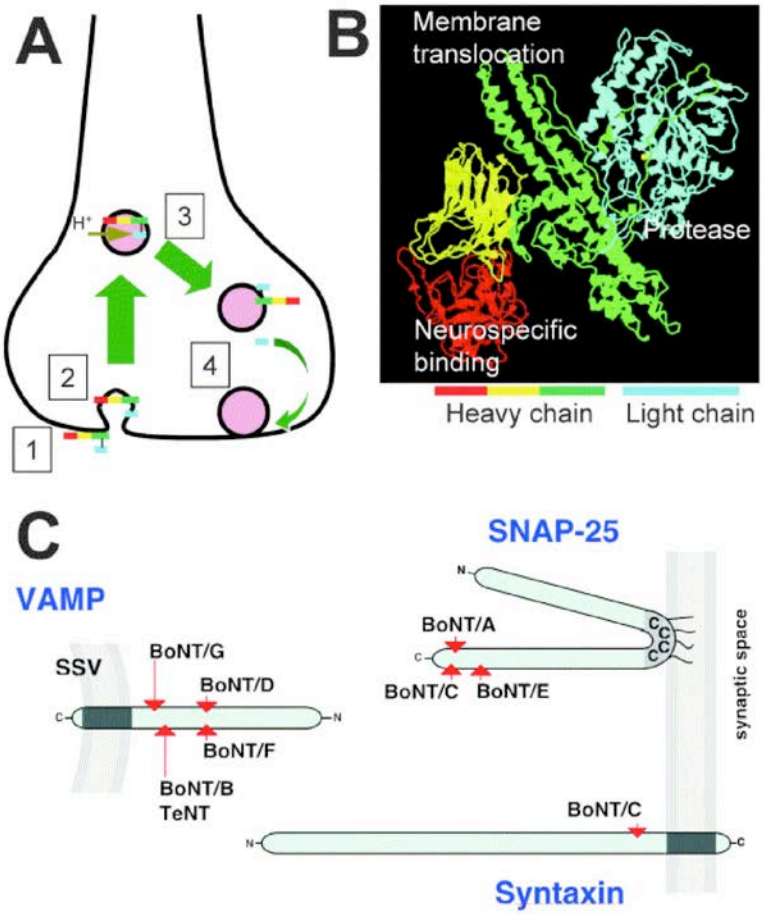

Fig. 1.4.1.1 Mode of action of botulinum neurotoxins at the neuromuscular junction. (A) The neurotoxin selectively binds (1) to a yet to be identified neuronal acceptor on the nerve terminal axolemma, (2) is internalised and (3) the heavy chain undergo a conformational change driven by acidification of the compartment. This allows the translocation of the light chain into the cytoplasm where it is released by reduction of the disulfide bridge. (4) The metallo-protease activity of the light chains cleaves SNAREs proteins thereby inhibiting regulated neurotransmitter secretion. (B) Three-dimensional crystal structure of BoNT/A highlighting (in red and yellow) the neuroacceptor binding domains, (in green) the translocation domain, and (in blue) the light chain responsible for the zinc-dependent (yellow dot) metallo-protease activity. (C) Cleavage sites of the various CNTs on VAMP/synaptobrevin (located on small synaptic vesicles (SSV), SNAP-25 and syntaxin situated on the nerve terminal axolemma.
Figure copied from FA Meunier et al. Journal of Physiology Paris. 96, 105-113 (2002)

in fusion pore formation and expansion. Manipulations in the Ca^{2+} concentration of the solutions applied to whole cells, permeabilised cells or membrane patches allow the study of the effect of Ca^{2+}. The proteins that are thought to mediate the Ca^{2+} stimulus can also be studied in this way. Martin and Kolwalchyk (1997) demonstrated that the

Ca^{2+} -activated fusion mechanisms were preserved after cell homogenisation (Martin and Kowalchyk, 1997). They also demonstrated that ATP and cytosol where required for fusion of large dense core vesicles and plasma membrane.

1.4.2.1 ATP

ATP plays a role in exocytosis and is a required factor for exocytosis. ATP plays a role in priming the vesicles through PI transfer protein and phosphoinostide kinases catalyse the synthesis of $PI(4,5)P_2$ which is required for Ca^{2+} triggered fusion (Avery *et al*., 1999). ATP is also required as a co-factor in NSF and a- SNAP disassembly of the cis-SNARE complex. Variations in the ATP concentration have been used to demonstrate that there is a readily releasable pool of vesicles that are docked to plasma membrane that do not require ATP to undergo membrane fusion (Chestkov *et al*., 1998).

1.4.2.2 Protein kinase C (PKC)

Phorbol ester PMA has been shown to stimulate evoked cathecholamine release from adrenal chromaffin cells by increasing the size of the readily releasable pool (Gillis *et al*., 1996). PMA activates PKC and also binds to munc-13 (Betz *et al*., 1998). By using the PKC inhibitor bisindolylmaleimide is used to block the PKC ATP-binding site it has been shown that the effect of PMA on exocytosis is due to PKC activation (Graham *et al*., 2000).

1.4.2.3 Guanylate Cylcase (PKG)

Activation of PKG by nitric oxide slows down the amount of granule content released (Machado *et al*., 2000). This is an interesting observation and if confirmed will demonstrate the ability of nitric oxide to modulate the amount of granule content released. The actions of nitric oxide on exocytosis remain controversial, as not all the findings are consistent.

1.4.2.4 Protein kinase A (PKA)

Activation of PKA with mild stimuli, b-adrenergic agonists, results in a slowing of exocytosis similar to PKG activation by nitric oxide. Stronger stimuli, forskolin treatment, result in an apparent increase in granule content. This may be due to two or more granules fusing together prior to fusion (Borges *et al*., 2002). The underlying mechanism seems to be PKA potentiation of Ca^{2+} entry to the cell.

1.4.3 Purified proteins

The ability to insert c-DNA into bacterial plasmids allows the production of purified proteins or domains of proteins and antibodies to proteins. These purified proteins can then be added to a permeabilised cell or membrane patch to investigate the effect. For example, bacterially expressed soluble coil domain of neuronal VAMP/synaptobrevin and syntaxin inhibit docked dense core vesicle release. The soluble coil domain formed SDS-resistant complexes with endogenous SNAREs and thus prevented the SNAREs anchoring the two target membranes together (Scales *et al*., 2000). Another example is the SNAP-25 specific Cl 71.1 Fab fragment that have been demonstrated to inhibit the sustained phase of exocytosis (release of vesicles after the initial release of the docked vesicles of the readily releasable pool) after stimulation of an adrenal chromaffin cell by caged Ca^{2+} release (Xu *et al*., 1999).

1.5 Concluding comments

1.5.1 Reconstitution of Exocytosis

The goal of a cell free *in vitro* assay is to be able to reconstitute vesicle exocytosis on a plasma membrane. A number of added components are required to produce the end result and theoretically each of these can be manipulated to produce evidence about the function of individual proteins and molecules involved in regulated exocytosis.

Preparation of vesicles from a number of tissues and cell types, including adrenal chromaffin cells, have been described. These isolated secretory vesicles have been shown to be functional in that they can fuse with plasma membranes and they will exocytose their contents. Preparation of cytosol from chromaffin cells has also been described. The addition of isolated vesicles and cytosol to the membrane is the basic requirement of the cell-free assay.

The manipulation of the cytosol to alter change the concentrations of known factors in exocytosis, such as NSF, a-SNAP, ATP and Ca^{2+}, and potentially other soluble proteins should provide insight into the requirement and function of these factors. Further the use of specific inhibitors of proteins (eg. neurotoxins that cleave SNARE proteins) or specific effectors will further add to the assay as a tool to examine regulated exocytosis.

Modification of the vesicle attached (v-SNAREs) and other membrane associated proteins by mutation or by labelling them with GFP would provide new information about their interactions with plasma membrane attached proteins.

1.5.2 Proposal

To further current knowledge in the field of regulated exocytosis better methods of investigating the interactions at the cell membrane need to be developed. These methods should be robust and reliable to allow cell free investigation of regulated exocytosis in mammalian cells.

The aim of this project was to develop such a method. The basic requirements of this method would include an optical technique that could acquire images fast enough and with high enough resolution to image exocytotic events occurring in a sub-second time frame and TIRFM was chosen for the features described in section 2. Subsequently this method has been commended as the best technique to study granule motion (Borges and Machado, 2002). A cell model for regulated exocytosis that is well characterised would be an important requirement. Bovine adrenal chromaffin cells have been used in a variety of such experiments and were chosen for use in our method development. A further requirement is a means of adhering cells tightly to a glass coverslip allowing the disruption of the membrane and retaining a membrane patch that remains closely adhered to the glass. This has been described for other applications and the methods required investigation in our particular setting.

Once developed the method would require validation by the current means of regulating exocytosis, including demonstrable Ca^{2+} activation, ATP dependence and blockade by neurotoxins. The images of single vesicles would need to be of reasonable clarity, these vesicles would need to be tracked and be recorded during exocytosis by demonstration of the flash in fluorescence as the dye leaves the vesicle. The ultimate experiment would be the addition of prepared vesicles in a cytosol solution over the membrane patch and being able to record exoctysois of these vesicles from the membrane patch. It would also be useful to demonstrate the existence of two pools of exocytotically competent vesicles, the readily releasable pool and the reserve pool.

In conclusion the introductory chapters have set the scene behind the idea of a mammalian cell free model for the study of regulated exocytosis. Robert H Chow initiated and produced the concept and funding was provided by a Sir Henry Wellcome Commemorative Award for Innovative Research.

2.1 Total Internal Reflectance Fluorescence Microscopy

Hirschfeld first described Total Internal Reflectance Fluorescence Microscopy (TIRFM) in 1965 as a technique for selective surface illumination (Hirschfeld, 1965). Since then it has been used for a number of applications in biochemistry and cell biology. The theory of TIRF is described in this section along with its application to the development of the method.

TIRF is a method of exciting fluorophores very near a solid surface, depth of field between 100 and 200nm, without exciting fluorescence from regions further from the surface (Axelrod *et al.*, 1992). This overcomes the potential difficulty in observing surface-associated molecules with conventional epi-fluoresence (in which the whole area and depth has fluorescence excited) if there are non surface-associated molecules in the adjacent medium. As the cell membrane and associated attachment proteins are in the order of 30nm in thickness TIRF is ideally suited to investigating cellular trafficking at the cell membrane (Axelrod, 2001).

2.1.1 Evanescent field

The evanescent field is a very thin electromagnetic field with the same frequency as the incident light. This electromagnetic field is able to excite fluorophores near the surface while not exciting those further away. The evanescent field decays exponentially from the interface. The decay characteristic is defined by the refractive indices of the media, incident angle and illumination wavelength. The intensity is also dependent on the polarisation of the incident light. For an infinitely wide beam, the intensity of the

$$I(z) = I(0)e^{-z/d}$$

$d = \lambda_0 / 4\pi (n_3^2 \sin^2\theta - n_1^2)^{-1/2}$

d , depth dependant on with λ_0, the wavelength of the incident light in a vacuum and the refractive indices of the two media

evanescent wave decays exponentially with perpendicular distance ‘z’ from the interface. This is measured in units of energy per unit area, per second.

Fig 2.1.1 demonstrates the decay of the evanescent field as calculated for the BK7 glass coverslips, interface with water and incident light at λ = 488nm. These are approximations for the conditions of our experiments.

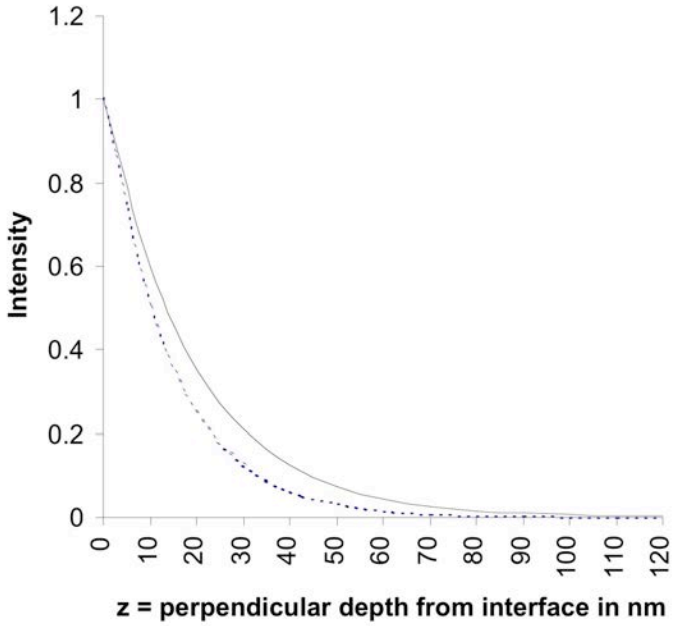

Fig 2.1.1 Intensity of the evanescent wave from the interface.
The solid line demonstrates the intensity of the evanescent wave for the glass water interface. The dashed line demonstrates the intensity for a glass cytoplasm interface. Both of these are calculated with a 68.86° angle of incidence.

2.1.2 Evanescent wave

Total internal reflection (TIR) relies on the physical properties of light that are described by Snell's law (figure 2.1.2). As a beam of light crosses from one medium to another with a different refractive index it will be refracted. When the incident angle of the light beam is above a critical angle (defined by Snell's law) light will be totally reflected back into the medium with the higher refractive index rather than pass through into the medium with lower refractive index. When the light beam reflects, an evanescent field is created in the lower index medium (Axelrod *et al*., 1992).

The critical angle q_c for TIR is given by:

$$q_c = \sin^{-1}(n_1/n_3)$$

Where n_1 and n_3 are the refractive indices of the liquid (lower refractive index) and the solid (higher refractive index), respectively. (Use of n_2 will be reserved for discussing an optional intermediate layer below.) The ratio n_1/n_3 needs to be ≤ 1 for TIR to occur. Figure 2.1.2 demonstrates the principal of Snell's law. Incident light with $q < q_c$ will

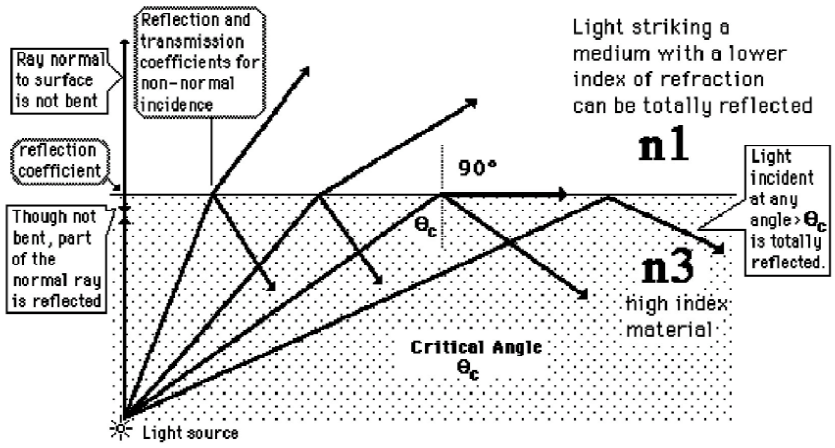

Fig 2.1.2 Diagram demonstrating the basic principal of Snell's law.

refract through the interface with a refraction angle, also given by Snell's law. There

will be some reflection of the incident light back into the solid medium. For $q > q_c$ all of the incident light reflects back into the solid medium. Some of the incident energy penetrates through the interface and propagates parallel to the surface in the plane of incidence. This evanescent field is capable of exciting fluorescence.

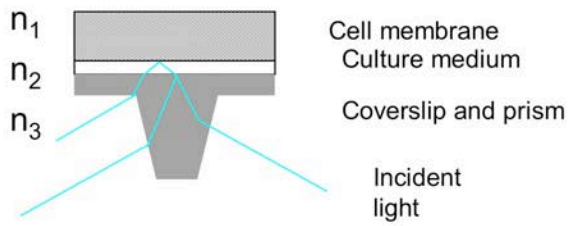

Fig 2.1.2.1 Diagram demonstrating the intermediate layer in a biological system. There are potentially other layers in cytoplasm and intracellular organelle membranes etc. The lines represent the incident light and the potential points for TIR. The depth of the evanescent wave is measured from the surface of n_3. The culture medium is represented by n_2 and the cell membrane by n_3.

2.1.2.1 Intermediate layers

Due to the higher complexity of preparations needed for laboratory measurements, the theoretical bi-layer approach may not always be appropriate. For example a cell membrane (lipid bilayer) interfacing with a glass coverslip is a complex stratified multilayer system consisting of glass, culture medium, lipid bilayer and cytoplasm.

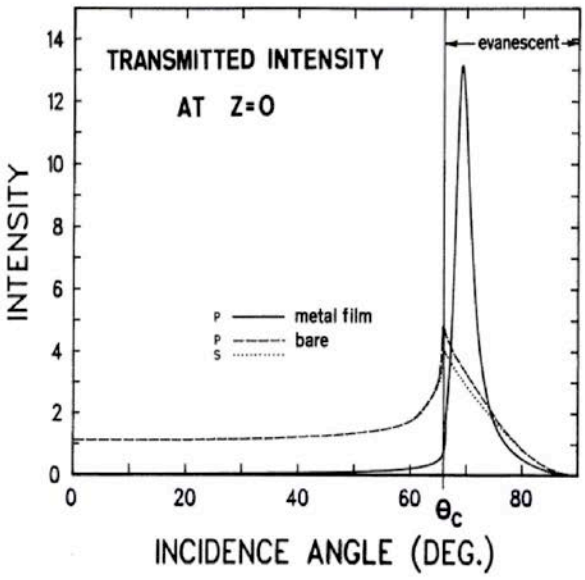

Figure 2.1.2.2 : Evanescent intensities *I p,s* at z=0 vs θ, assuming the incident intensities in the glass are set equal to unity. At angles θ > θc the transmitted light is evanescent; at anglesθ < θc, it is propagating. Both s- and p-polarizations are shown. Refractive indices n_3 =1.46 (fused silica) and n_1 =1.33 are assumed here, corresponding to θc =65.7°. Also shown is the evanescent intensity that would be obtained with a thin (20nm) aluminum film coating. Figure copied from D Axelrod. *Traffic.* 2 , 764-774 (2002).

To consider the implication of a multilayer system a theoretical 3 layer system is discussed briefly. The full consideration of the physics and mathematics of the implication has been reviewed by Axelrod (Axelrod *et al*., 1992).

For a three layer system with medium 3, refractive index n_3, medium 2, refractive index n_2 and medium 1 refractive index n_1, with light travelling from medium 3 to medium 1, several features have been noted. Qualitatively there is no particular change to TIR. The question of whether TIR occurs at the n_3:n_2 or the n_2:n_3 interface is interesting but appears to have little importance in qualitative studies. This is because, in practice, the n_2 layer is often very thin.

The evanescent wave profile in medium 1 will follow the characteristic exponential decay as given in the section 2.1.1. This will be the identical regardless of the refractive index (n_2) and thickness of the intermediate layer (medium 2). There will be a difference in depth of penetration as this is measured from the surface of medium 3. Figure 2.1.2.1 demonstrates the potential TIR points in a simple diagrammatic format. Further, it should be noted that irregularities of the intermediate layer could theoretically give rise to incident light scattering in all directions. There may be an advantage in placing a thin metal film as the intermediate layer, as this provides much greater intensity in a range from 10-200nm from the metal surface, as is used in plasma resonance spectroscopy. This is demonstrated in fig 2.1.2.2 (Axelrod, 2001). Potential advantages of a thin metal layer include not having to use a collimated incident light beam and the production of a highly polarised evanescent wave regardless of the purity of the incident polarisation. Specialised coverslips with thin metal films applied by the manufacturer are available commercially. A few of these where purchased to enable us to assess them for use. Unfortunately they were not suitable for cell culture work.

2.1.3 Optical configurations for TIRF with a microscope

A number of systems have been designed for TIRF microscopy (Axelrod *et al*., 1992; Oheim *et al*., 1999; Axelrod, 2001). These may use inverted or upright microscopes, with or without a prism. Each of these will be briefly discussed with more detail provided on the upright prism system that was in use in our laboratory. The excitation incident light source may be from a laser or from an epifluorescent lamp.

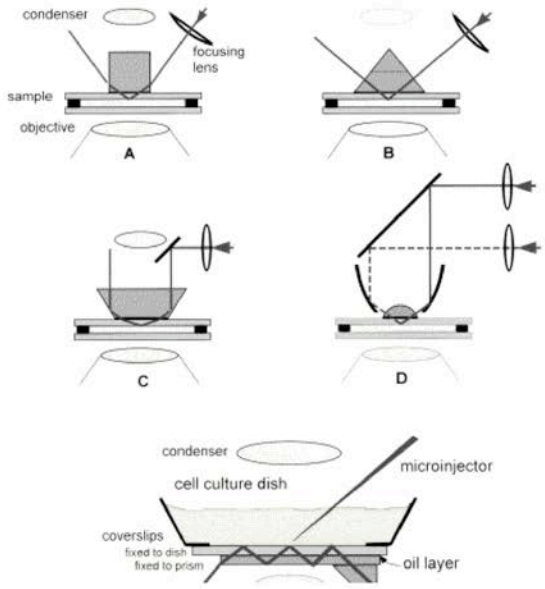

Figure 2.1.3.1 : Schematic drawings for prism-based TIR in an inverted microscope, all using a laser as a light source
The vertical distances are exaggerated for clarity. The first four configurations (A-D) use a TIR prism above the sample. In these configurations, the buffer-filled sample chamber consists of a lower bare glass coverslip , a spacer ring (made of 60-µm-thick Teflon or double-stick cellophane tape) and the cell coverslip inverted so the cells face down. The upper surface of the cell coverslip is put in optical contact with the prism lowered from above by a layer of immersion oil or glycerol. The lateral position of the prism is fixed but the sample can be translated while still maintaining optical contact. The lower coverslip can be oversized and the Teflon spacer can be cut with gaps so that solutions can be changed by capillary action with entrance and exit ports. Alternatively, commercially available solution-changing cell chambers (e.g. Sykes -Moore chamber from Bellco Glass Co. or rectangular cross-section microcapillary tubes from Wilmad Glass Co.) can be used. In configuration D, two incident beams split from the same laser intersect at the TIR surface, thereby setting up a striped interference pattern on the sample which is useful in studying surface diffusion (34). Configuration E places the prism below the sample and depends on multiple internal reflections in the substrate. This configuration thereby allows complete access to the sample from above for solutions changing and/or electrophysiology studies. However, only air or water immersion objectives may be used because oil at the substrate's lower surface will thwart the internal reflections. Figure copied from D Axelrod. *Traffic.* 2 , 764-774 (2002).

2.1.3.1 Inverted microscope with a prism

Fig 2.1.3.1 represents the basis of this design. The first four diagrams (A-D) show the prism above the sample. The prism was in optical contact with the coverslip or microscope slide. Optical contact was achieved with a drop of immersion oil or glycerol with refractive index equal to that of the prism glass and coverslip glass. The prism produces an incident light beam of greater than the critical angle, and hence TIR. Only

air or water lenses can be used with these systems, as oil immersion will prevent internal reflection because the refractive index of oil will not allow total reflection of the incident beam at the chosen incident angle.

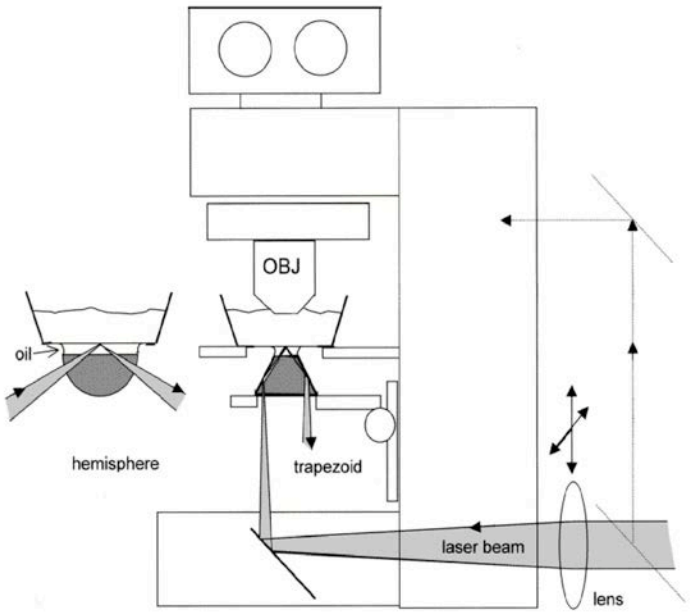

Figure 2.1.3.2.1 : TIRF for an upright microscope utilizing the integral optics in the microscope base and a trapezoidal prism on the condenser mount and movable up and down.
The position of the beam is adjustable by moving the external lens. An alternative hemispherical prism configuration for variable incidence angle is also indicated to the left. Vertical distances are exaggerated for clarity. An extra set of mirrors can be installed to deflect the beam into an -illumination light path (shown with dashed lines). Figure copied from D Axelrod. Traffic. 2 , 764-774 (2002).

2.1.3.2 Upright Microscope with a prism

This is a convenient and low cost way of setting up TIRF. Figure 2.1.3.2.1 demonstrates the instrument arrangement. A water immersion lens is used for biological experiments, while any lens that does not require oil immersion can be used in other applications. The water immersion lens can be immersed directly in the culture medium in which the cells are growing and provides high quality images.

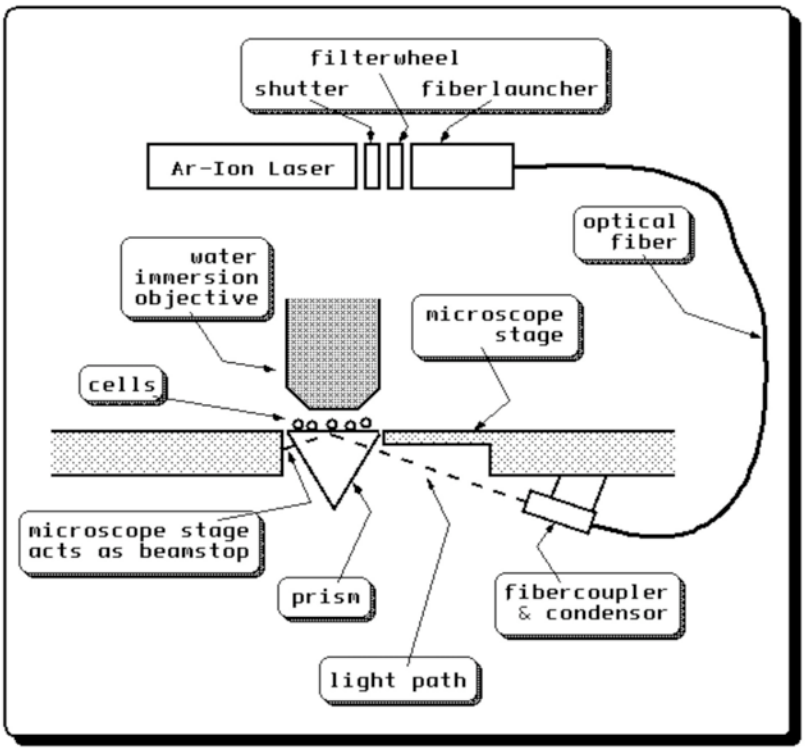

Fig 2.1.3.2.2 The Edinburgh TIRF Setup -- an implementation of the prism approach

The optical system is based around a Zeiss Axioskop upright microscope.The implementation of the system requires additionally an Ar-ion laser light source, shutter (here: Uniblitz), light guide, modified microscope stage, x-y stage for fine positioning of the laser beam in the prism , commercially available BK7 prism, and an intensified CCD camera. Ease of use, minimal implementation cost, and low cost of ownership were important design criteria. For example, the prism can be easily removed for cleaning, and the laser beam can be brought into the appropriate position without major difficulties. However, one major disadvantage of this approach is the use of an upright microscope which makes electrophysiological measurements difficult because of the limited accessibility to the culture dish for cell handling and environmental conditioning.

This is the system adapted for use in our laboratory. We retained the light microscope attachments and introduced the laser beam through an optic cable and holding device. The holding device allowed 2 dimensional (X-Y) movement of the laser beam, allowing accurate placing of the TIR area. The microscope also had an epifluorescent lamp attached to the rear of the microscope and a filter block allowing the insertion of specific light filters to allow different excitation wavelengths. A water immersion lens (Zeiss 63X NA 0.9) with working distance of 1.4mm allowed us to place micropipettes onto cells under imaging. A 70^{o} prism was placed in an engineered holder allowing some lateral (X- Y) movement above the condenser. This enabled us to produce a means of

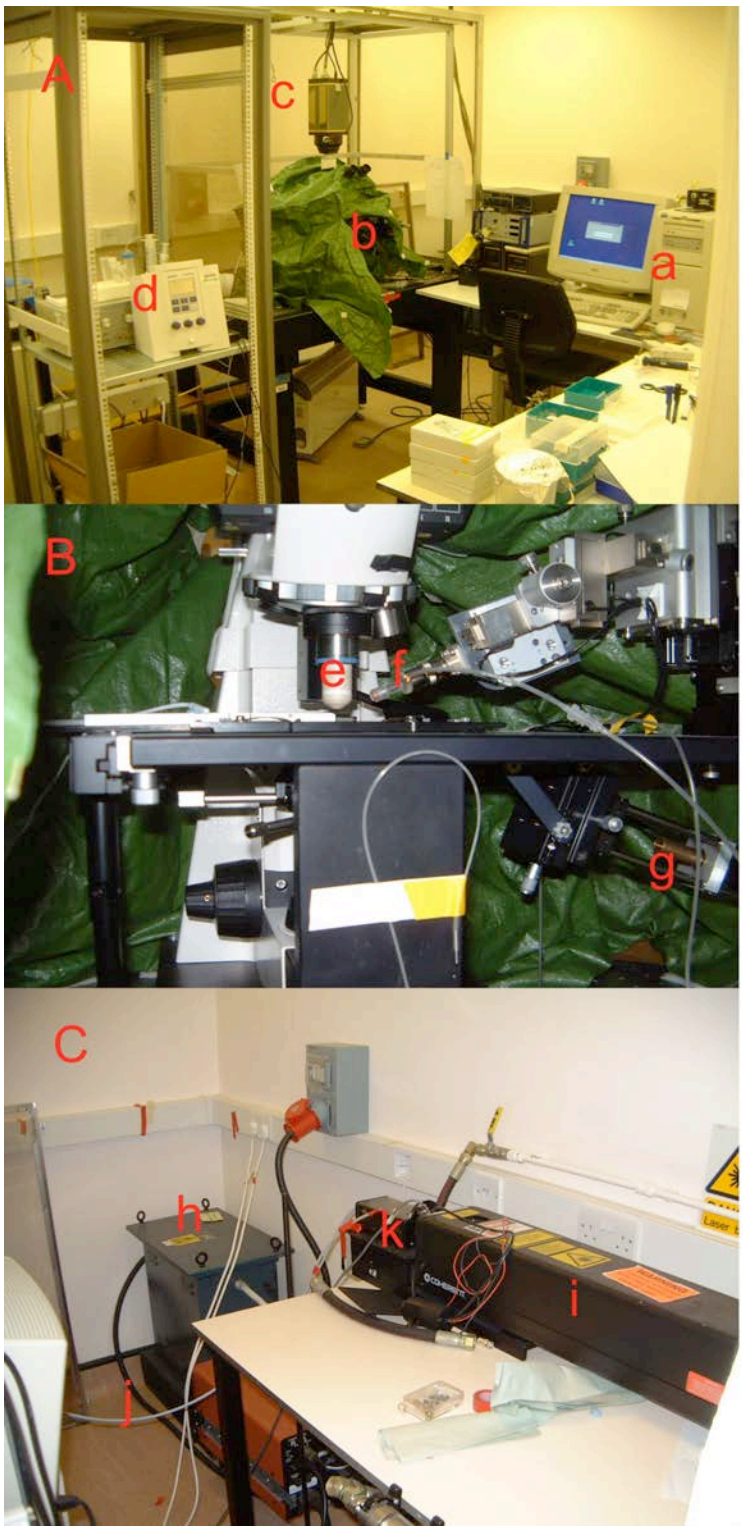

Figure 2.1.3.2.3 Photographs of the instruments used to configure the TIRFM in our Laboratory

A shows the workstation with the PC (a), the microscope (b), draped in green plastic, cooled CCD camera (c), injector equipment (d). The laser seen in **C** was behind the PC. The work bench was used for preparing pipettes and solutions for use in the experiments.

B is a close up of the microscope stage showing the water immersion lens(e), micro-pipette holder(f), laser beam holder and positioner (g) and tubing for the injector system. The green plastic background was in place to retain the heat that we pumped into the enclosed area to heat the whole stage to 30^{O}C. The prism holder is behind the vertical black piece of stage support.

C is a photograph of the laser equipment. The power supply and transformer (h) is on the floor and the tube(i) for the laser is on the bench.The fiber optic cable (j) for linking to the laser holder (g) runs from the shutter driver (k) at the end of the laser case.

holding 35mm cell culture dishes in place above the prism. We could then produce a small focussed area of TIR in the cell culture dish. The transmitted light fittings were retained on the microscope allowing us to select cells and manipulate them with pipettes. Figure 2.1.3.2.2 is an illustration demonstrating the configuration used in our TIRFM experiments. The microscope is an upright-style instrument. For routine non-fluorescence observation, a lamphouse is positioned below the microscope stage to enable visualization of specimens through conventional techniques. To the right of the microscopy body is an argon laser system. Control of the laser is achieved through mechanical units and an electronic shutter linked to the controlling computer, The laser is linked to the microscope stage through an optic fibre coupling. A cooled CCD camera (Pentemax, Princeton Instruments) is attached to the microscope allowing detection and digital image capture of the emitted light. Digital images collected by the camera are processed and analysed by an accompanying computer workstation with specialised imaging software from Universal Imaging Corporation. Figure 2.1.3.2.3 shows some photographs of the instruments in use in our laboratory.

2.1.3.3 Prismless TIR

TIR without a prism can be achieved by using an objective with high enough numerical aperture (NA). The incident beam must be constrained to pass through the periphery of the objective's pupil and must emerge with only a narrow spread of angles. This can be achieved with focussing the incident beam off-axis at the back focal plane. The further the beam is focussed off axis, the larger the angle of the beam emerging from the objective. The maximum possible angle of emergence θ_m is given by a formula containing the refractive index of the oil and NA.

$NA = n_{oil} - \sin\theta_m \ (n_3 \sin\theta_3)$ where 3 is the coverslip substrate.

For TIR to occur with an aqueous medium of refractive index n_1, θ_3 must be greater than the critical angle θ_c. Thus to view TIR in water the NA must be greater than the refractive index of water, i.e. > 1.33. This is achievable with the 1.4 NA lenses. However it is more difficult within a cell with n= 1.38 as TIR is just possible due to the

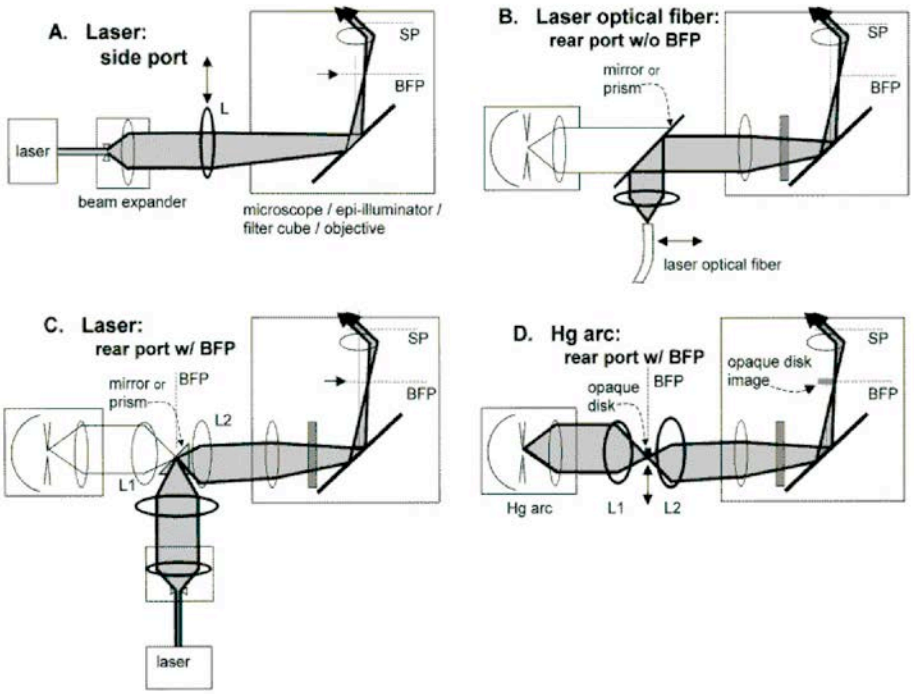

Figure 2.1.3.3: Four arrangements for prismless TIRF in an inverted microscope.
In all these configurations, SP refers to sample plane, and BFP refers to the objective's back focal plane or its equivalent planes (also called aperture planes). Components drawn with heavier lines need to be installed; components in lighter lines are possibly pre-existing in the standard microscope. (A) Laser illumination through a side port (requires a special dichroic mirror cube facing the side, available for the Olympus IX-70 microscope). The beam is focused at the back focal plane at a radial position sufficient to lead to supercritical angle propagation into the coverslip Moving the lens L transversely changes the angle of incidence at the sample and allows switching between subcritical (EPI) and supercritical (TIR) illumination. This is how Figure 1 was produced. (B) Laser illumination introduced by an optical fiber through the rear port normally used by the arc lamp, This scheme is employed by the commercial Olympus TIRF device. (C) Laser illumination in microscope systems containing an equivalent BFP in the rear path normally used by an arc lamp. The laser beam is focused at the BFP where the arc lamp would normally be imaged. The Zeiss Axiovert 200 provides this BFP, marked as an aperture plane. If (as in the Olympus IX-70) an aperture plane does not exist in the indicated position, it can be created with the pair of lens L1 and L2. (D) Arc lamp TIR illumination with no laser at all. The goal is to produce a sharp-edged shadow image of an opaque circular disk at the objective back focal plane such that only supercritical light passes through the objective. The actual physical opaque disk (ideally made of aluminized coating on glass) must be positioned at an equivalent upbeam BFP which, in Kohler illumination, also contains a real image of the arc. The Zeiss Axiovert provides this BFP, marked as an aperture plane. If (as in the Olympus IX-70) an aperture plane does not exist in the indicated position, it can be created with the pair of lens L1 and L2. The illumination at the back focal plane is a circular annulus; it is shown as a point on one side of the optical axis for pictorial clarity only. The through-the-lens arc-lamp TIRF configuration D can be switched easily to laser TIRF configuration C by insertion of the reflecting prism in the arc lamp light path. Figure copied from D Axelrod. Traffic. 2 , 764-774 (2002).

limitations to the angle of incidence and the refractive indices of the two media, giving a deeper penetration of the evanescent field. The deeper evanescent wave results in higher levels of scattered fluorescence propagation due to cellular organelles and other dense heterogeneity's in the layer of excitation. Higher NA objectives are now available and this is less of a problem than previously described. Fig 2.1.3.3 demonstrates the options for prismless TIR.

2.1.4 Advantages of TIRFM

At the time this project was being planned TIRFM has a number of distinct advantages over the two other methods described. Some of these advantages have been eroded with the subsequent improvement in the technology of the other two microscopy methods.

The first advantage was in the area of excitation. Laser scanning confocal microscopy excites a large area but only collects the image from the pinhole. This results in significant photobleaching and cell damage. Multiphoton and TIRFM excite much more specific areas of the cell resulting in less photobleaching and cell damage (Oheim, 2001).

The second advantage was in the speed of image acquisition. The TIRFM system used a cooled CCD camera that was capable of imaging at up to 200 Hz. These rates were not possible with either multiphoton or laser scanning confocal (~0.1-5Hz) imaging at the time. It was also noted above that the faster scan speed in laser scanning confocal microscopy results in more background noise (Toomre and Manstein, 2001).

The third advantage is in section thickness. TIRFM has a thinner plane of excitation (100nm) than the 500 – 800nm obtained in laser scanning confocal layers (Toomre and Manstein, 2001).

The final advantage was in the actual cost of the equipment. The TIRFM system was built in the laboratory at a reasonable cost whereas the laser scanning confocal equipment and multi-photon equipment were purpose-built commercial microscopes and could incur a significant cost.

2.2 Other Microscopy techniques

Confocal microscopy and multiphoton excitation enable observation of the details within cells by a process known as optical sectioning, without the artefacts that accompany specimen preparation by physical sectioning. We used confocal microscopy for related experiments to localise EGFP protein constructs. Due to slower acquisition times on the Leica laser scanning confocal microscope, the technique was not suitable for the planned experiments for exocytosis. Multiphoton excitation microscopy was not readily available at the onset of this study. However as we have considered its use in future experiments a description is included here.

When fluorescent specimens are imaged using a conventional wide-field optical microscope, secondary fluorescence emitted by the specimen that appears away from the region of interest often interferes with the resolution of the features that are in focus. This situation is especially problematic for specimens having a thickness greater than about 2 micrometers. The confocal imaging approach provides a marginal improvement in both axial and lateral resolution, but it is the ability of the instrument to exclude from the image the "out-of focus" flare that occurs in thick fluorescently labelled specimens, which has caused the recent popularity of the technique. Multiphoton imaging also has the ability to remove the out-of-focus flare (Oheim, 2001; White *et al*., 2001).

2.2.1 Laser scanning confocal microscopes

The laser scanning confocal microscopes employ a pair of pinhole apertures to limit the specimen focal plane to a confined volume approximately one micron in size. Relatively thick specimens can be imaged in successive volumes by acquiring a series of sections along the optical (z) axis of the microscope. The excitation laser scans the specimen and the emission light is filtered by a pinhole, whose aperture can be varied. Small pinholes afford the greatest resolution with the confocal microscope, while successively larger pinholes permit more of the fluorescence background noise to appear in the image.

Further, the scan speed can be adjusted. Increases in the scan speed result in a corresponding increase in the amount of background noise captured by the photomultipliers.

Figure 2.2.1 illustrates the confocal principle, as applied in epifluorescence microscopy, which has become the basic configuration of most modern confocal systems used for fluorescence imaging. Light passing through a pinhole is focussed by an objective lens at the desired focal plane in the specimen.

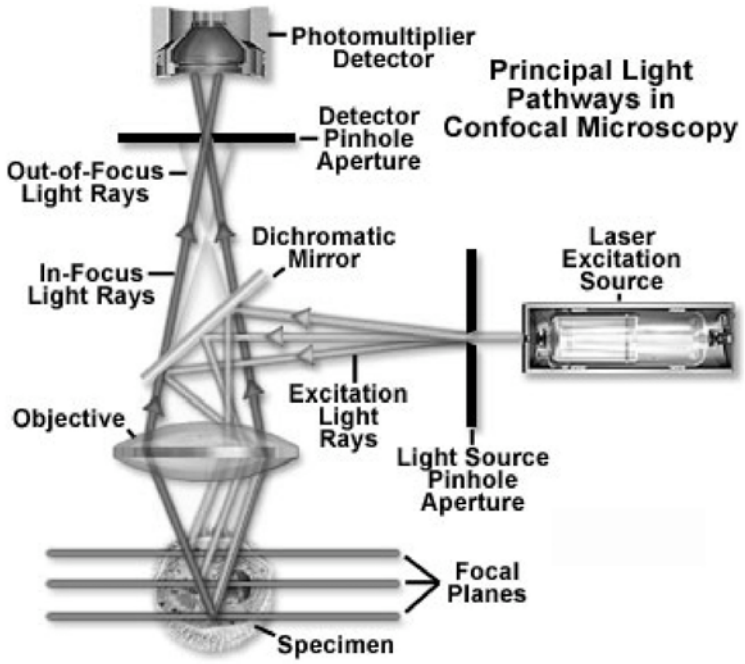

Fig 2.2.1 Basic principal of confocal microscopy, demonstrating laser light source, dichromatic mirror, the ability to move the laser spot to different planes within the sample, the detector pinhole and the photomulitiplier detector.

A second objective lens at a second pinhole with the same focus as the first pinhole (confocal) allowed the emitted fluorescence from the chosen focal plane to be collected in a low-noise photomulitiplier. The photomulitiplier generates a signal related to the brightness of the emitted light. The second pinhole prevents light from other planes reaching the photomultiplier.

Limitations of laser scanning confocal microscopes include:

1- the whole field is illuminated by the excitation light (in common with wide-field fluorescence microscopy).This results in a higher potential for photo-damage.

2- for individual vesicle imaging the depth of the confocal section is a trade off between time resolution and signal resulting in the inefficient use of excitation light leading to higher degree of photo-damage.

The laser scanning microscope continues to be widely used in cell biology imaging.

2.2.2 Multi photon microscopy

Two photon microscopy (TPM) is another method that allows optical sectioning. This is true optical sectioning in that only the plane of interest is excited. TPM is not limited to any particular plane but the plane remains thicker than in TIRFM.

The basic principles of multiphoton excitation are that at high photon densities, two photons can be simultaneously absorbed (mediated by a virtual state) by combining their energies to provoke the electronic transition of a fluorophore to the excited state. The energy of a photon is inversely proportional to its wavelength. Therefore the two photons should have wavelengths about twice that required for single-photon excitation. This means that longer wavelengths, extending into the infrared region, can be utilised to excite chromophores in a single quantum event, which subsequently emit secondary radiation at lower wavelengths.

High photon densities are necessary in multiphoton fluorescence to ensure a sufficient level of fluorophore excitation. Photon concentration must be approximately a million times that required for an equivalent number of single-photon absorptions. This is accomplished with high-power mode-locked pulsed lasers. Brief, but intense, pulses emitted by the laser increase the average two-photon absorption probability for a given fluorophore at a constant average incident laser power level. Minimizing the average excitation power level reduces the amount of single photon absorption. It is these events

that lead to a majority of the heating and some of the photo-damage that occurs during fluorescence experiments.

Excitation in multiphoton microscopy occurs only at the focal point of a diffraction-limited microscope. This provides the ability to optically section thick biological specimens in order to obtain three-dimensional resolution. Individual optical sections are acquired by raster scanning the specimen in the x-y plane, and a full three-dimensional image is composed by serially scanning the specimen at sequential z positions. The position of the focal point can be accurately determined and controlled by the software. For this reason multiphoton microscopy is useful for exciting fluorescence in selected regions inside the specimen. The highly localised excitation energy minimises photobleaching of the fluorophores and reduces photodamage of the cell. This allows for a longer duration of experiments when compared to laser scanning confocal microscopy. Higher excitation wavelengths permit deeper penetration into biological materials and reduce the high degree of light scattering that is observed at shorter wavelengths. The disadvantages of the multiphoton microscope include in-plane photobleaching and some photo-damage from single photons. The cost of these microscopes is a further disadvantage. For single-vesicle events the scanning nature of the excitation limits the suitability of the multi-photon microscope. However the possibility of using a localised wide-field approach may overcome this limitation.

3 Methods

3.1 Introduction to methods

The aim of the project was the development of an optical method of monitoring regulated exocytosis in a cell-free environment. The methods described required modification and adaptation over the time course of the project. Not all the possibilities had been considered at the beginning of the project and thus there were a number of methodological alterations during the first year. The descriptions in this text are of those methods in use at the end of the first year when I was still working full-time on the project.

The aim of the method development was to produce a cell-free environment for the study of regulated exocytosis using the total internal reflectance fluorescence microscope (TIRFM) as the analytical platform. For this I required a cell culture and specialised culture dishes for the TIRFM. Methods related to these requirements are: a primary cell culture; transfection of the cells with Semliki Forest Virus to enable transduction of cDNA encoding fluorescent constructs of secreted proteins; and the procedure for producing culture dishes and promoting cell adherence to glass. Procedures for operating the microscopes, data collection and processing will be described. Experimental methods for planned experiments will also be described.

Each method is described in this section with more detailed laboratory standard operating procedures (SOP) for specific methods included for reference purposes, as appendix B. Working COSHH forms for each of the main procedures are available in the laboratory.

3.2 Cell Culture

Primary cultures of bovine adrenal chromaffin cells have been used for many studies of regulated exocytosis. These are neuroendocrine cells that secrete adrenalin and noradrenalin as well as nucleotides and various proteins from large dense core vesicles

(LDCVs). The release process (exocytosis) can be studied at the single-cell level by amperometry, membrane capacitance measurements and microscopy.

3.2.1 Primary culture

Bovine adrenal chromaffin cells were prepared from adrenal glands freshly obtained from an abattoir. The collection was performed under the supervision of the health inspector at the abattoir and all regulations were adhered to. The adrenal glands were collected after the inspector had completed the health inspection of the offal. Excess connective tissue and fat was trimmed with dissecting scissors, taking care to protect the adrenal artery and vein. Once cleaned the gland was perfused with iced Locke's solution using a syringe and then placed in ice-cold Locke's solution and transported to the laboratory covered by ice. In the laboratory the glands were perfused again with Locke's solution until no blood returned from the blood vessels. The gland was then filled with digesting solution, Collagenase 0.25mg/ml (Worthington type 2) and DNAse 0.18mg/ml (Mannheim) in Locke's solution, and placed in a 37°C water bath for 5 minutes. This was repeated 4 times before the gland was bisected by careful dissection to remove the medullary portion .The medulla was placed in a petri dish containing a few millilitres of the digesting solution. Mechanical dispersion of the adrenal medulla was performed using scalpel blades and the dispersed tissue was placed in a sterile jar containing a stir bar. The jar was then placed in the 37°C water bath and stirred gently for 20 minutes. The larger remains of the dispersed and digested medullary tissue were removed from the solution using forceps. The remaining solution was aspirated into a syringe and then filtered through a 100 mm filter moistened (with digesting solution) into a 20 ml sterile centrifuge tube. The centrifuge tube was placed in the bench-top centrifuge and spun at 700 rpm for 5 minutes. The supernatant was removed using the aspirator pipette. The cell pellet was resuspended gently using 5 ml of culture medium, then a further 15 ml of culture medium was addedto bring the volume up to 20ml. The centrifugation and resuspension were repeated for a second time, and a cell count was carried out using a haemocytometer after the second resuspension with 5mls of culture medium. Calculations of cell numbers were then performed to allow an appropriate cell

concentration for the planned experiment. The cells were then reconstituted in the appropriate amount of culture medium. The dispersed cells were maintained in culture for up to 5 days in a variety of different culture chambers and glass coverslips in Dulbecco's modified Eagle's medium supplemented with 1% (v/v) 1x insulin/transferring/selenium supplement (ITS-X), 0.1% penicillin/streptomycin and 1% (w/v) sodium pyruvate (all from Gibco BRL Life Technologies) at 37°C in 95% air, 5% CO_2.

3.2.2 Infection protocol.

Approximately 1 x 10^6 freshly prepared chromaffin cells were plated onto the glass coverslips attached to the bespoke culture dishes (see later). After 24 hours of culture at 37°C in 95% air, 5% CO_2 the conditioned medium was removed and stored for later use. Virus stock was activated by the addition of chymotrypsin A4 (250mg/ml; Sigma-Aldrich) and digestion for 10 minutes on ice. Proteolysis was halted by the addition of aprotonin (0.67mg/ml; Sigma-Aldrich). A 1:10 dilution of the virus stock was made in the conditioned chromaffin cell medium, and approximately 1ml was overlaid onto the cells. The cells were incubated with the virus for 2 hours at 37°C in 95% air, 5% CO_2, then the medium was removed and replaced again with conditioned chromaffin cell medium.

Alternatively, the infection was carried out during the last reconstitution step of the primary culture process. In this instance conditioned medium was not available and the unconditioned medium was used. The cells were incubated with viral stock for 2 hours prior to final reconstitution and plating into the bespoke dishes or culture wells. The infected cells were cultured for specific times before experiments on the TIRFM or confocal microscope.

3.2.3 Modifications to primary culture

Modifications to the original cell culture specification included:

(1) Changes in the perfusion of the gland;

(2) Changes to the timing of the digestion steps;

(3) Modifications to the cell culture medium and;

(4) Alterations to the timing of the centrifugation steps.

The optimised cell culture method produced fairly consistent batches of cells that were used for the experiments described.

3.3 Bespoke Dish preparation

The use of an upright microscope and the requirement for a glass coverslip for TIRFM required the design and testing of bespoke dishes. See figure 3.3 for images of the different dishes used and a brief description of the characteristics.

The requirements for the dishes were:

- That they could be used for cell culture, allowing cells to live for up to 5 days.
- The dishes had to be sterilisable.
- That a 16-19 mm glass coverslip could be attached to a dish in a manner that allowed use of the microscope stage.

The microscope stage had been built to hold a 35mm Nunc plastic cell culture dish. The original dish design used these 35 mm cell culture dishes that had a 12-14 mm hole drilled through the centre of the base (fig 3.3 Ai-ii). The 19mm glass coverslip could then be attached with Silgard and the dishes were sterilised under UV light.

The first modification was engineered initially by Dr M Oheim, who was hoping to perform amperometry or capacitance measurements on cells at the same time as imaging with TIRFM. He produced a dish that was flat at the base and the body angled back from the opening where the coverslip could be placed. This design allowed for the use of pipettes under the upright microscope lens (fig 3.3 A iii-vi). The prototype dish was prepared in aluminium and the interaction between the aluminium surface and the physiological solutions for cell culture was found to be deleterious to good cell survival. For this reason plastic compounds were investigated. The first was a black vinyl

compound (polyvinyl chloride) that was rigid, allowing the engineering department to manufacture the dishes to the shape shown in figure 3.3 (A iii-vi), from 40mm diameter cylinders of black vinyl. These dishes performed well until they had been through the glass attachment and sterilising cycles a few times when it was noticed that the cells did not survive well. The next product tested was Teflon“ (tetrafluoroethylene); a white Teflon“ product was available in 40mm diameter cylinders. The dishes engineered from the Teflon“ cylinder produced excellent results with the cells but often became slightly misshapen during the heat-curing step for Silgard resulting in problems with the coverslip attachment and fitment to the microscope stage. The final product was engineered from aluminium and coated with black Teflon“ and these met all the requirements (figure 3.3 A vi). The black Teflon“ used to coat the aluminium dishes was available to the specialist-engineering firm for a pressurised spray coat application.

The test dishes were all engineered in the University of Edinburgh workshop under the care of John Lissimore and Peter Frew. The Teflon® coat was applied by a specialist engineering firm in Glasgow.

3.3.1 Preparation of Dishes for use on the microscope

The edge of the hole in the dish was lined with a thin layer of Silgard using an orange stick as the applicator. A coverslip was fixed evenly over the hole using Silgard as glue. The Silgard was allowed to cure overnight or cured in the 60^{o}C oven for 1 hour and then the glass was cleaned using an acid wash by soaking the dishes in a 0.1N sulphuric acid for 1 hour followed by an alkaline wash by soaking the dishes in 0.1N sodium hydroxide for 10 minutes and then rinsed with distilled water. The dishes were sterilised using 70% alcohol by soaking for 1 hour. The dishes were then rinsed in distilled water and collagen type I 0.4mg/ml (Sigma-Aldrich) was placed centrally on the glass and left to incubate at 37°C for 1 hour. The remaining solution was then aspirated off the coverslip and the coverslip rinsed with sterile filtered water and left to dry in a cupboard or drying oven as seen in figure 3.3.

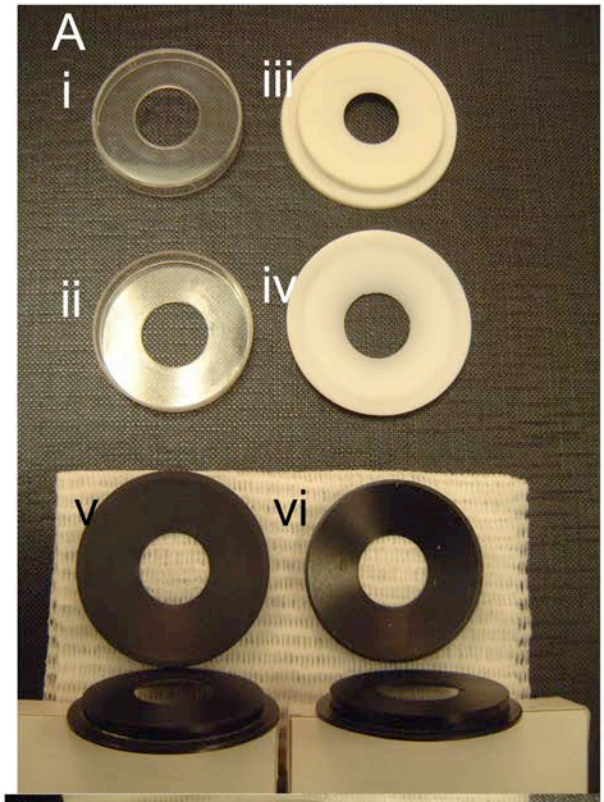

Figure 3.3.1 Photograph of the different dishes produced during the project. Ai and Aii are 35mm Nunc cell culture dishes with a 14 mm hole drilled in the base. Aiii and Aiv are the white Teflon® product, Av is the black vinyl dish and Avi the aluminium dish coated in black Teflon®. The inner aspect of dishes iii to vi is sloped to allow a pipette to gain access underneath the upright microscope. The dishes engineered from the cyclinders of material have a lip that allows insertion and removal of the dish from the 35mm diameter hole in the microscope stage.

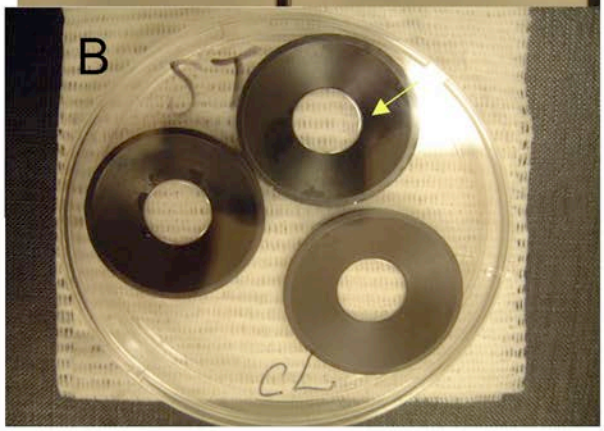

(B) demonstrates the dishes as prepared for use. The ST indicates sterile and CL that the dishes are treated with collegen IV. Usually a date of sterilization would also appear on the lid. The yellow arrow points at the line of silgaurd at the edge of the coverslip.

3.3.1.1 Other glass treatments

Flame sterilisation and cleaning

The coverslip was picked up and dipped into 70% alcohol and then passed through the flame of a Bunsen burner and placed into the culture well.

Protein treatment

Poly-L-Lysine 0.1mg/ml (Sigma-Aldrich), Collagen type IV 0.4mg/ml (Sigma Aldrich), Fibronectin 0.01mg/ml (Sigma Aldrich) and a 1:1 mixture of collagen type 1 and IV 0.4mg/ml were placed on the glass. 3ml of protein solution was placed centrally on the coverslip and left to incubate at 37°C for 1 hour. The remaining solution was then aspirated off the coverslip and the coverslip rinsed with sterile filtered water and left to dry as described above (Aplin and Hughes, 1981; Macklis *et al*., 1985).

Silane treatment

3-aminopropyltriethoxysilane (APTS) was placed on the cover-slips (one side) and then left for 4mins. The APTS was then removed and disposed of with copious water down the drain in fume hood. The coverslips were then washed carefully with distilled water. The coverslips then had 1% w/v glutaraldehyde (diluted in HBSS) placed on them to cover the area treated with APTS and then they were incubated at room temp for 30 minutes. A further washing step was then carried out by rinsing 3 times with HBSS prior to sterilizing the glass with 70% ethanol by soaking them for 1 hour and a final wash step with HBSS and filtered sterile water. The treated coverslips were then left to dry in a drying oven (Aplin and Hughes, 1981; Nobles and Abbott, 1996).

3.4 Microscopy

3.4.1 Cell Selection

The aim of this project was to create a cell membrane patch from which regulated exocytosis could be triggered. To make a patch of membrane it was important to choose living, healthy cells for the imaging experiments. Figure 3.4.1 demonstrates the appearance of healthy cells in transmitted light. The cell should adhere tightly to glass to allow rupture of the cell membrane and removal of the cell content. Tapping the side of the microscope stage gently can test the attachment to the glass; a little or no movement indicated attachment and large movements of the cell indicated poor attachment. The cell shape was another important aspect in evaluating firm attachment. The cells that appear flattened out, or spindle-shaped are usually the most firmly attached. The cell should appear healthy. This is subjective and difficult to describe, but involves looking at cytoplasmic features and the nucleus of the cell. I avoided cells that appeared to have a very granular appearance, as these cells were often apoptotic. A dense granular nucleus often indicated a dead cell. Under fluorescence microscopy, stained nuclear DNA indicates an unhealthy or dead cell. Fluorescence in transduced cells is not always an indicator of a good cell and the distribution of the fluorescence needs to be assessed. The images of transduced cells in figures 3.4.2 a and b demonstrate appropriate cells imaged on the confocal microscope.

3.4.2 Confocal microscopy

The use of the confocal microscope is described as it was used to establish co-localisation of the LDCV-associated fusion protein DOC2b EGFP with the secretory protein chromogranin A and later for similar experiments with pre-proANF EGFP. DOC2b is a vesicle membrane associated protein that we investigated and the initial paper was to demonstrate that DOC2b was co-localised to LysoTracker Red-stained

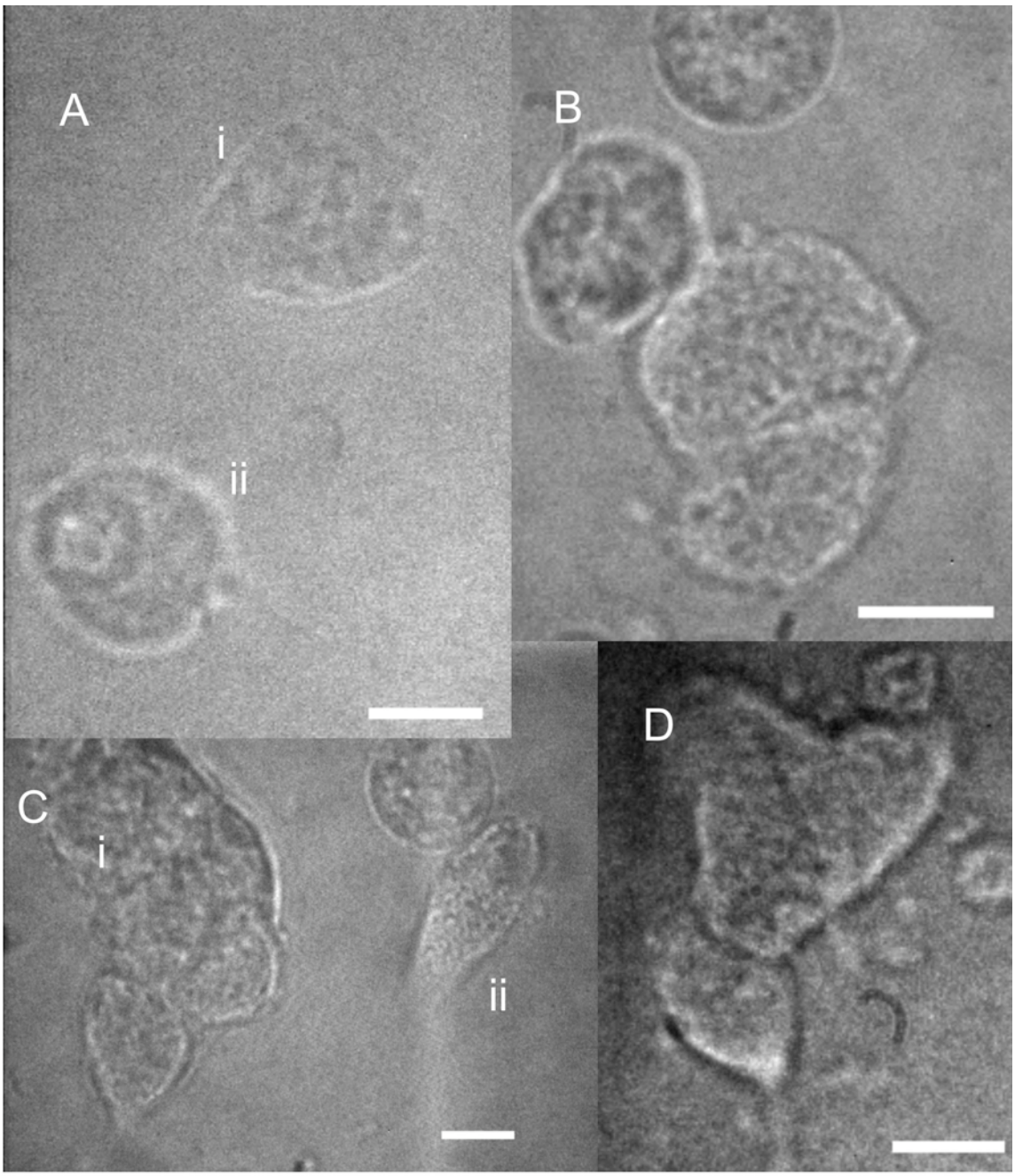

Figure 3.4.1 Images of cells as seen by transmitted light. These cells have been selected to demonstrate the cells chosen for TIRFM experiments. For electrophysiology other cell configurations would have been chosen. A demonstrates a cell (i) that is fairly well adhered to the cover slip and another that is dead (ii). B demonstrates two well adhered cells and two cells that are not adhered. C demonstrates a clump of cells (i) on the left with some well attached and another cell on the right (ii) that demonstrates the spindle appearance of a well attached cell. D demonstrates three cells well adhered to the cover slip and lying closely adjacent to one another. All scale bars are 10 μm in length.

vesicles in living cells and colocalised with chromogranin A in fixed cells (Duncan *et al*., 1999), preproANF is a protein that is directed to large dense core vesicles for exocytosis (Nguyen *et al*., 1988). c-DNA for preproANF EGFP was obtained from Dr E Levitan in Pittsburgh (Burke *et al*., 1997, Johns *et al*., 2001) and Dr R Duncan inserted the c-DNA into the Semliki Forest Virus vector. The preproANF-EGFP has been shown to co-localise to LysoTracker Red-stained vesicles in chromaffin cells (Greaves *et al*., 2002). I will include some of my own results for preproANF-EGFP and LysoTracker Red stained vesicles that have not been published using the analytical method used for the results presented previuosly (Duncan *et al*., 1999). The usefulness of preproANF-EGFP was investigated initially by myself but Dr I Matskevich performed the majority of the confocal studies as well as the TIRFM studies with the preproANF EGFP chromaffin cells. Later Ms J Greaves performed further confocal experiments.

The confocal microscope was run and managed by Ms L Wilson. Experimental planning and cell selection for the experiment were very important and Ms L Wilson performed the actual microscopy and image collection. For the purposes of localising the expressed protein, a single healthy chromaffin cell imaged with the 63X oil immersion lens and zoom 4X was ideal for demonstrating the required features. Another choice was a group of cells as this provided more information about the level of expression of the transfected c-DNA and for these localisation and expression experiments a zoom 2X was required on the confocal microscope settings. Cell selection was important, as there was no point in selecting cells that were not expressing the protein of interest in the expected way. Obviously this requires knowledge of where the particular protein should be distributed within the cell. Figure 3.4.2 demonstrates the appearance of DOC2b-EGFP (a) and preproANF-EGFP (b), both of which should localise to vesicles, preproANF-EGFP to the vesicle lumen as a packaged protein for exocytosis (Nguyen *et al*., 1988) and as shown in the paper by Duncan *et al* (Duncan *et al*., 1999) DOC2b-EGFP is cytoplasmic, but bound to the large dense core vesicles. Once the cell had been selected a scan was made through the cell to collect data on distribution of granules. We

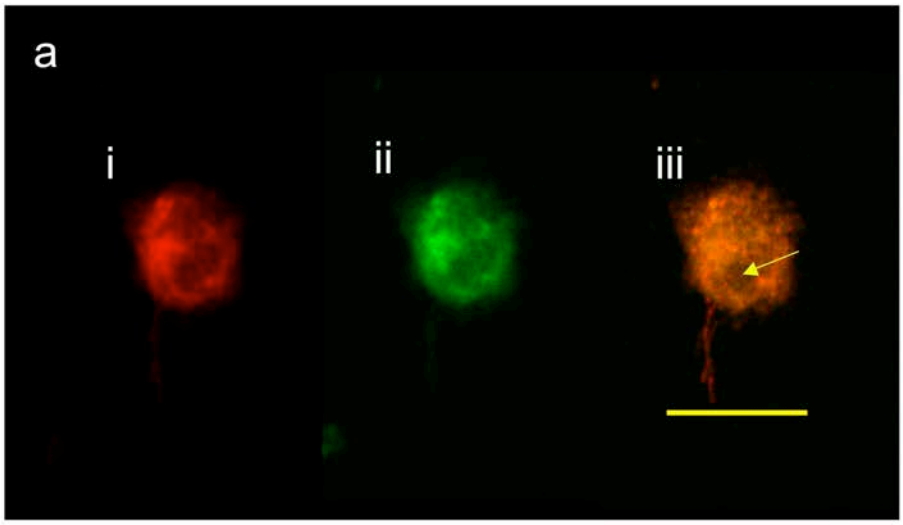

Figure 3.4.2.a Bovine Adrenal Chromaffin cell transfected with DOC2β EGFP(ii) and stained with lysotracker red(i).
The cell shows a punctate appearance , particularly on the overlay version(iii) and also demonstrates the nuclear sparing(arrow). Scale bar 10 μm.

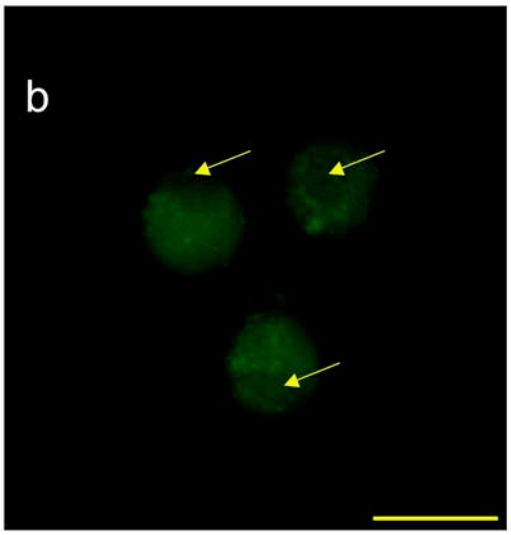

Figure 3.4.2.b Bovine Chromaffin Cells transfected with pre-proANF EGFP
All three cells demonstrate punctate expression of the expressed EGFP tagged protein. All three also have areas of nuclear sparing and have been imaged at slightly different levels hence the nuclear sparing is not as clear in the cell at the base of the image as it is the cell at the top. Scale bar is 10μm.

needed to produce 3D reconstruction models for the localisation experiments and so thin (500 nm) slices were standard.

Thereafter the procedure for experiments requiring the addition of a stimulatory medium was as follows:

- Select the plane with most visible granules of correct size for any experiments.

- Prepare the software for the fastest possible scans (or the appropriate time lapse)
- Decide on which cycle to use for adding medium for the chosen experiment.
- Begin the time lapse.
- Add the medium to the dish carefully so that the cell moves as little as possible.
- Save files as *.tif export files and an overall image of the fluorescent channel.

Analysis of the saved images was performed by selecting corresponding planes from the red and green channels. The planes were then overlaid and merged producing a new image. The areas that appeared yellow indicated compartments that had stained with both fluorescent markers. The numbers of red and green compartments were recorded along with the number of yellow. From this we calculated the total percentage of co-localisation. Another method of determining co-localisation is demonstrated in figure 4.4.1 (Duncan *et al*., 1999). This produced very similar results that are not shown in the thesis.

3.4.3 TIRFM

TIRFM was the method of choice for our experiments for the reasons described in section 2. The microscope was situated in a purpose-built room and the instructions for running it are included as an appendix to this thesis (Appendix A). As for confocal microscopy the choice of cell for experimentation was important, since for TIRFM the cells needed to be firmly adhering to give a good footprint visible in the 200nm layer of excitation. The TIRFM was not as robust as the confocal microscope and it often required fine adjustment to optimise performance. Figure 3.4.1 illustrates healthy-appearing cells for TIRFM as seen by light microscopy. A number of experimental procedures were planned for use and the description of these follows in section 3.6.

Data collection from the microscope was initially in the form of large image files, collected for each time point in an experiment. Good file management is essential for managing the image data collection and a data file system was set up before collecting images. It was useful to allocate a specific directory for collecting series of images as this facilitated the running of journals (macros) within the Metamorph‘ (Universal Imaging Corporation) software package that was used for camera control, image collection and processing. It was a very versatile package and extremely good for imaging.

3.5 Analysis of Images

Metamorph‘ software was used to analyse the images for single vesicles. When patches of cell membrane had been produced the number of vesicles present docked on the cell membrane was generally not high and this permitted analysis without the aid of image de-convolution. Most of the data presented here were taken from vesicles that could easily be identified without the aid of a de-convolution algorithm. In whole cells there were many more vesicles present and the use of de-convolution was required. To define a suitable algorithm fluorescent latex beads of diameter of 200nm (similar in size to large dense core vesicles) were used, to construct a de-convolution algorithm using the Metamorph‘ software. Figure 3.5.1 shows an image of 200nm beads before and after running the de-convolution algorithm. The method used to produce the data presented in the thesis was based on work done by a colleague, Dr U Wiegand (Wiegand *et al.*, 2002). I had attempted a number of different

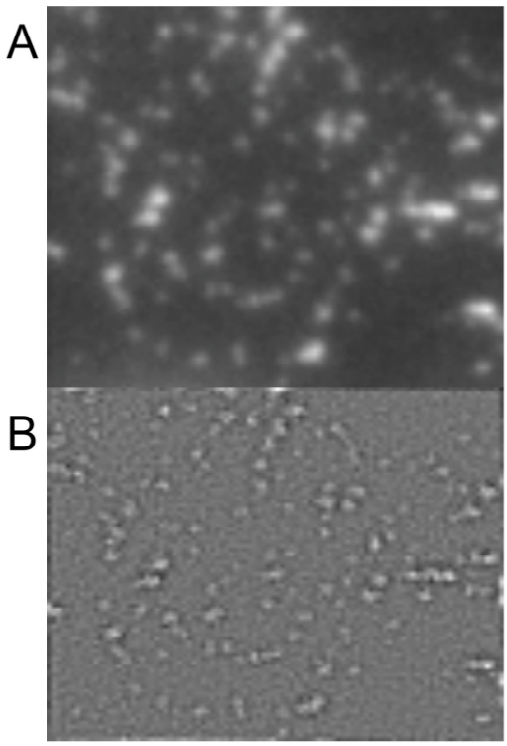

Figure 3.5.1 200nm beads before and after the de-convolution algorithm.
A is the raw image of 200nm beads with TIRFM and B is the image following the de-convolution process. If there are many possible areas of vesicle then this process is able to assist in distinguishing between two nearby but distinct objects.

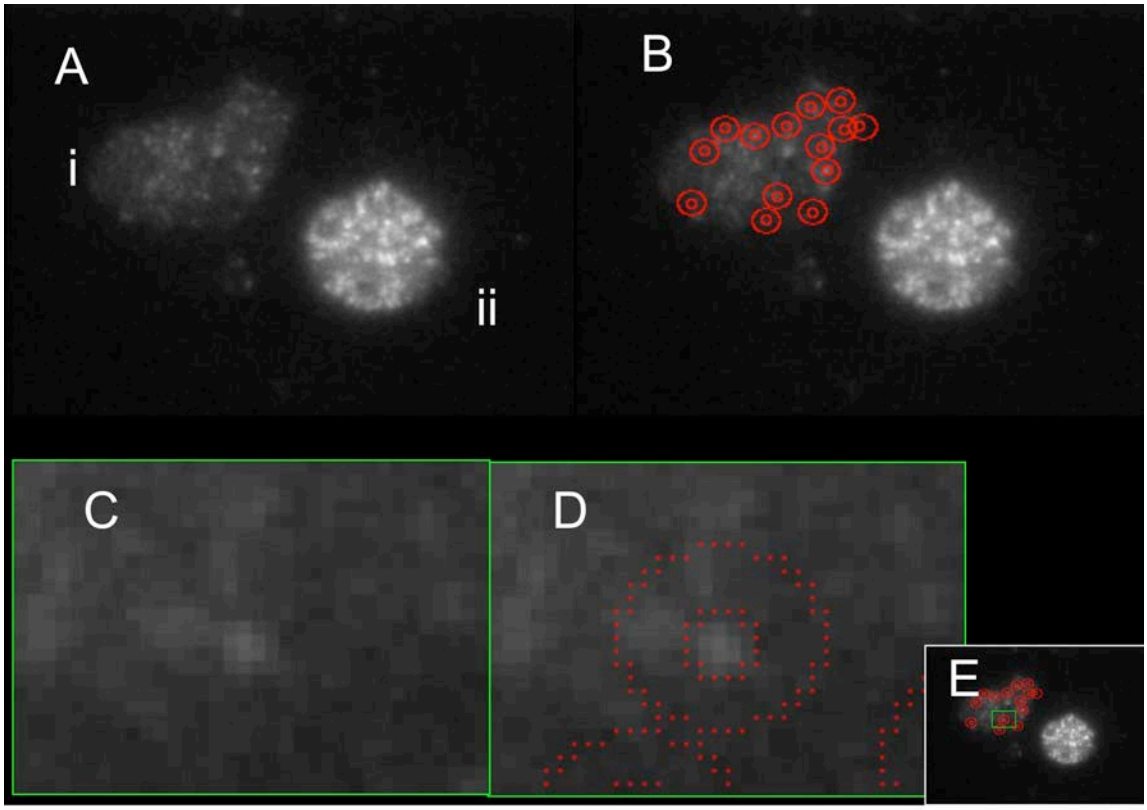

Figure 3.5.2 Description of the analytical steps for exocytosis
A) Demonstrates two cells, i) is a well adhered cell and ii) is less well adhered, i) was ruptured by a jet of fluid and what is visible is a large membrane patch. B) Demonstrates the vesicles chosen for analysis on this patch. C and D demonstrate in more detail the area highlighted in green in E. The two red circles on D are the two areas used for the calculation of average intensity. The inner circle surrounds the vesicle and the outer a larger area of cell membrane etc.

methods of assessing vesicle exocytosis on the membrane patches but none was as successful as that adapted from Dr U Wiegand. The technique is described in figure 3.5.2 which demonstrates the concepts behind the method. The published method was based on a higher frequency of imaging resulting in the ability to detect a “flash” of exocytosis. My images had been collected at a lower frequency and had been averaged to produce a clearer image. This made the exact analysis performed by Dr Wiegand difficult to apply. I used a similar technique that demonstrated a clear drop in intensity difference when a vesicle disappeared. This used two regions of different size, the first being 7 X 7 pixels, covering the vesicle itself, and the second 16 X 16 pixels that included the vesicle and a wider surrounding area. Metamorph‘ calculated the average

intensity for each area and the difference between the two average intensities was calculated in Microsoft Excel. The difference of intensity was then plotted against decimal time to achieve a standardised time course. Decimal time is a conversion of time units from the standard time to metric units. This produced a standardised axis for plotting the time course data. Experiments in which Ca^{2+} was added to the Ca^{2+}-buffered medium had the time of Ca^{2+} addition recorded as time zero. With this method each vesicle was viewed graphically as reported in the results.

3.6 Experimental Procedures

3.6.1 Cell adherence to glass coverslips

The aim of this experiment was to determine the best means of attaching the cell to the glass so as to leave behind a membrane patch following rupture of the cell.

To allow good cell health and attachment it was important to clean any debris from the glass. The use of flamed glass is well established for patch clamp experiments and acid-cleaned glass is well described. As we needed to have a method that we could use for a coverslip attached to a plastic dish, we wanted to investigate the acid washing methods to ensure that the acid cleaned glass was as good for cell health as flame-cleaned glass.

The second part of this experiment was to determine the ability of cells to adhere tightly to the glass surface. The experimental design was to prepare coverslips with different coatings and to then subjectively examine cell health and adherence of the cell to the coverslip. The methods have been described in section

Initially cell health and adhesion were investigated by:-

(1) Comparing acid-washed glass with alcohol (Saltzman *et al.*, 1991) and flamed glass as means of cleaning glass cover-slips.

(2) Comparing the four protein products used elsewhere (poly-L-lysine, fibronectin, collagen types I and IV) (Macklis *et al.*, 1985; Aplin and Hughes, 1981) on glass coverslips placed in 12-well cell culture chambers.

(3) Experimenting with silane treated glass (Nobles and Abbott, 1996).

(4) Subsequently cell adherence was investigated with the rupturing technique using the acid-washed glass treated with protein.

3.6.2 Measuring exocytosis by TIRFM

The aim of this experiment was to measure exocytotic events by use of TIRFM and to establish the how long after cell culture we could still achieve exocytosis.

Cells plated on glass coverslips in the bespoke dishes were investigated on days 2-4 after culturing. A single cell was chosen in each dish following the criteria outlined above. Once the cell had been imaged by light microscopy, it was imaged by TIRFM to check that individual vesicles could be seen in the evanescent field. The cell was then stimulated by addition of a K^+-containing solution to allow exocytosis. Potassium ion at a concentration of around 60mM depolarises bovine adrenal chromaffin cells resulting in regulated exocytosis. We planned to measure "flashes" of exocytosis as described by Steyer and colleagues (Steyer and Almers, 1999) for these experiments indicating the presence of regulated exocytosis.

3.6.2.1 Basic stimulation experiment

A bespoke dish of cells was removed from the incubator and stained with one of the following acidophilic dyes: Acridine Orange (2 mmol/L) use 10㎖ per 2ml of culture medium; LysoTracker Red™(40 nM) use 20㎖ per 2ml of culture medium; LysoSensor Green™ (40 nM) use 20㎖ per 2ml of culture medium. The cells were then incubated with the dye for 20 minutes. The bespoke dish was removed from incubator and the culture medium with dye was aspirated, the cells were washed twice with HBSS warmed to 37^{o}C and the culture medium was replaced with 500 ㎖ external solution (KCl 2.8mM, NaCl 140mM, $CaCl_2$ 2mM, Mg Cl_2 0.2mM, HEPES NaOH10mM and glucose 10mM) warmed to 37^{o}C. The bespoke dish was carefully transported to the TIRFM laboratory and placed in the holder on the microscope stage. A cell was selected under transmitted light and imaged with TIRFM. If the cell was suitable then the imaging

sequence was selected and the cell stimulated by adding 500 ml of excitation solution (KCl 60mM, NaCl 82,8mM, $CaCl_2$ 2mM, Mg Cl_2 0.2mM, HEPES NaOH 10mM and glucose 10mM) with a micro-pipette at the correct time in the sequence. Images were collected for the required period of time for the experiment. Exocytosis was expected to occur within 2 minutes of the addition of the excitation medium. The data stack was saved.

3.6.3 Preparing the membrane patch and monitoring release of the docked vesicles

The aim of this procedure is to produce a piece of membrane from a single cell that remains attached firmly to the glass coverslip after removal of the opposing (upper) cell membrane and most of the cell contents. These patches should theoretically still have docked large dense core vesicles attached to them that could be released under the correct stimulation. This method required development, as it had not been described before in mammalian cells. Most methods of preparing cell membranes rely on membranes produced from the rupture of a population of cells (Vacquier, 1975; Crabb and Jackson, 1985; MacLean and Edwardson, 1992; Martin and Kowalchyk, 1997) and these ideas were adapted for single adrenal chromaffin cells. The measure of exocytosis was originally taken to be the "flash" of dye being released from the vesicle but because of difficulty in capturing images of flashes, we ended up using the loss of fluorescence intensity (section 3.5) as a substitute (Steyer and Almers, 1999).

3.6.3.1 Basic membrane patch preparation

A bespoke dish of cells was removed from the incubator and stained with Acridine Orange (2 mmol/L) and incubated for 20 minutes. The bespoke dish was removed from incubator and the culture medium with dye was aspirated, the cells were washed twice with HBSS warmed to 37^{o}C and the culture medium was replaced with 500 ml modified internal solution (L- glutamic acid 145mM, NaCl 8mM, Mg Cl_2 1mM, MgATP 4mM, HEPES NaOH 10mM, EGTA 1mM, GTP 0.3mM and glucose 10mM) warmed to 37^{o}C. The rupturing pipette was prepared, placed in the holder and flushed through with

internal solution without MgATP or GTP. The bespoke dish was carefully transported to the TIRFM laboratory and placed in the holder on the microscope stage. A cell was selected under transmitted light and imaged with TIRFM. The rupturing pipette was placed over the cell and the cell was broken open by using the jet of internal fluid and the cell contents were washed away, leaving behind a patch of membrane adhering to the glass surface. The imaging sequence was started and recorded. Stimulation of exocytosis was produced by adding 10 ml 1M Ca^{2+} with a micropipette to overcome the EGTA 1mM at the chosen time point.

3.6.4 Other planned experiments

The grant proposal to the Wellcome Trust mentioned further experiments using Clostridial neurotoxins to block exocytosis, addition of prepared large dense core vesicles to the area above the membrane and the manipulation of certain cytosolic proteins with addition of cloned proteins of interest. None of these were performed due to the technical difficulties with the procedure, which made the method unreliable. This will be discussed in detail in the discussion chapter.

4 Results

The aim of the experiment was to produce a patch of cell membrane that remains closely adhered to the glass coverslip after rupture allowing imaging with TIRFM. Following this demonstration of exocytosis of the LDCV's still attached to the membrane by Ca^{2+} stimulation was to be demonstrated by a flash of extruding dye. Parallel experiments on the confocal microscope are also shown.

Sections 4.1, 4.2 and 4.3 review the results of the basic experiments performed prior to the membrane patch experiments. The two methods for cleaning the glass are compared in 4.1 by looking at the cell health both subjectively and by capacitance. Section 4.2 compares the subjective results from the different protein substrates used to assist the cells adherence to the glass. The results of confocal experiments are given in 4.4 and the results of the membrane patch experiments in 4.5.

4.1 Cell adherence and health under different conditions.

The two conditions investigated were acid-washed coverslips compared to flame-cleaned coverslips. The flame-cleaned coverslips are used routinely in electophysiological techniques and these were taken as the standard against which the acid washed glass was compared. The requirement for tightly adhering cells for the rupturing procedure meant that these experiments had to be carried out prior to any microscope-based experiments.

The findings suggested that there was a slight improvement in cell attachment with the acid-washed glass compared to the flame-cleaned glass. Capacitance measurements performed on these cells showed no significant differences in the responses of cells on the two different types of coverslip. *(Personal communication Dr S Tapechum)* As the adherence and health are subjective findings actual results have not been reported, what was important is that there was no obvious disadvantage presented by the use of acid-washed glass when compared to flame-cleaned glass.

4.2 Comparison of different protein substrates.

The results are reported in table 4.2.1. The results demonstrated that all the protein substrates improve cell adherence compared with cleaned, untreated glass. There was a slight preference for collagen type I from the results in table 4.2.1. Table 4.2.2 reports the subjective appearance for health of the cells. From this table it becomes clear that the

Table 4.2.1 Adherence experiments with Bovine Chromaffin cells with different protein substrates

Protein	Day 1	N	Day 2	N	Day 3	N
Control	90%	21	88%	21	86%	7
Poly-L-lysine	95%	21	94%	21	80%	7
Fibronectin	81%	21	92%	21	93%	7
Collagen type I	88%	17	95%	13	98%	3
Collagen type IV	95%	17	87%	13	98%	3
Collagen types I & IV	95%	8	95%	8		

N is the number of coverslips. The percentage adherence is a subjective opinion based on observation under a microscope. The number of attached cells was estimated by tapping the side of the chamber.

advantage of collagen type I was the interesting finding in that it did not promote fibroblast growth as much as did collagen type IV or fibronectin. This was an important finding as the chromaffin cells, when well adhered, may appear similar to fibroblasts

Table 4.2.2 Subjective Health of Cells (N=60 coverslips)

Protein	Day 1	Day 2	Day 3
Control	good	good	poor
Poly-L-lysine	poor	poor	poor
Fibronectin	good	good, but fibroblast proliferation	good, but fibroblast proliferation
Collagen type I	good	good	good
Collagen type IV	good	good, but fibroblast proliferation	good, but fibroblast proliferation
Collagen types I & IV	good	good, but fibroblast proliferation	good, but fibroblast proliferation

under light microscopy. Chromaffin cells have not been reported to proliferate under cell culture conditions whereas fibroblasts are well known to proliferate in chromaffin cell primary preparations.

Table 4.2.3 Percentage of cells ruptured with membrane patch adhered to the glass with the different protein substrates.

Protein	Day 2	N	Day 3	N
Control	None	5	None	5
Fibronectin	None	5	None	5
Collagen type I	80%	5	80%	5
Collagen type IV	60%	5	40%	5
Collagen types I & IV	None	5	None	5

N is the number of cells used in the rupturing experiment.

The use of silane to treat glass prior to treatment with proteins was not very successful. All the coverslips (control and protein treated) demonstrated poor cell survival on the three occasions that this was attempted.

The final part of this experiment was to compare the adherence under rupturing conditions. Only fibronectin and collagen treatments (type I, type IV and a mixture of type I and type IV) were used for this part of the experiment. 5 cells were chosen from each preparation for the rupturing experiment. The results shown in table 4.2.3 indicated that the use of collagen type I alone was the most suitable preparation for good cell health and adherence under the rupturing technique chosen.

4.3 Exocytosis experiments in whole cells

These were some of the earlier experiments carried out and as I was still learning the technique the results are rather poor and have not been presented. However, this line of experimentation was also undertaken by another member of the research group, Dr I Matskevich, who performed a much larger number of TIRFM experiments on whole cells, in parallel to my membrane patch experiments. These cells came from the same primary cultures and the results demonstrated that our cell preparation was suitable to

demonstrate exocytosis as published by others (Steyer, *et al*. 1997). A total of 28 cells are recorded, 25 of these underwent exocytosis as measured by a flashes of exocytosis on TIRFM. The video file 43 on the CD-ROM included with the thesis demonstrates the flashes of exocytosis that were seen. The cells were transfected at primary culture and experiments were done at 48, 72 and 96 hours. Both acridine orange and pre-proANF-EGFP were used as vesicle markers. There was a lead-in period during which Dr I Matskevich was becoming familiar with the experimental technique and when the results were unreliable, and this period of time coincided with the time when I was performing the bulk of my experiments. As the technique improved better results were obtained.

The next section covers the parallel experiments performed by myself on the confocal microscope.

4.4 Confocal experiments with DOC2b-EGFP and preproANF-EGFP

Confocal microscopy was performed with whole cells that were handled in the same manner as those for the TIRFM experiments. Table 4.4.1 demonstrates the results from a few cells transfected with DOC2b-EGFP cDNA. The results show that 98% of the DOC2b-EGFP labelled structures were also labelled by LysoTracker Red. This indicated that DOC2b is a vesicle-associated protein (Duncan *et al*., 1999). These results also confirmed the usefulness of the Semliki Forest Virus vector (Duncan *et al*., 1999).

Table 4.4.1 DOC2β-EGFP expressed in Bovine Chromaffin cells labelled with LysoTracker Red and imaged with a confocal laser scanning microscope (Leica)

Cell	Green vesicles	Red vesicles	Overlay
fA	17	20	17
d	19	22	18
fB	9	9	9
Total	**45**	**51**	**44**

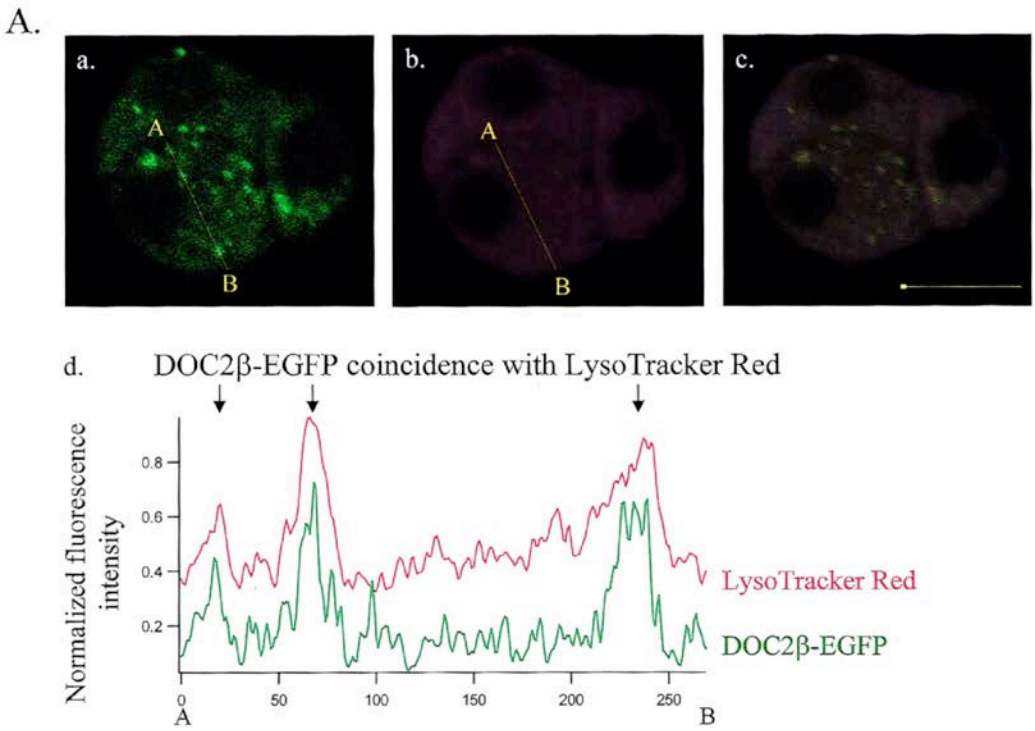

Figure 4.4.1 Confocal microscopy of DOC2β-EGFP-expressing chromaffin cells

(A) High-power confocal images of a group of three DOC2β-EGFP 2–expressing chromaffin cells 48 h post-infection. A single 1 μm-thick confocal optical section, illuminated at 488 nm and 577nm, was used to produce these images. (a) The EGFP fluorescence is seen distributed throughout the chromaffin cell in punctate distribution with nuclear sparing, reminiscent of vesicular localisation. This coincides with the distribution of LysoTracker Red in the same cell (b), which also shows a punctate distribution with nuclear sparing. (c) Superimposition of the two images revealed the fluorescent spots to be overlapping as indicated by yellow. A yellow line AB shown on (a) and (b), was measured for fluorescence intensity. (d) Shows the normalized intensity under the line proceeding in arbitrary distance units from point A to point B. Similar vertical lines were drawn through 55 vesicular areas in 5 cells. DOC2β-EGFP peaks were coincident with LysoTracker Red peaks in 98% of vesicles. Conversely LysoTracker Red peaks were coincident with DOC2β-EGFP peaks in 76% of vesicles. The arrows mark peaks that are representative of vesicular fluorescence. Scale bar: 10 μm with bold inset (yellow square on left hand edge of scale bar in panel c: 0.39 μm) representing the approximate size of a large dense core vesicle.
(Copied from Figure 2 A from Duncan RR, AC Don-Wauchope etal 1999)

The figure published in Duncan *et al*. (1999) is reprinted as Figure 4.4.1 and this illustrates a group of cells and the technique used to evaluate co-localisation of the two fluorescent markers.

Table 4.4.2 preproANF-EGFP expressed in Bovine Chromaffin cells labelled with LysoTracker Red and imaged with a confocal laser scanning microscope (Leica)

Cell	Green vesicles	Red vesicles	Overlay
c8	16	20	16
c2a	21	35	21
c6	8	11	8
c 5a	7	20	7
c5b	16	20	16
c5c	1	8	1
c5d	13	22	13
c2b	19	20	19
Total	**101**	**156**	**101**

The preproANF-EGFP experiments were imaged by the same method and analysed in a similar way. Table 4.4.2 shows the results from a number of cells. These are consistent with preproANF-EGFP being a vesicle-packaged 'cargo' protein as all the green areas co-localise with LysoTracker Red and have a very punctate appearance. There is a 100% co-localisation of preproANF-EGFP with LysoTracker Red while not every LysoTracker Red labelled structure appears in the green channel. This is because vesicles containing preproANF-EGFP are young ones, assembled after transfection of the cells, whereas LysoTracker red labels the entire population of LDCVs, irrespective of age; furthermore this acidophilic dye also labels other subcellular compoents with acidic lumens, such as lysosomes and endosomes. The experiments reported here have not been reported previously but similar results were published by another member of the research group, Ms J Greaves (Greaves *et al*., 2002). The purpose of these experiments was to confirm that virally-transfected cells expressing preproANF-EGFP were healthy and that the fluorescent marker could be detected. All of the cells investigated showed some degree of expression of the fluorescent marker indicating that there was a high efficiency of transfection. The relatively small number of vesicles labelled with preproANF-EGFP was an important finding, as this would allow easier monitoring of the movement and function of the tagged vesicle (Duncan *et al*., 2003).

These experiments led on to the confidence to start producing membrane patches with labelled vesicles. These results are presented in the next section.

4.5 Exocytosis from membrane patches

Table 4.5.1 provides a summary of the successful experiments on membrane patches. A summary of the TIRFM experiments is shown in Table 4.5.2. Acridine Orange was used most often as the fluorescent marker of the vesicle lumen and more detail of the success and failure of these experiments is provided in Table 4.5.3. A total of 179 cells were examined with only 42 producing a successful result. These included 19 cells that were ruptured for the membrane patch validation experiments as shown in table 4.5.1. The other successful rupturing experiments included observation of the membrane patch without collecting data and membrane patches where it was impossible to follow vesicles throughout the image stack because of movement of the coverslip during the procedure. The initial whole-cell imaging where the successful outcome was seeing vesicles with TIRF, imaging of cells transfected with DOC2b-EGFP to look for evidence of transfection and a number of other once one-off experiments were listed as successful in tables 4.5.2 and 4.5.3. The other 137 cells did not appear to secrete or were not stimulated, for reasons that are unknown but that presumably reflect uncontrolled parameters in the experimental process. This high failure rate of 77% is discussed in section 5. The experimental failure rate in the rupturing experiments was slightly higher at 80% and since rupturing required physical shearing of the cells, this was not an unexpected finding. The reasons for experimental failure are not always clear-cut. For example the cells that do not demonstrate exocytosis may be of poor quality from the primary culture, may not adequately demonstrate TIRFM either before or after the addition of the stimulating medium because of poor adhesion, the medium may be added incorrectly or the collection and processing of the images to report exocytosis may be inadequate. The categorization in table 4.5.3 is based on the comments entered in the laboratory book. Due to the high failure rate both in my experiments and subsequently in those of Dr U Wiegand (data not shown) the more interesting further experiments, to examine molecular interaction at the cell membrane, were not undertaken.

Table 4.5.1 Exocytosis From Membrane Patch Experiment Data

date	cell number	Number of Vesicles analysed	Vesicles that undergo "exocytosis"
Calcium added		**77**	**11**
17/8/99	2	6	4
16/10/99	4	8	0
17/8/99	3	13	3
18/8/99	7	8	2
20/8/99	1	5	0
24/8/99	3	6	2
7/11/00	2	4	0
28/11/00	1	4	0
20/2/01	1	5	0
9/5/01	1	5	0
9/5/01	2	4	0
7/6/01	1	5	0
7/6/01	2	4	0
Calcium free		**40**	**1**
6/10/99	1	12	1
18/8/99	1	7	0
19/8/99	1	10	0
24/8/99	1	4	0
29/8/99	1	3	0
24/4/01	1	4	0

Table 4.5.2 Summary of all TIRFM Experiments

	AO	LSG	DOC2β	ANF
total	**179**	**15**	**9**	**19**
observed	19	5	7	8
exocytosis	4		2	11
rupturing	156	10	nil	nil

This table includes all experiments and categorises them into experiment type an vesicle tagging method: Acridine Orange (AO); LysoSensor Green (LSG); DOC2β-EGFP (DOC2β) and preproANF-EGFP (ANF).

Table 4.5.3 Experimental success in the Arcidine Orange group

			Reason for Failure				
	Successful	Failed	Cell Culture Problems	Adherence and Rupturing Failure	TIRFM and Associated Equipment Failure	Optical and software failure	Solution error
total	**42**	**137**	**34**	**27**	**50**	**21**	**5**
observed	10	9			7	2	
exocytosis	1	3					3
rupturing	31	125	34	27	43	19	2

Descriptive features of the total number of experiements with Acridine Orange are included in this table. Successful is broadly used as any experiement that met the target set. The reason for failure is arbiterily categorised to try and show the main areas of error in the experimental method.

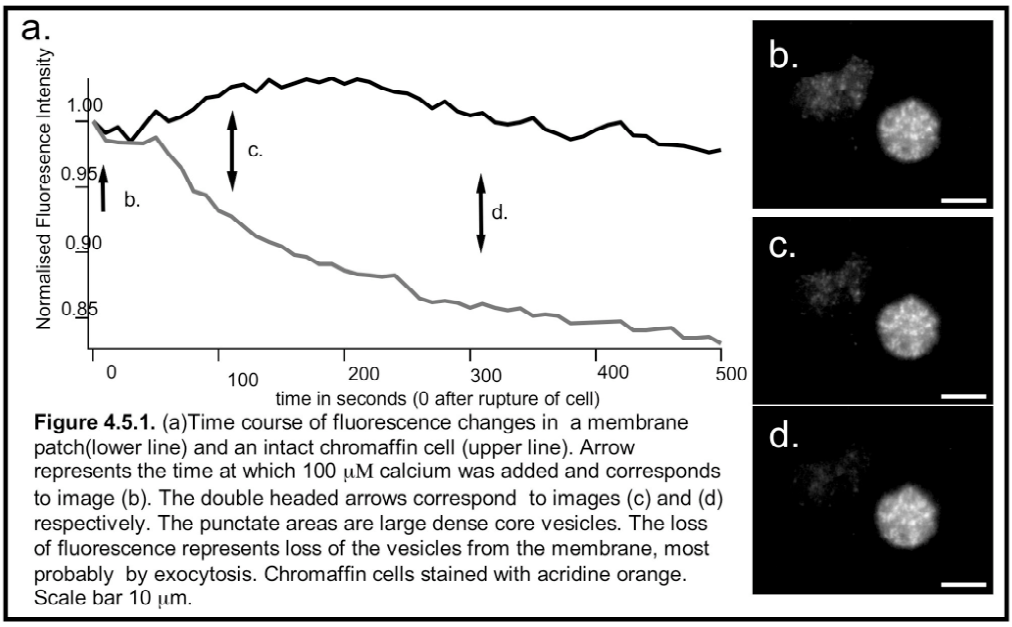

Figure 4.5.1. (a)Time course of fluorescence changes in a membrane patch(lower line) and an intact chromaffin cell (upper line). Arrow represents the time at which 100 μM calcium was added and corresponds to image (b). The double headed arrows correspond to images (c) and (d) respectively. The punctate areas are large dense core vesicles. The loss of fluorescence represents loss of the vesicles from the membrane, most probably by exocytosis. Chromaffin cells stained with acridine orange. Scale bar 10 μm.

Figure 4.5.1 illustrates the loss of total fluorescence and the appearance of the membrane patch before and after the experiment. Images of the membrane patch are shown in the panels on the right and the traces on the left are from a membrane patch and, for comparison, a whole cell (in which addition of external Ca^{2+} cannot trigger exocytosis). The video file 45 in the CD included with the thesis demonstrates the same cell pair throughout the experiment. The video demonstrates the gradual loss of intensity in the footprint during the time-lapse recording. The sudden loss of vesicles was also apparent. Figure 4.5.2 shows a series of recordings of the fluorescence of individual LDCVs, taken from a cell in which vesicles appeared to undergo exocytosis. The recordings are superimposed so that the time of Ca^{2+} addition (time 0) coincides; exocytosis appeared as a drop in the average intensity. Exocytosis was presumed to have occurred when the intensity difference line dropped suddenly and continued at the lower level. A single example of such a vesicle line (taken from a different cell) is shown in figure 4.5.3. This particular cell has been excluded from analysis as there was some doubt regarding the addition of Ca^{2+} to the medium (a drop of fluid was noted on the objective at the end of the experiment and therefore it was not certain that the Ca^{2+} containing medium had in fact been added). The second line on the figure shows a second vesicle that slowly loses

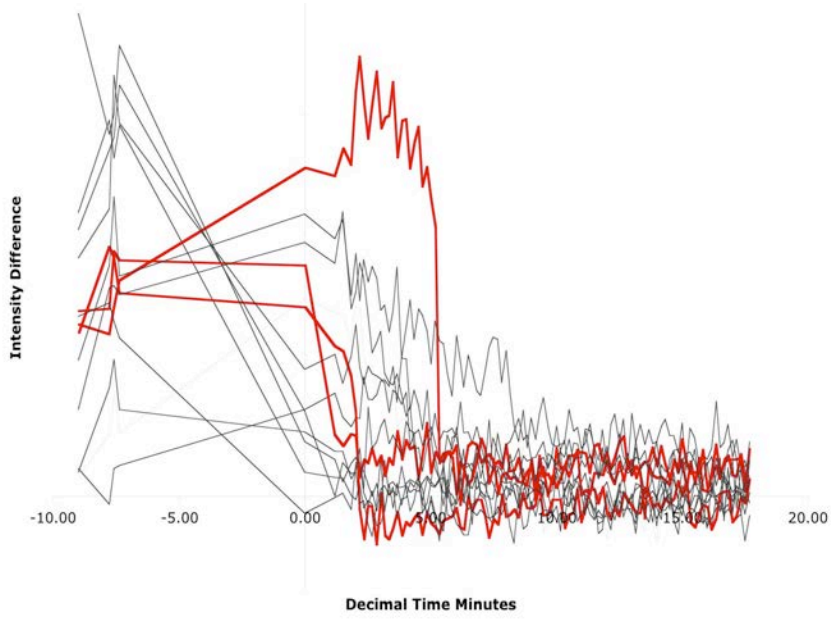

Figure 4.5.2 Cell 3 from 17/8/99. The vesicle marker was acridine orange and the cells where 48 hours from primary culture and had been grown on dishes coated with collagen type 1. The membrane patch was imaged with the Pentemax CCD camera and the images were processed with Metamorph and Excel. 100 μmol Calcium was added to membrane patch at decimal time 0 min. The Y axis is intensity difference that is the average intensity of the vesicular area subtracting the average intensity of the wider surrounding area as described in Figure 3.5.2.2. The red lines demonstrate 3 vesicles that show a sudden drop in intensity difference that is taken to represent exocytosis. In this particular experiment series of images where taken 10 seconds apart and the average of 4 images taken as a series with exposure of 25ms per image is used to create each time point. The averaging used in the data collection made it impossible to look for the flash of exocytosis that may be seen as a large negative deflection in the trace. The sudden drop of intensity difference between the two regions selected for each vesicle is matched by disappearance of the vesicle from the image.

intensity throughout the experiment. We can only speculate to the cause of intensity loss but we need to consider photo-bleaching, alteration in vesicle pH and movement away from the evanescent field as possibilities. Figure 4.5.4 shows fluorescence traces from 12 vesicles that appeared to fuse with the membrane. The variation in time between Ca^{2+} addition and fusion (shown as a rapid drop in fluorescence) was wide, perhaps reflecting the unpredictable arrival of Ca^{2+} at the membrane-bound vesicle. The fall in fluorescence intensity was variable and there were large fluctuations in background intensity. The total number of vesicles selected for investigation (Table 4.5.1) was

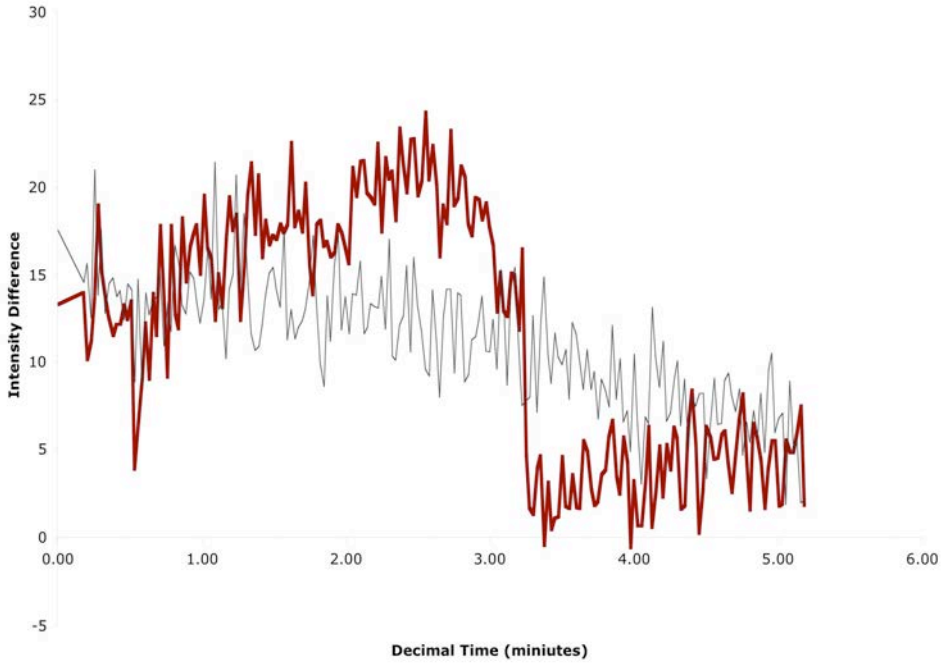

Figure 4.5.3 Cell 2 from 12/06/2001. These vesicles were tagged with acridine orange, The cell was grown on a glass coverslip coated with collagen type 1, analysed 48 hours following primary culture and images were collected in series of 2.5 seconds apart. The average of each series is used to provide the image that was analysed as described in figure 4.5.2. Calcium addition to this membrane patch was questionable and then vesicle analysis has been excluded from the overall data analysis. The red line demonstrates a sudden drop in intensity difference and the grey line demonstrates a single example of a vesicle that does not undergo exocytosis. A total of 6 vesicles where analysed in this cell only one of which demonstrated exocytosis. The black line demonstrates a downward trend in the line due to a degree of fluorescent decay.

117, of which 77 were from patches that had Ca^{2+} added at some point during the observation and 40 had no Ca^{2+} added. A total of 12 vesicles were deemed to have undergone exocytosis, 11 of these after the addition of Ca2+ and 1 when no Ca2+ was present. Using a one-tailed Fishers exact test a p value of 0.04 is obtained indicating that Ca2+ was an important requirement to the ability of vesicles to undergo exocytosis in this experimental procedure.

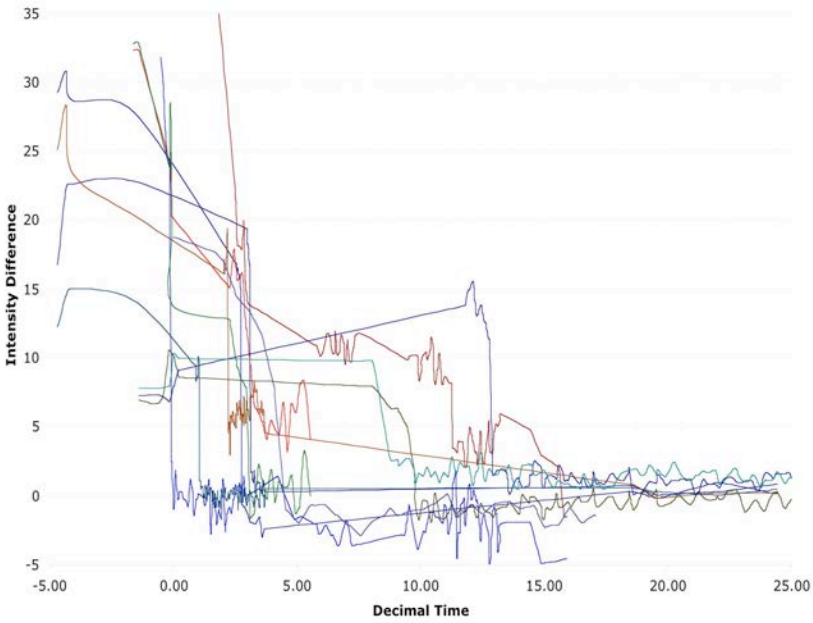

Figure 4.5.4 The 12 Vesicles That Demonstrated Exocytosis From The Membrane Patches.
The lines have been smoothed and some data points have been removed to enable the figure to demonstrate the loss of fluorescence intensity for each the 12 vesicles that exocytosed. The timing of loss of fluorescence intensity was variable occurring from time 0 to 13 minutes after addition of calcium. The line that enters from above the scale on the Y axis started with a fluorescence intensity difference of 82.

4.6 Summary

The method development has produced a reliable means of producing chromaffin cells adhering tightly to glass coverslips, allowing cell rupture and removal of cell membrane and cell content. The experiments to demonstrate functionality of the membrane patch have not been completed due to the high rate of variability in the experimental outcome. The results presented here are encouraging and justify further development of the method. The methodological problems described here and that are discussed in more detail in the next section should not be insurmountable, and recommendations for improvements are suggested in section 5.

5 Discussion

In the introduction a number of potential methods for investigating exocytosis in a cell-free environment were reviewed (section 1.3). The optical methods have produced some successful experiments but none has resulted in major advances or discoveries. When this is compared to electrophysiological methods, where much has been learned about the dynamics of exocytosis in whole and permeabilised cells one realises that methods using imaging techniques have been comparatively unproductive. The biochemical approach developed in the sea-urchin egg model is an exception, but this has not yet been successfully applied to a mammalian cell type. The lack of a biochemical mammalian cell-free model and the difficulty with the optical methods highlights the challenge of producing an optical cell-free assay for monitoring exocytosis.

The results from our experiments are encouraging as we were able to produce a model system that appeared to function in accordance with current knowledge. The successful experiments confirm previous work using different experimental approaches that regulated exocytosis can be triggered under specific conditions. The experimental design potentially provides an excellent platform for the investigation of the required factors for regulated exocytosis, however, we reluctantly decided not to pursue this interesting direction as the experiments did not appear to be robust in my hands nor in the hands of my colleague Dr U Wiegand (data not shown). The main limitation of the experimental process was our confidence in the equipment and the technique. This will be discussed in more detail later in this section.

As the aim of this project was to develop a method for *in vitro* study of exocytosis the discussion will revolve around the method development and the process of this method development. Initially the features that demonstrated that the method fulfilled its task as described in section 1.4 are discussed. The features of good experimental method are then discussed in relation to the method under development. The weaknesses of the method are commented on with suggestions for improvement and further investigation.

5.1 Meeting the Aims stated in section 1.5

The method development met several of the aims stated in section 1.5, but not all of them. Each of the aims mentioned is discussed under its own heading. Another successful aspect of the method development was the development of a cell culture dish that allowed healthy cell culture and also gave access to a pipette under the upright microscope. These dishes have been used for other applications as well as continued use on the TIRFM platform. The method for coating the glass with collagen has been successful for the rupturing experiments and continues to be used for these experiments. There could be improvements made in the dish preparation method and this is discussed in section 5.2.

5.1.1 Demonstration of Calcium sensitivity

Table 4.5.1 shows that we are able to demonstrate a significant difference ($p=0.039$) between Ca^{2+}-stimulated patches and unstimulated patches with respect to exocytosis as measured in this experimental design. This confirms that this *in vitro* system does exhibit Ca^{2+}-stimulated exocytosis and therefore meets this expected standard. This is an important base for the rest of the method investigation as if this had not been confirmed then further work on this method would have been difficult to justify. This measurement is however rather a gross measure of the Ca^{2+} relationship with the membrane patch. The technique used to apply Ca^{2+} was imprecise in that we cannot be certain of the exact concentration of Ca^{2+} that reached the membrane patch. The diffusion time from application of the Ca^{2+} containing solution to the Ca^{2+} free medium to the required environment at the membrane patch is uncertain. Suggested improvements are made later in section 5.3.2.

5.1.2 Blockade of regulated exocytosis by Clostridial neurotoxins

These experiments were not performed, as we could not reliably record Ca^{2+}-stimulated exocytosis from every membrane patch. If we could not be certain that the exocytotic

stimulus would work on each occasion that it was applied, we could not demonstrate that by applying a Clostridial neurotoxin light-chain that is expected to inhibit evoked LCDV release that we had in fact blocked exocytosis. This aim has therefore not been met.

5.1.3 Imaging of single vesicles, tracking of these vesicles and the "flash" at exocytosis

Figure 4.5.3 demonstrates an example of single vesicles on a membrane patch. This is similar to other published images achieved with TIRFM (Han *et al*., 1999;Oheim *et al.*, 1999; Steyer *et al.*, 1997) and is comparable to confocal images of whole cells that we obtained with the same cell culture techniques. This confirms the system's ability to visualise single large dense core vesicles. The stack of images available as a video file (43) (data from Dr I Matskevich) on the CD included with this thesis demonstrates the systems ability to follow a vesicle moving in the intact cell with the "flashes" of exocytosis. Movement of vesicles on a cell patch is shown in a video file (45). The software tracking of these vesicles was a little less robust but with more use better results would have been obtained. Finally we have images that demonstrate a flash when exocytosis occurs. My own experiments only achieved this in whole cells, however Dr U Wiegand (personal communication, data not shown) has successfully demonstrated this in membrane patches. TIRFM has proved to be a successful technique for these purposes. With improvements in certain aspects of the set-up it should be a very useful technique in the future for imaging both living cells and cell membrane patches.

5.1.4 Addition of prepared vesicles to the membrane patch

The experiments to demonstrate the addition of prepared vesicles to the membrane patches were not attempted, as we could not be confident in the reliability of the method to produce repeatable experiments nor had we completed the confirmatory experiments with neurotoxins.

5.1.5 Demonstration of two pools of vesicles

We could postulate that the flashes seen are often from vesicles recruited from the reserve pool of vesicles, as they seem to approach the membrane prior to undergoing exocytosis. However we do not have enough data to adequately validate the method. This aim has not been met.

5.2 Experimental Method Assessment

Good experimental method is not always well defined but yet is an important concept that is essential to method development. For a method to produce results that are acceptable to peer review it should meet certain quality standards. In method development the need for the new method must first be established, the new method must be evaluated against other methods that measure similar parameters and finally the method must meet quality standards. The quality standards are based on reproducibility and accuracy allowing other investigators to produce similar results. The basis of most quality standards is a reference method but in new method development there is not always a reference method. Performance parameters such as accuracy, analytical range, analytical sensitivity, analytical specificity, blank reading, detection limit, interferences, precision and reagent stability may be useful in assessing a method. The basis of quality standards is often a comparison with reference methods. When no reference method is available what quality standard is appropriate? Repeatability and reproducibility are the basics of quality control and quality assessment and thus these must be the principal tests of a new method.

To what extent does the method we have developed method meet the criteria described above? The need for a different approach to measuring exocytosis and the proteins involved in regulated exocytosis has been proposed in the introduction. There are many unanswered questions and much more knowledge is required to finally establish the exact mechanism of regulated exocytosis. The introduction also reviews a number of other methods of monitoring regulated exocytosis and we can compare what we find with the knowledge gained from other experimental methods. There is no reference

method for comparison and thus an alternative, the response to well documented stimuli, was chosen for comparison, the responsiveness to change in free [Ca^{2+}] at the cytoplasmic side of the cell membrane. This is well documented in a variety of systems and is therefore the most robust measure of the ability of the method to reproduce regulated exocytosis. As demonstrated in the results section the method does in fact meet these criteria but it fails on the reproducibility and repeatability criteria in that only 4 out of the 13 membrane patches actually demonstrated a vesicle that underwent exocytosis. It is also of concern that, for various technical reasons, more than 75% of attempted patch experiments yielded no image data at all. It was because of this high experimental failure rate that the clostridial neurotoxin experiments were not performed and because we could not validate the method by the neurotoxin method the other planned experiments were not performed.

5.3 Limitations of the method

The fact that so many experiments failed completely is the most worrying issue and this is discussed in the following section. As the method has four main areas of potential failure these will be discussed individually (Table 4.5.3). These areas of weakness have mostly been identified, and probably none is insurmountable, although they all posed problems at the time that the work was being carried out.

5.3.1 Cell Culture

The method is based on a primary cell culture that in an individual's hands was reproducible but still suffered from some seasonal and circumstantial variation. When different members of staff undertook cell culture a wider variation was noted. This can be overcome by training an individual to perform the primary cell culture on all occasions but the seasonal and circumstantial variations are difficult to control and difficult to quantify. We and others have noticed changes in our cell culture depending on the season. Possibly this is indicative of changes to the bovine adrenal axis (hypothalamus-pituitary-adrenal) brought on by exposure to sunlight. Use of a cell line may be the way to improve this aspect of the method but no cell line has LDCVs in the

quantity and size of bovine chromaffin cells. As imaging ability increases to allow better resolution of smaller vesicles, cell lines such as PC-12 cells will become more useful for these experiments. These cells contain smaller secretory vesicles than do chromaffin cells, but a larger proportion of them are docked at the plasma membrane; this is not necessarily an advantage for TIRFM studies, since it greatly increases the complexity of image analysis. Other secretory cells that have a better propensity to growth and adherence, such as endothelial cells or AtT-20s, may also improve certain aspects of the experimental process. Dr U Wiegand is currently working with AtT-20 cells with some success (personal communication). This mouse pituitary cell line has fewer LDCVs than are found in chromaffin cell (only a few hundred per cell) but they are of about twice the diameter of chromaffin granules.

The cells demonstrated different survival patterns in the different bespoke dishes that were produced and also in the standard cell culture dishes. Some cultures produced good batches of cells while others were very poor. Attempts to improve cell survival included variations in the medium, supplements and actual technique of primary culture. The description in the methods section (3.2s) is the one that I found produced the most reliable batch of cells.

The bespoke dishes required investigation to find a combination of chemical and physical treatment that was compatible with reasonable cell survival. In some instances the cells did not survive in any number beyond a few hours whereas in others we had a much better result and occasionally found cells surviving up to 7 days (data not shown), which matched untreated commercial cell culture dishes. Tables 4.2.1 and 4.2.2 cover these aspects of the investigation. The use of collagen type I was continued throughout the experiments and the data on cell survival (Table 4.2.3) does not include the cells cultured for the rupturing and experimentation phase of the method development.

The bespoke dishes performed well on most occasions but there was a degree of difficulty in preparing standardised dishes on all occasions. A more robust dish manufacturing process with demonstrable quality control would improve this aspect. Again this could be achieved by training an individual to perform the task on a regular

basis to a standardised protocol. The step that was probably most important and most variable was protein coating. As this step relies on the proteins attaching to the glass surface as the medium evaporates, the final product can have variable degrees of protein layering. Using a liquid spray application and quicker drying steps would achieve a more even and reliable coat. Such methods are difficult to establish locally but a commercial organisation with specialised equipment would be able to produce the dishes in this way. The cost of producing these dishes commercially will be prohibitive until there is a widespread demand for them. With the advancement of microscopy techniques there may well come a time when this is a feasible product.

5.3.2 Rupturing of adhered cells

Rupturing of the cells to produce a cell membrane attached to the glass worked well once the technique had been practised. Initially attempts were made to lance the cell with a pulled pipette but this technique did not leave visible cell membrane on the glass surface. The technique described in the methods, which used a jet of fluid over the cell to rupture the membrane, worked well on most occasions. One problem was that cells that were poorly attached to the glass surface rolled away rather than rupturing. It was noted on more than one occasion that these cells left behind a fluorescent footprint that may well have confounded the experimental technique. This was a particular problem with LysoSensor Green and also noted with Acridine Orange. It has been demonstrated that cells do not adhere smoothly to glass or other surfaces and TIRFM appears to be the best method for investigating adherence proteins and contact regions of cell membranes (Reichert and Truskey, 1990). The footprint noted may well be residual dye in compartments between the cell membrane and the substrate. The footprint did not seem to be an issue with cells expressing preproANF-EGFP and this more specific vesicle marker is recommended for future work, although it has the disadvantage that the fluorescence of LDCVs is much less bright than when they are labelled with the acidophilic dyes. Once ruptured the cellular components were washed away with a jet of fluid to leave behind a patch of cell membrane with attached vesicles and cytosolic components. The membrane did not reseal immediately as the medium in which the cell

was ruptured was Ca^{2+}-free: a Ca^{2+} chelator was present in a concentration well above that of Ca^{2+} likely to be released from intracellular stores when the cell was ruptured. Initially the cell was ruptured without washing the content of the cell away from the membrane attached to the coverslip. In these cells it was noted that the membrane resealed once Ca^{2+} was added back to the solution. This is not unexpected, as it has been shown that Ca^{2+} is important in resealing of injured cell membranes (Steinhardt *et al*., 1994). The force of the jet of fluid from the pulled pipette often resulted in the membrane lifting from the glass. This technique required practice but with regular use produced enough cell membrane patches for experimental use. Injection of fluid was done manually as described in the methods section. One improvement would be with the use of a pressure injector allowing a constant and even jet that may produce more reliable results. Further use of the pressure injector would be the application of the Ca^{2+} containing medium and the other experimental media (reconstituted cytosol, vesicles and other molecules of interest). In our experiments we relied on Ca^{2+} diffusing to the membrane patch after being applied with a pipette to the medium in the cell culture dish. This technique, Ca^{2+} addition by pipette, did result in a number of failed experiments. Initially the increased volume of fluid resulted in focus drift and later when smaller volumes were used there were the occasional experiments in which the drop of Ca^{2+} containing fluid was found on the edge of the dish above the culture medium. Overall the technique worked but for a more reliable method the other stages of the planned experiments would have required the development of a precise method of applying the experimental media. As mentioned above a pressure injector could be used for this purpose, allowing a more controlled application of medium into the direct environment of the membrane patch.

5.3.3 Vesicle Staining

Visualising LDCVs by fluorescence microscopy requires some form of vesicle labelling. Acridine Orange, an acidophilic dye, was used most commonly in my experiments. Other acidophilic dyes such as LysoTracker and LysoSensor dyes were tested and some time was spent investigating the use of cells that were virally transfected so as to express

the fluorescent secretory chimeric protein preproANF-EGFP. My experiments with preproANF-EGFP demonstrated that it did label vesicles suitably. Most of the early TIRFM experiments with the preproANF-EGFP construct were performed by Dr I Matskevich and later continued by Dr U Wiegand. The reason for investigating at an alternative label was the non-specificity of labelling by the acidophilic dye, which results in cellular compartments other than LDCVs, such as lysosomes and endosomes, becoming fluorescent. Further the footprint effect (when cells rolled away) of the acidophilic dyes had been noted and a means of avoiding this complicating area of fluorescence was required. The fluorescent chimeric protein, introduced by Dr E Levitan in Pittsburgh, seemed an ideal candidate as it is specifically targeted to vesicles for regulated exocytosis (Burke *et al*., 1997;Johns *et al.*, 2001). Dr Levitan kindly provided me with the cDNA, and Dr R Duncan then inserted the cDNA into the Semliki Forest Virus vector that allowed us transduce chromaffin cells with great efficiency. Much exciting work has come from this in the hands of other members of the research group (Duncan *et al*., 2002; Greaves *et al*., 2002; Wiegand *et al*., 2002; Duncan *et al*., 2003; Wiegand *et al*., 2003).

5.3.4 Equipment issues

The microscope was a bespoke unit purpose built for these experiments by Dr G Bodammer, a colleague with training in physics. It was limited in that there was a large proportion of downtime and it required regular adjustment to keep it working. Errors in the adjustment of the laser, fibre optics, prism placement and piezo focus device all contributed to physical mishaps in the experiments. Further the microscope stage was occasionally affected by vibration resulting in lateral movement of vesicles. The most difficult problem, however, was the drift in focus during time-lapse experiments. After much consideration the problem was diagnosed to be the weight of the camera bearing down on the focus mechanism of the microscope. This resulted in a slow drift in the focal plane that affected the fluorescence intensity of most of the experiments. With some engineering a counterbalance device was rigged into the microscope stage. This eventually produced a steady image that was suitable for analysis. Adjustment of the

counterbalance weight was still required on occasion. More recently commercially produced microscopes with purpose-built digital cameras have become available. It would be interesting to see if they are more reliable for experimental purposes as we had experienced a 19% (Table 4.5.3) failure due to microscope equipment problems.

Imaging software and the interface between the digital camera and the computer created another group of problems related to equipment. Data transfer from the camera to the computer was not usually an issue. The frequency of imaging was limited by the data transfer rate to 200Hz but this did not produce particular problems in our experiments as imaging was done at a lower frequency. The software package, MetaMorph‰(Universal Imaging), usually produced good images and allowed analysis. On occasion good experimental data was lost due to errors in writing data to the hard drive. This occurred when the software application crashed due to a processing error. Few experiments were lost in this way (1%) but this was particularly frustrating if all the other factors had worked satisfactorily. All the computing issues will presumably be improved as technology advances. Already computer processing speeds have increased and the available hard drive space is no longer an issue now that larger capacity hard drives and better quality CD writers have become available.

Data analysis was limited by the protocol that I used to collect data and work carried out later by my colleague, Dr U Wiegand, achieved a better confirmation of exocytosis. I routinely employed a short burst of high frequency imaging and then created an average image from 4 images taken in sequence. All the final images presented in the results section are constructed from a series of 4 images taken as fast as the camera was capable (25ms exposure per image and using half the CCD chip for each image with a data transfer occurring from the one half while the other half was exposed, resulted in the 4 images being collected in approximately 120 ms) and then averaged. The series of averaged images was then analysed for vesicles as described in the methods. This was limited because Dr U Wiegand has subsequently demonstrated that by using the individual images one can distinguish between vesicles that exocytose and those that simply move away from the cell membrane (area of TIR excitation). The ‘mushroom

flash' (Nature, issue no.6928, cover picture) is another way of presenting such data. Some of the first images to be analysed in this way were those produced using preproANF-EGFP transfected into bovine chromaffin cells and imaged on the same microscope by Dr U Wiegand. For future experiments it would be recommended to collect the images individually at predetermined frequency that is shown to allow analysis as described by Dr U Wiegand (Wiegand *et al*., 2002).

5.4 Recommendations for future work in this field

The total number of experiments that produced a result that could be analysed was small but the results were interesting and do offer the potential further development of the method. Most importantly the method does demonstrate the sensitivity of vesicle fusion to the free Ca^{2+} concentration and it would be interesting to establish the [Ca^{2+}] that was able to release the vesicles attached to the membrane in this system, as has been done using permeabilised cells and by flash photolysis of patch-clamped cells (Smith *et al*., 1998). Considering that many of the problems with the method are simply related to technical limitations the potential for further work on this method still exists once the technical limitations are overcome.

5.4.1 Chromaffin cells

If further work with this method is to be attempted with chromaffin cells it would be sensible to study conformational changes in the chromaffin cell architecture that occur when the chromaffin cell flattens itself against the glass. Use of dopamine-beta-hydoxyalse as a chromaffin granule marker could identify where in the flattened cell the granules lie, if required studies of fixed cells to determine cytoskeletal changes may be interesting. Further the effect of the solution used for rupturing should also be investigated in the chromaffin cells to look at the effect of the high potassium concentration. We presumed that by having a 1mM calcium buffer in the solution that even if the cells depolarized that the chromaffin granules would not undergo exocytosis as the Ca^{2+} signal would not occur. It would be therefore be beneficial to demonstrate the presence of chromaffin granule at the cell membrane in fixed cells that had been

exposed to the internal solution. This could be done with confocal microscopy using one of the vesicle markers or by electron microscopy.

The effect of the collagen type I coating of the coverslips on the physiology of the chromaffin cells should also be investigated. Capacitance measurements of cells on the coated coverslips should be compared with uncoated coverslips. Both cell configurations (normal round chromaffin cell and flattened chromaffin cell) should be investigated as the capacitance measurements are expected to be different.

5.4.2 Solutions

The solution used for rupturing the cells requires further consideration. The solution used in these experiments used a concentration of potassium ion that would under normal circumstances depolarise the cell, allowing [Ca^{2+}] to enter through the calcium channels and thereby triggering exocytosis. The calcium buffer was presumed to block the signal for exocytosis but this should be confirmed by a biochemical assay. Other supplements that could be added to the solution include protease inhibitors to block the effect of proteases released on cell rupture and a reducing agent to neutralise the oxidative products released on cell rupture. These factors may allow better functioning of regulated exocytosis, however the changes would require experimental evidence to confirm this. The ionic components of the solution could also be adjusted, particularly if [K^+] is found to allow Ca^{2+} into the cell following depolarization. Use of Na^+ is a possibility with a lower amount of K^+. A control solution for Ca^{2+} induced exocytosis should also be formulated and here Mg^{2+} could replace Ca^{2+}.

5.4.3 Membrane patch preparation

Improvements to the dish preparation could be made but for the purposes of these experiments they are adequate, as is the method of applying a collagen coat. The primary cell culture is suitable but the use of a line of cells that naturally adhered to glass/collagen better than chromaffin cells would be recommended. These cells would need to demonstrate regulated exocytosis and be able to direct the preproANF-EGFP to the appropriate vesicle. PreproANF-EGFP would be the recommended fluorescent

marker as it specifically labels a small population of LDCVs (i.e. those assembled between cell transfection and the imaging experiment – usually 48h). This amounts to no more than 150 vesicles per chromaffin cell (Duncan *et al*., 2003) making it easier to follow and analyse the marked vesicles. It also does not produce the footprint under the cell membrane that was noted with the acidophilic dyes.

Membrane patch preparation could be improved by the use of a pressure injector producing a more regulated flow of medium. The addition of stimulatory media, prepared vesicles, protein products and neurotoxins could also be done with more precision with a pressure injector.

5.4.4 Imaging

Imaging of the experiments could continue with TIRFM but as the laser scanning confocal and multi-photon microscopes now have faster acquisition speeds the advantage of the purpose-built TIRFM equipment is less. Both the other systems could be investigated for suitability for the planned experiments as the equipment is now more readily accessible. As the rupturing technique requires a number of other fitments to the microscope stage the equipment may have to be dedicated to this work. The commercially available TIRFM equipment could also be investigated, as it may be less prone to some of the problems we faced with the equipment at our disposal.

Finally image data analysis is improving with more powerful and more specialised computers. My experience with these is minimal but much more analytical work is now possible than when this project started.

References

Alberts, B., Johnson, A., Lewis, J., Raff, M., Roberts, K. and Walter, P. (eds.) (2002) *Molecular biology of the cell*. Garland Science.

Almers, W. (1990) Exocytosis. *Annu Rev Physiol*, **52**, 607-24.

Angleson, J.K. and Betz, W.J. (1997) Monitoring secretion in real time: capacitance, amperometry and fluorescence compared. *Trends Neurosci*, **20**, 281-7.

Aplin, J.D. and Hughes, R.C. (1981) Protein-derivatised glass coverslips for the study of cell-to substratum adhesion. *Anal Biochem*, **113**, 144-8.

Archer, D.A., Graham, M.E. and Burgoyne, R.D. (2002) Complexin regulates the closure of the fusion pore during regulated vesicle exocytosis. *J Biol Chem*, **277**, 18249-52.

Aunis, D. and Langley, K. (1999) Physiological aspects of exocytosis in chromaffin cells of the adrenal medulla. *Acta Physiol Scand*, **167**, 89-97.

Avery, J., Ellis, D.J., Lang, T., Holroyd, P., Riedel, D., Henderson, R.M., Edwardson, J.M. and Jahn, R. (2000) A cell-free system for regulated exocytosis in PC12 cells. *J Cell Biol*, **148**, 317-24.

Avery, J., Jahn, R. and Edwardson, J.M. (1999) Reconstitution of regulated exocytosis in cell-free systems: a critical appraisal. *Annu Rev Physiol*, **61**, 777-807.

Axelrod, D. (2001) Total internal reflection fluorescence microscopy in cell biology. *Traffic*, **2**, 764-74.

Axelrod, D., Hellen, E. and Fulbright, R. (1992) Total Internal Reflection Fluorescence. *Topics in Fluorescence Spectroscopy*, **3**, 289-344.

Baumert, M., Maycox, P.R., Navone, F., De Camilli, P. and Jahn, R. (1989) Synaptobrevin: an integral membrane protein of 18,000 daltons present in small synaptic vesicles of rat brain. *Embo J*, **8**, 379-84.

Bayer, M.J., Reese, C., Buhler, S., Peters, C. and Mayer, A. (2003) Vacuole membrane fusion: V0 functions after trans-SNARE pairing and is coupled to the Ca2+-releasing channel. *J Cell Biol*, **162**, 211-22.

Bennett, M.K. (1997) Ca2+ and the regulation of neurotransmitter secretion. *Curr Opin Neurobiol*, **7**, 316-22.

Bennett, M.K. and Scheller, R.H. (1993) The molecular machinery for secretion is conserved from yeast to neurons. *Proc Natl Acad Sci U S A*, **90**, 2559-63.

Betz, A., Ashery, U., Rickmann, M., Augustin, I., Neher, E., Sudhof, T.C., Rettig, J. and Brose, N. (1998) Munc13-1 is a presynaptic phorbol ester receptor that enhances neurotransmitter release. *Neuron*, **21**, 123-36.

Bittner, M.A. (2000) Alpha-latrotoxin and its receptors CIRL (latrophilin) and neurexin 1 alpha mediate effects on secretion through multiple mechanisms. *Biochimie*, **82**, 447-452.

Bittner, M.A., Krasnoperov, V.G., Stuenkel, E.L., Petrenko, A.G. and Holz, R.W. (1998) A Ca2+-independent receptor for alpha-latrotoxin, CIRL, mediates effects on secretion via multiple mechanisms. *J Neurosci*, **18**, 2914-22.

Bock, J.B., Matern, H.T., Peden, A.A. and Scheller, R.H. (2001) A genomic perspective on membrane compartment organization. *Nature*, **409**, 839-41.

Borges, R. and Machado, J.D. (2002) Chromaffin cell research in the new millennium. *Trends in Pharmacological Sciences*, **23**, 53-55.

Borges, R., Machado, J.D., Betancor, G. and Camacho, M. (2002) Pharmacological regulation of the late steps of exocytosis. *Ann N Y Acad Sci*, **971**, 184-92.

Bruns, D. and Jahn, R. (2002) Molecular determinants of exocytosis. *Pflugers Arch*, **443**, 333-8.

Burgoyne, R.D. and Barclay, J.W. (2002) Splitting the quantum: regulation of quantal release during vesicle fusion. *Trends in Neurosciences*, **25**, 176-178.
Burgoyne, R.D. and Morgan, A. (2003) Secretory granule exocytosis. *Physiol Rev*, **83**, 581-632.
Burke, N.V., Han, W., Li, D., Takimoto, K., Watkins, S.C. and Levitan, E.S. (1997) Neuronal peptide release is limited by secretory granule mobility. *Neuron*, **19**, 1095-102.
Chamberlain, L.H. and Burgoyne, R.D. (1998) Cysteine string protein functions directly in regulated exocytosis. *Mol Biol Cell*, **9**, 2259-67.
Chamberlain, L.H. and Burgoyne, R.D. (2000) Cysteine-string protein: the chaperone at the synapse. *J Neurochem*, **74**, 1781-9.
Chen, Y.A., Scales, S.J., Patel, S.M., Doung, Y.C. and Scheller, R.H. (1999) SNARE complex formation is triggered by Ca2+ and drives membrane fusion. *Cell*, **97**, 165-74.
Chernomordik, L., Chanturiya, A., Green, J. and Zimmerberg, J. (1995) The hemifusion intermediate and its conversion to complete fusion: regulation by membrane composition. *Biophys J*, **69**, 922-9.
Chernomordik, L.V., Kozlov, M.M., Melikyan, G.B., Abidor, I.G., Markin, V.S. and Chizmadzhev, Y.A. (1985) The shape of lipid molecules and monolayer membrane fusion. *Biochim Biophys Acta*, **812**, 643-45.
Chestkov, V.V., Radko, S.P., Cho, M.S., Chrambach, A. and Vogel, S.S. (1998) Reconstitution of calcium-triggered membrane fusion using "reserve" granules. *J Biol Chem*, **273**, 2445-51.
Chizmadzhev, Y.A., Kumenko, D.A., Kuzmin, P.I., Chernomordik, L.V., Zimmerberg, J. and Cohen, F.S. (1999) Lipid flow through fusion pores connecting membranes of different tensions. *Biophys J*, **76**, 2951-65.
Chow, R.H., Klingauf, J., Heinemann, C., Zucker, R.S. and Neher, E. (1996) Mechanisms determining the time course of secretion in neuroendocrine cells. *Neuron*, **16**, 369-76.
Chow, R.H., Klingauf, J. and Neher, E. (1994) Time course of Ca2+ concentration triggering exocytosis in neuroendocrine cells. *Proc Natl Acad Sci U S A*, **91**, 12765-9.
Chow, R.H. and Von Ruden, L. (1995) Electrochemical detection of secretion from single cells. In E, S.B.a.N. (ed.) *Single Channel Recording*. Plenum Press, New York.
Chow, R.H., von Ruden, L. and Neher, E. (1992) Delay in vesicle fusion revealed by electrochemical monitoring of single secretory events in adrenal chromaffin cells. *Nature*, **356**, 60-3.
Coorssen, J.R., Blank, P.S., Tahara, M. and Zimmerberg, J. (1998) Biochemical and functional studies of cortical vesicle fusion: the SNARE complex and Ca2+ sensitivity. *J Cell Biol*, **143**, 1845-57.
Crabb, J.H. and Jackson, R.C. (1985) In vitro reconstitution of exocytosis from plasma membrane and isolated secretory vesicles. *J Cell Biol*, **101**, 2263-73.
Cuchillo-Ibanez, I., Michelena, P., Albillos, A. and Garcia, A.G. (1999) A preferential pole for exocytosis in cultured chromaffin cells revealed by confocal microscopy. *FEBS Lett*, **459**, 22-6.
Del Castillo, J. and Katz, B. (1954) Quantal components of the end-plate potential. *J Physiol*, **124**, 560-73.
Duncan, R.R., Don-Wauchope, A.C., Tapechum, S., Shipston, M.J. and Chow, R.H. (1999) High-efficiency Semlike Forest virus-mediated transduction in bovine adrenal chromaffin cells. *Biochemical Journal*, **342**, 497-501.
Duncan, R.R., Greaves, J., Tapechum, S., Apps, D.K., Shipston, M.J. and Chow, R.H. (2002) Efficacy of Semliki Forest virus transduction of bovine adrenal chromaffin cells: an analysis of heterologous protein targeting and distribution. *Ann N Y Acad Sci*, **971**, 641-6.

Duncan, R.R., Greaves, J., Wiegand, U.K., Matskevich, I., Bodammer, G., Apps, D.K., Shipston, M.J. and Chow, R.H. (2003) Functional and spatial segregation of secretory vesicle pools according to vesicle age. *Nature*, **422**, 176-80.

Eccles, J.C. (1990) Developing concepts of the synapses. *J Neurosci*, **10**, 3769-81.

Edwardson, J.M. (1998) A cell-free system for Ca2+-regulated exocytosis. *Methods*, **16**, 209-14.

Elhamdani, A., Palfrey, H.C. and Artalejo, C.R. (2001) Quantal size is dependent on stimulation frequency and calcium entry in calf chromaffin cells. *Neuron*, **31**, 819-30.

Evans, G.J., Wilkinson, M.C., Graham, M.E., Turner, K.M., Chamberlain, L.H., Burgoyne, R.D. and Morgan, A. (2001) Phosphorylation of cysteine string protein by protein kinase A. Implications for the modulation of exocytosis. *J Biol Chem*, **276**, 47877-85.

Fasshauer, D., Sutton, R.B., Brunger, A.T. and Jahn, R. (1998) Conserved structural features of the synaptic fusion complex: SNARE proteins reclassified as Q- and R-SNAREs. *Proc Natl Acad Sci U S A*, **95**, 15781-6.

Fatt, P. and Katz, B. (1950) Membrane potentials at the motor end-plate. *J Physiol*, **3**, 46p-7p.

Fatt, P. and Katz, B. (1951) An analysis of the end-plate potential recorded with an intracellular electrode. *J Physiol*, **115**, 320-70.

Fatt, P. and Katz, B. (1952) Spontaneous subthreshold activity at motor nerve endings. *J Physiol*, **117**, 109-28.

Gillis, K.D., Mossner, R. and Neher, E. (1996) Protein kinase C enhances exocytosis from chromaffin cells by increasing the size of the readily releasable pool of secretory granules. *Neuron*, **16**, 1209-20.

Gonzalez, L., Jr. and Scheller, R.H. (1999) Regulation of membrane trafficking: structural insights from a Rab/effector complex. *Cell*, **96**, 755-8.

Graham, M.E. and Burgoyne, R.D. (2000) Comparison of cysteine string protein (Csp) and mutant alpha-SNAP overexpression reveals a role for csp in late steps of membrane fusion in dense-core granule exocytosis in adrenal chromaffin cells. *J Neurosci*, **20**, 1281-9.

Graham, M.E., Fisher, R.J. and Burgoyne, R.D. (2000) Measurement of exocytosis by amperometry in adrenal chromaffin cells: effects of clostridial neurotoxins and activation of protein kinase C on fusion pore kinetics. *Biochimie*, **82**, 469-79.

Greaves, J., Duncan, R.R., Tapechum, S., Apps, D.K., Shipston, M.J. and Chow, R.H. (2002) Use of ANF-EGFP for the visualization of secretory vesicles in bovine adrenal chromaffin cells. *Ann N Y Acad Sci*, **971**, 275-6.

Han, W., Ng, Y.K., Axelrod, D. and Levitan, E.S. (1999) Neuropeptide release by efficient recruitment of diffusing cytoplasmic secretory vesicles. *Proc Natl Acad Sci U S A*, **96**, 14577-82.

Heinemann, C., Chow, R.H., Neher, E. and Zucker, R.S. (1994) Kinetics of the secretory response in bovine chromaffin cells following flash photolysis of caged Ca2+. *Biophys J*, **67**, 2546-57.

Henry, J.P., Darchen, F. and Cribier, S. (1998) Physical techniques for the study of exocytosis in isolated cells. *Biochimie*, **80**, 371-7.

Hille, B., Billiard, J., Babcock, D.F., Nguyen, T. and Koh, D.S. (1999) Stimulation of exocytosis without a calcium signal. *J Physiol*, **520**, 23-31.

Hirschfeld, T. (1965) Total reflection fluorescence. *Can. Spectrosc*, **10**, 128.

Hu, C., Ahmed, M., Melia, T.J., Sollner, T.H., Mayer, T. and Rothman, J.E. (2003) Fusion of cells by flipped SNAREs. *Science*, **300**, 1745-9.

Jahn, R. and Niemann, H. (1994) Molecular mechanisms of clostridial neurotoxins. *Ann N Y Acad Sci*, **733**, 245-55.

Jahn, R. and Sudhof, T.C. (1999) Membrane fusion and exocytosis. *Annu Rev Biochem*, **68**, 863-911.

Johns, L.M., Levitan, E.S., Shelden, E.A., Holz, R.W. and Axelrod, D. (2001) Restriction of secretory granule motion near the plasma membrane of chromaffin cells. *J Cell Biol*, **153**, 177-90.

Katz, B. (1996) Neural transmitter release: from quantal secretion to exocytosis and beyond. The Fenn Lecture. *J Neurocytol*, **25**, 677-86.

Klenchin, V.A., Kowalchyk, J.A. and Martin, T.F. (1998) Large dense-core vesicle exocytosis in PC12 cells. *Methods*, **16**, 204-8.

Kozlovsky, Y., Chernomordik, L.V. and Kozlov, M.M. (2002) Lipid intermediates in membrane fusion: formation, structure, and decay of hemifusion diaphragm. *Biophys J*, **83**, 2634-51.

Lang, T., Margittai, M., Holzler, H. and Jahn, R. (2002) SNAREs in native plasma membranes are active and readily form core complexes with endogenous and exogenous SNAREs. *J Cell Biol*, **158**, 751-60.

Lang, T., Wacker, I., Steyer, J., Kaether, C., Wunderlich, I., Soldati, T., Gerdes, H.H. and Almers, W. (1997) Ca2+-triggered peptide secretion in single cells imaged with green fluorescent protein and evanescent-wave microscopy. *Neuron*, **18**, 857-863.

Lansing Taylor, D. and Salmon, E.D. (1989) Basic Fluorescence Microscopy. *Methods in Cell Biology*. Academic Press, Vol. 29, pp. 207-37.

Lindau, M. and Almers, W. (1995) Structure and function of fusion pores in exocytosis and ectoplasmic membrane fusion. *Curr Opin Cell Biol*, **7**, 509-17.

Machado, J.D., Segura, F., Brioso, M.A. and Borges, R. (2000) Nitric oxide modulates a late step of exocytosis. *J Biol Chem*, **275**, 20274-9.

Macklis, J.D., Sidman, R.L. and Shine, H.D. (1985) Cross-linked collagen surface for cell culture that is stable, uniform, and optically superior to conventional surfaces. *In Vitro Cell Dev Biol*, **21**, 189-94.

MacLean, C.M. and Edwardson, J.M. (1992) Fusion between rat pancreatic zymogen granules and plasma membranes. Modulation by a GTP-binding protein. *Biochem J*, **286**, 747-53.

Mahal, L.K., Sequeira, S.M., Gureasko, J.M. and Sollner, T.H. (2002) Calcium-independent stimulation of membrane fusion and SNAREpin formation by synaptotagmin I. *J Cell Biol*, **158**, 273-82.

Martin, T.F. and Kowalchyk, J.A. (1997) Docked secretory vesicles undergo Ca2+-activated exocytosis in a cell-free system. *J Biol Chem*, **272**, 14447-53.

Melia, T.J., Weber, T., McNew, J.A., Fisher, L.E., Johnston, R.J., Parlati, F., Mahal, L.K., Sollner, T.H. and Rothman, J.E. (2002) Regulation of membrane fusion by the membrane-proximal coil of the t-SNARE during zippering of SNAREpins. *J Cell Biol*, **158**, 929-40.

Meunier, F.A., Schiavo, G. and Molgo, J. (2002) Botulinum neurotoxins: from paralysis to recovery of functional neuromuscular transmission. *J Physiol Paris*, **96**, 105-13.

Misura, K.M., Scheller, R.H. and Weis, W.I. (2000) Three-dimensional structure of the neuronal-Sec1-syntaxin 1a complex. *Nature*, **404**, 355-62.

Monck, J.R., Oberhauser, A.F. and Fernandez, J.M. (1995) The exocytotic fusion pore interface: a model of the site of neurotransmitter release. *Mol Membr Biol*, **12**, 151-6.

Morgan, A., Wilkinson, M. and Burgoyne, R. (1993) Identification of Exo2 as the catalytic subunit of protein kinase A reveals a role for cyclic AMP in Ca(2+)-dependent exocytosis in chromaffin cells. *EMBO J.*, **12**, 3747-3752.

Murthy, V.N. (1999) Optical detection of synaptic vesicle exocytosis and endocytosis. *Current Opinion in Neurobiology*, **9**, 314-320.

Nguyen, T.T., Ong, H. and De Lean, A. (1988) Secretion and biosynthesis of atrial natriuretic factor by cultured adrenal chromaffin cells. *FEBS Lett*, **231**, 393-6.
Nobles, M. and Abbott, N. (1996) Adhesion and Growth of Brain Microvascular Endothelial Cells on Treated Glass. *Endothelium*, **4**, 297-307.
Oheim, M. (2001) Imaging transmitter release. I. Peeking at the steps preceding membrane fusion. *Lasers Med Sci*, **16**, 149-158.
Oheim, M., Loerke, D., Chow, R.H. and Stuhmer, W. (1999) Evanescent-wave microscopy: a new tool to gain insight into the control of transmitter release. *Philosophical Transactions of the Royal Society of London. Series B: Biological Sciences*, **354**, 307-318.
Oheim, M., Loerke, D., Stuhmer, W. and Chow, R.H. (1998) The last few milliseconds in the life of a secretory granule. Docking, dynamics and fusion visualized by total internal reflection fluorescence microscopy (TIRFM). *Eur Biophys J*, **27**, 83-98.
Pabst, S., Margittai, M., Vainius, D., Langen, R., Jahn, R. and Fasshauer, D. (2002) Rapid and selective binding to the synaptic SNARE complex suggests a modulatory role of complexins in neuroexocytosis. *J Biol Chem*, **277**, 7838-48.
Palade, G.E. and Palay, S.L. (1954) Electron microscope observations of interneuronal and neuromuscular synapses. *Anat Rec*, **118**, 335.
Palay, S.L. (1956) Synapses in the central nervous system. *J Biophys Biochem Cytol*, **2**, 193-202.
Rae, J.L. and Fernandez, J. (1991) Perforated Patch Recordings in Physiology. *Int.Union Physiol Sci*, **6**, 273-77.
Reichert, W.M. and Truskey, G.A. (1990) Total internal reflection fluorescence (TIRF) microscopy. I. Modelling cell contact region fluorescence. *J Cell Sci*, **96**, 219-30.
Rizo, J. and Sudhof, T.C. (2002) Snares and Munc18 in synaptic vesicle fusion. *Nat Rev Neurosci*, **3**, 641-53.
Saltzman, W.M., Parsons-Wingerter, P., Leong, K.W. and Lin, S. (1991) Fibroblast and hepatocyte behavior on synthetic polymer surfaces. *J Biomed Mater Res*, **25**, 741-59.
Scales, S.J., Bock, J.B. and Scheller, R.H. (2000) The specifics of membrane fusion. *Nature*, **407**, 144-6.
Schiavo, G., Benfenati, F., Poulain, B., Rossetto, O., Polverino de Laureto, P., DasGupta, B.R. and Montecucco, C. (1992) Tetanus and botulinum-B neurotoxins block neurotransmitter release by proteolytic cleavage of synaptobrevin. *Nature*, **359**, 832-5.
Segura, F., Brioso, M.A., Gomez, J.F., Machado, J.D. and Borges, R. (2000) Automatic analysis for amperometrical recordings of exocytosis. *J Neurosci Methods*, **103**, 151-6.
Shepherd, G.M. and Erulkar, S.D. (1997) Centenary of the synapse: from Sherrington to the molecular biology of the synapse and beyond. *Trends Neurosci*, **20**, 385-92.
Sherrington, C.S. (1897) In Foster, M. (ed.) *Textbook of Physiology*.
Shin, O.H., Rizo, J. and Sudhof, T.C. (2002) Synaptotagmin function in dense core vesicle exocytosis studied in cracked PC12 cells. *Nat Neurosci*, **5**, 649-56.
Smith, C., Moser, T., Xu, T. and Neher, E. (1998) Cytosolic Ca2+ acts by two separate pathways to modulate the supply of release-competent vesicles in chromaffin cells. *Neuron*, **20**, 1243-53.
Smith, C.B. and Betz, W.J. (1996) Simultaneous independent measurement of endocytosis and exocytosis. *Nature*, **380**, 531-4.
Sollner, T., Bennett, M.K., Whiteheart, S.W., Scheller, R.H. and Rothman, J.E. (1993a) A protein assembly-disassembly pathway in vitro that may correspond to sequential steps of synaptic vesicle docking, activation, and fusion. *Cell*, **75**, 409-18.

Sollner, T., Whiteheart, S.W., Brunner, M., Erdjument-Bromage, H., Geromanos, S., Tempst, P. and Rothman, J.E. (1993b) SNAP receptors implicated in vesicle targeting and fusion. *Nature*, **362**, 318-24.
Steinhardt, R.A., Bi, G. and Alderton, J.M. (1994) Cell membrane resealing by a vesicular mechanism similar to neurotransmitter release. *Science*, **263**, 390-3.
Steyer, J.A. and Almers, W. (1999) Tracking single secretory granules in live chromaffin cells by evanescent-field fluorescence microscopy. *Biophys J*, **76**, 2262-71.
Steyer, J.A., Horstmann, H. and Almers, W. (1997) Transport, docking and exocytosis of single secretory granules in live chromaffin cells. *Nature*, **388**, 474-478.
Sudhof, T.C. (2002) Synaptotagmins: why so many? *J Biol Chem*, **277**, 7629-32.
Sutton, R.B., Fasshauer, D., Jahn, R. and Brunger, A.T. (1998) Crystal structure of a SNARE complex involved in synaptic exocytosis at 2.4 A resolution. *Nature*, **395**, 347-53.
Tahara, M., Coorssen, J.R., Timmers, K., Blank, P.S., Whalley, T., Scheller, R. and Zimmerberg, J. (1998) Calcium can disrupt the SNARE protein complex on sea urchin egg secretory vesicles without irreversibly blocking fusion. *J Biol Chem*, **273**, 33667-73.
Toomre, D. and Manstein, D.J. (2001) Lighting up the cell surface with evanescent wave microscopy. *Trends in Cell Biology*, **11**, 298-303.
Tooze, S.A., Martens, G.J. and Huttner, W.B. (2001) Secretory granule biogenesis: rafting to the SNARE. *Trends Cell Biol*, **11**, 116-22.
Trimble, W.S., Cowan, D.M. and Scheller, R.H. (1988) VAMP-1: a synaptic vesicle-associated integral membrane protein. *Proc Natl Acad Sci U S A*, **85**, 4538-42.
Umbach, J.A., Saitoe, M., Kidokoro, Y. and Gundersen, C.B. (1998) Attenuated influx of calcium ions at nerve endings of csp and shibire mutant Drosophila. *J Neurosci*, **18**, 3233-40.
Vacquier, V.D. (1975) The isolation of intact cortical granules from sea urchin eggs: calcium lons trigger granule discharge. *Dev Biol*, **43**, 62-74.
Verhage, M., Maia, A.S., Plomp, J.J., Brussaard, A.B., Heeroma, J.H., Vermeer, H., Toonen, R.F., Hammer, R.E., van den Berg, T.K., Missler, M., Geuze, H.J. and Sudhof, T.C. (2000) Synaptic assembly of the brain in the absence of neurotransmitter secretion. *Science*, **287**, 864-9.
Vitale, M.L., Seward, E.P. and Trifaro, J.M. (1995) Chromaffin cell cortical actin network dynamics control the size of the release-ready vesicle pool and the initial rate of exocytosis. *Neuron*, **14**, 353-63.
Voets, T., Moser, T., Lund, P.E., Chow, R.H., Geppert, M., Sudhof, T.C. and Neher, E. (2001a) Intracellular calcium dependence of large dense-core vesicle exocytosis in the absence of synaptotagmin I. *Proceedings of the National Academy of Sciences of the United States of America*, **98**, 11680-11685.
Voets, T., Toonen, R.F., Brian, E.C., de Wit, H., Moser, T., Rettig, J., Sudhof, T.C., Neher, E. and Verhage, M. (2001b) Munc18-1 promotes large dense-core vesicle docking. *Neuron*, **31**, 581-91.
von Gersdorff, H. and Matthews, G. (1999) Electrophysiology of synaptic vesicle cycling. *Annual Review of Physiology*, **61**, 725-752.
Weber, T., Zemelman, B.V., McNew, J.A., Westermann, B., Gmachl, M., Parlati, F., Sollner, T.H. and Rothman, J.E. (1998) SNAREpins: minimal machinery for membrane fusion. *Cell*, **92**, 759-72.
Weimbs, T., Low, S.H., Chapin, S.J., Mostov, K.E., Bucher, P. and Hofmann, K. (1997) A conserved domain is present in different families of vesicular fusion proteins: a new superfamily. *Proc Natl Acad Sci U S A*, **94**, 3046-51.

White, J.G., Squirrell, J.M. and Eliceiri, K.W. (2001) Applying multiphoton imaging to the study of membrane dynamics in living cells. *Traffic*, **2**, 775-80.

Wiegand, U.K., Don-Wauchope, A., Matskevich, I., Duncan, R.R., Greaves, J., Shipston, M.J., Apps, D.K. and Chow, R.H. (2002) Exocytosis studies in a chromaffin cell-free system: imaging of single-vesicle exocytosis in a chromaffin cell-free system using total internal reflection fluorescence microscopy. *Ann N Y Acad Sci*, **971**, 257-61.

Wiegand, U.K., Duncan, R.R., Greaves, J., Chow, R.H., Shipston, M.J. and Apps, D.K. (2003) Red, yellow, green go!--A novel tool for microscopic segregation of secretory vesicle pools according to their age. *Biochem Soc Trans*, **31**, 851-6.

Wightman, R.M., Jankowski, J.A., Kennedy, R.T., Kawagoe, K.T., Schroeder, T.J., Leszczyszyn, D.J., Near, J.A., Diliberto, E.J., Jr. and Viveros, O.H. (1991) Temporally resolved catecholamine spikes correspond to single vesicle release from individual chromaffin cells. *Proc Natl Acad Sci U S A*, **88**, 10754-8.

Xu, T., Rammner, B., Margittai, M., Artalejo, A.R., Neher, E. and Jahn, R. (1999) Inhibition of SNARE complex assembly differentially affects kinetic components of exocytosis. *Cell*, **99**, 713-22.

Yang, B., Steegmaier, M., Gonzalez, L.C., Jr. and Scheller, R.H. (2000) nSec1 binds a closed conformation of syntaxin1A. *J Cell Biol*, **148**, 247-52.

Yoshihara, M., Adolfsen, B. and Littleton, J.T. (2003) Is synaptotagmin the calcium sensor? *Curr Opin Neurobiol*, **13**, 315-23.

Zimmerberg, J., Coorssen, J.R., Vogel, S.S. and Blank, P.S. (1999) Sea urchin egg preparations as systems for the study of calcium-triggered exocytosis. *J Physiol*, **520**, 15-21.

Zucker, R.S. (1996) Exocytosis: a molecular and physiological perspective. *Neuron*, **17**, 1049-55.

Appendix A

The TIRF Setup -- a guide

Georg Bodammer
20. August 1998
Modified
Andrew Don-Wauchope
14. May 1999

System Start-up

Decide if epifluoresence will be used. If so, then switch on the mercury lamp before switching on any other equipment.

CAUTION! Mercury lamp generates an electromagnetic wave that can damage electronic equipment that is powered.

1. Ensure that microscope camera shutter is closed (i.e. beampath to oculars is open)
2. Switch camera cooling-unit on.
3. Switch camera on.
4. Switch piezo-focus device on. (not yet linked to software)
5. Start computer. [Screensaver password is 'sommer'.]
6. Switch Uniblitz shutter on, flick the reset button, make sure shutter is closed (when both the green and red light on the right hand side of the controller are off).
7. Start MetaMorph and ensure that software and hardware are synchronised, i.e. the physical shutter state corresponds with the state the software thinks the shutter is in by opening the window *Set shutter state* from the Devices menu.
8. Make sure that heat indicator on controller shows -20. Should be running for half hour for optimum cooling.
9. Activate door interlock system and insure laser warning light in the corridor is illuminated.
10. Turn on cooling water supply.
11. Turn on 3-phase power behind apple stand.
12. Ensure that on the laser control panel the current control dial is set to its highest level (fully to right), the light control dial is turned fully off, and power selector pushbutton .2 W is pressed. Also, check that the Autostart button is pressed.
13. **CAUTION! Ensure again that mechanical shutter is closed and the prism is in its proper position on the microscope stage! Permanent damage to your eyes is otherwise possible.**

14. Insert safeties key and activate laser control panel. The warning about too little water flow should disappear after a few seconds. If not, try to adjust the water pressure by closing/ opening the valve at the short-circuited taps. Once all warning lights have disengaged press start on the control panel. After approximately 30 seconds the laser will have the potential to lase as indicated by the upper bar strip.
15. If the laser power is too high, the control panel will indicate an overpressure fault. D**o not** operate the laser for any length of time in this regime. The fault condition will be reset after turning the laser power (in these circumstances, the light regulator dial) below the fault indication threshold.
16. **CAUTION:** If any other fault (apart from the above mentioned ones) conditions occur, reduce laser power immediately and shut system down.

2. System shutdown

Emergency procedure

1. Stay calm. Move towards exit sign/ door and press emergency shutdown switch that is located to the right of the door.
2. Vacate the room, make sure door closes behind you.
3. Raise the alarm.

Scheduled shutdown

1. Set laser light regulator dial to lowest level. Press *off* switch on the control panel. Remove key and leave in secure place.
2. Raise microscope turret.
3. Switch 3-phase power at main isolator panel off.
4. After 5-10 minutes switch off laser cooling-water.
5. Shut computer down.
6. Switch camera and it's cooling water unit off.
7. Switch Uniblitz shutter off.
8. Switch piezo-focus driver unit off.
9. Remove culture dish.
10. Clean prism.
11. Reassemble microscope stage.

3. Trouble shooting

Laser

1. **Fault:** low water flow rate. **Solution:** close valve at short further to increase water flow through recirculation system. Make sure you do not cut off flow completely.
2. **Fault:** water high temperature.**Solution:** shut laser system down and contact departmental supervisor Bill Mitchell.
3. **Fault:** overpressure. **Solution:** reduce laser light power.
4. **Fault:** laser does not lase after pressing the start button.
   4.1. **Solution:** check for faults on the laser power control panel and look under the relevant section above.
   4.2. **Cause:** have you waited for less than 30 seconds? **Solution:** wait for at least 30 seconds after pressing the start button.
   4.3. **Cause:** has the door interlock been activated? **Solution:** activate door interlock.
   4.4. **Cause:** laser mirrors are not aligned properly. **Solution:** realign laser mirrors following the procedure outlined in the laser handbook: coarse vertical alignment. If you see a bright flash whilst wobbling the rear mirror using the big handle on top of the laser case at the rear, stop wobbling and try to find lasing conditions with the wavelength selector.**DO NOT TOUCH the rear mirror adjustment screws.**

Optics

1. **Fault:** low light level at fiber output.
   1.1. **Cause:** shutter closed. **Solution:** Check both shutters (i.e. the shutter at the end of the laser tube and the mechanical external shutter).
   1.2. **Cause:** low laser power. **Solution:** increase laser power. **CAUTION:** do not exceed maximum power ratings for fiber optics (500 mW).
   1.3. **Cause:** neutral density with too large ND number in use.**Solution:** change to lower ND number filter.
   1.4. **Cause:** optical fiber not optimally aligned.**Solution:** realign optical fiber following instructions in the fiber launcher manual. Usually, the fiber alignment only needs to be optimised. This is accomplished by adjusting the two screws on the launch block downstream from the laser. Make only tiny adjustments. The assembly is very sensitive.
   If small adjustments do not increase throughput significantly, remove fiber from fiber holder. Insert alignment support tool with pinhole *towards* laser. Make sure pinhole is clean and open. Maximise power throughput by adjusting the two screws at the back of the launch block. Only if

absolutely necessary loosen the screws that attach fiber launcher to the base plate and carry out a coarse adjustment. Once the throughput has been optimised insert the alignment support tool with the pinhole pointing *away* from the laser. Optimise the throughput using the two forward screws of the launcher block. Finally, re-insert the optical fiber cable and optimise the throughput using only the two forward screws. A good indication of optimised throughput is saturation of the photodiode in the Spindler & Hoyer adapter holder at lowest laser power and with ND 3.0 in the beampath.

2. **Fault:** light level indicator on laser control panel changes when mechanical shutter is operated. **Cause:** laser is operated in current control rather than light control mode. **Solution:** turn the current control dial fully to the right, and the light control dial fully to the left. The green light next to the light control dial should illuminate indicating that the laser is operating in light control mode. Make sure you always work in the light control mode, as the laser control system will otherwise attempt to achieve a constant current that will result in light level fluctuations that are undesirable.
3. **Fault:** low light level at the prism interface. **Cause:** beam not centred on objective. **Solution:** centre beam using x-y stage beneath the microscope stage.
4. **Fault:** a lot of background light is observed without the filterset. **Cause:** iris on stage launcher is too wide open. **Solution:** close iris as much as possible.
5. **Fault:** a lot of light is transmitted into the ocular without the filterset. **Cause:** total internal reflection does not occur. Prism is not flush with the top of the microscope stage. **Solution:** adjust prism position.
6. **Fault:** a lot of stray light is observed. **Cause:** prism not properly cleaned before use. **Solution:** clean prism again.
7. **Fault:** a lot of light is transmitted into the ocular without the filterset and ripples are visible. **Cause:** too much index-matching oil has been applied. **Solution:** remove prism and clean. Apply less index-matching oil.
8. **Fault:** focal plane changes a lot when moving culture dish and total internal reflection is difficult to achieve. **Cause:** dust particles between cover slip and prism surface. **Solution:** remove prism etc, clean prism and coverslip more carefully.
9. **Fault:** no fluorescence emission can be detected.
   9.1. **Cause:** wrong fluorophore. **Solution:** check the excitation and emission characteristics of your fluorophore.
   9.2. **Cause:** wrong filterset. **Solution:** check your filterset specifications. The filterset specs can be found on the rim of the filters. The filters need to be removed from the filtercube to allow inspection. **CAUTION:** Do not touch any filter surface. During re-assembly make sure that the arrow on the filters point in the direction of light propagation.

9.3. **Cause:** wrong excitation wavelength.**Solution:** check laser wavelength (with 488 nm excitation filter) and adjust laser wavelength if necessary using the wavelength selector dial at the rear end of the laser.

9.4. **Cause:** emission intensity too low. **Solution:** increase excitation light level.

9.5. **Cause:** camera exposure time too short. **Solution:** increase exposure time.

9.6. **Cause:** camera not sensitive enough. **Solution:** get in contact with camera vendor.

9.7. **Cause:** camera shutter or ocular shutter not in correct position**Solution:** bring shutter in correct position for respective observation mode.

9.8. **Cause:** no total internal reflection. **Solution:** check prism position.

10. **Fault:** no total internal reflection.

10.1. **Cause:** prism not optimally placed.**Solution:** readjust prism position and ensure that its surface is flush with top of microscope stage.

10.2. **Cause:** fluorophores not close enough to interface**Solution:** check that your fluorophore (in the cell or on your bead) is close enough to the optical interface to be excited by the evanescent wave.

10.3. **Cause:** to little excitation intensity. **Solution:** increase laser power or open up iris at stage launcher. See also causes for too little light intensity at interface above.

4. Software/ Hardware

1. **Fault:** MetaMorph does not start up.

1.1 **Cause:** hardware key not inserted properly. **Solution:** check whether the appropriate hardware key (the one which has the serial number 4158 attached to it) has been inserted. If yes, remove hardware key and re-insert it into printer port 1 (marked parallel port on the computer's case). If this does not help contact Princeton Instruments at 01628 890858 and ask for John Wilkinson/ Andrew Philipps.

1.2 **Cause:** camera power is not on. **Solution:** switch on camera

2. **Fault:** MetaMorph does start up but gives an error message regarding the system identification code. **Cause:** this is most probably caused by an out-dated version**Solution:** of the camera driver. Contact at John Wilkinson/ Andrew Philipps john@princt.co.uk**.**

3. **Fault:** Camera does not initialise. **Cause:** wrong version of camera drive is used. **Solution:** update camera driver. Contact John Wilkinson/ Andrew Philipps john@princt.co.uk**.**

4. **Fault**: Shutter does not respond.

4.1. **Cause:** shutter device not powered up. **Solution:** switch shutter controller on.

4.2. **Cause:** shutter not connected with controller unit. **Solution:** check cable connection between shutter and its controller unit.

4.3. **Cause:** after powering the unit up the reset switch has not been flicked. **Solution:** Press reset switch.

4.4. **Cause:** connection between PC and shutter unit loose. **Solution:** check cable connections. The cable should connect pins 14 and 24 of printer port LPT2 at the bottom of the computer with *Pulse Input* on the back of the shutter controller unit.

4.5. **Cause:** MetaMorph software is not properly configured. **Solution:** go to menu point *Devices Install and configure devices*. Find the configuration dialog for the Uniblitz Shutter. Make sure LPT2 and pin 14 is selected. Make sure that *Illumination Device* is activated in the software.

4.6. **Cause:** Computer not properly configured. **Solution:** check in *Settings System* that the second printer port has base address 278.

5. **Fault:** Focus device does not respond.

5.1. **Cause:** Controller not switched on. **Solution:** Switch controller on.

5.2. **Cause:** Faulty cable connections. **Solution:** Check cable connections between piezo unit and its controller.

5.3. **Cause:** Connection between PC and piezo controller loose. **Solution:** check cable connections. The cable should connect the *Input* BNC connector with the D connector on the D/A card that is the second one from the bottom. Signal is connected with pin 18 and ground with pin 25.

5.4. **Cause:** MetaMorph software is not properly configured. **Solution:** reconfigure device driver through menu point *Devices Install and configure devices*. Find the configuration dialog for the Physick driver. Make sure base address 300 is selected.

6. **Fault:** Camera does not appear to work.

6.1. **Cause:** Camera not switched on. **Solution:** Check whether camera is powered up.

6.2. **Cause:** Camera overheated. **Solution:** Switch camera off and check power unit.

6.3. **Cause:** Camera not properly connected to frame grabber board. **Solution:** Check camera cable correctly connected to camera, power supply and computer.

6.4. **Cause:** Inappropriate camera driver loaded. **Solution:** Using the *Video Manager* confirm that the correct camera driver (i.e. Princeton Instruments) has been installed. Remember to restart the computer after you made a change.

6.5. **Cause:** Camera drive not appropriately configured **Solution:** Using the *Video Manager* confirm that the Princeton Instruments driver has been configured correctly (i.e. set to a resolution of 512 x 512 pixels).

6.6. **Cause:** Shutter on microscope turret in position that directs the light to the ocular. **Solution:** bring turret shutter in appropriate position.

7. **Fault:** The EPC-9 does not respond to remote trigger. ***NOT YET CONNECTED TO TIRF SETUP***

7.1. **Cause:** EPC-9 not switched on. **Solution:** Switch EPC-9 on.

7.2. **Cause:** connections between PC and EPC-9 are loose. **Solution:** check the connections. The cable should run from pin 16 on the second parallel card (i.e. LPT2) to the input BNC connector on the **back** of the EPC-9. Pin 23 provided the common ground.

7.3. **Cause:** software not configured properly. **Solution:** make sure that the *custom I/O device* is active. Also in the *Devices Install and configure devices* menu, ensure that the output stream is fed through pin 16.

7.4. **Cause:** Journal has been deleted. **Solution:** for triggering the EPC-9 a journal has to be written. If you cannot figure out yourself how to do it contact Georg Bodammer at g.bodammer@ed.ac.uk**.**

8. **Fault:** Metamorph cannot be triggered by the EPC-9.

8.1. **Cause:** EPC-9 switched off. **Solution:** Switch EPC-9 on.

8.2. **Cause:** faulty connections between the EPC-9 and the PC. **Solution:** Make

9. **Fault:** Icons for MetaMorph cannot be found on the desktop **Cause:** Someone has messed about with the desktop. **Solution:** Look under the start menu for Metamorph.

Appendix B

3.1s PRIMARY CELL CULTURE TECHNIQUES

Standard operating procedure

Purpose:

Routine primary culture of bovine chromaffin cells for use in excitation and membrane patch experiments. The transfection procedure for introducing cDNA into the cells is also described.

COSHH Status:

The risk was low when the procedure involved cells derived from pathogen-free animals or cell lines which are known to be free of adventitious agents.

General Comments

- Good laboratory practice was required for all handling of reagents and animal tissues.
- All work involving the handling of potential pathogens should be performed in a Class II laminar flow hood or other microbiological safety cabinet appropriate to the organism involved.
- Working area must be cleaned before use and maintained accordingly using 70% ethanol.
- It was recommended that gloves and a laboratory coat were worn throughout procedure.
- All disposable contaminated items and spent media were autoclaved following use.
- Any contaminated sharps were disposed of in a sharps bin.
- Cultures that harboured pathogens were clearly labelled. A separate incubator was used for such specimens.
- When work was finished, uncontaminated and autoclaved waste was disposed of through the appropriate waste management system.

References

Lindau, M. and Neher, E. Pfluegers Arch. 411, 137-146 (1988)
Duncan, RR. Don-Wauchope, AC. *et al* .Biochemical Journal. 342, 497-501 (1999)

Materials

Cell culture media.
Dulbeccos Modified Eagle’s medium (DMEM) with HEPES, Gibco BRL Life Technologies
Dulbeccos Modified Eagle’s medium (DMEM) without HEPES and without NaPyruvate, Gibco BRL Life Technologies
Locke's solution, (see formulation below).
Antibiotics (filter sterile)
Penicillin /Streptomycin 0.1%, Gibco BRL Life Technologies
Supplements (filter sterile)
Insulin Transferrin Selenium supplement (ITSX), Gibco BRL Life Technologies
Sodium Pyruvate 1% w/v, Sigma Aldrich
Foetal calf serum, Gibco BRL Life Technologies.

For primary culture

Collagenase ,Worthington type 2 CLS2, S6C157 or similar activity
DNAse, Mannheim 104159 84838420-29/31

For Semliki Forest Virus procedures

Chymotrypsin A4, 250 mg/ml, Sigma-Aldrich
Aprotonin, 0.67 mg/ml, Sigma-Aldrich

Other standard reagents

70% ethanol
NaCl
KCl
K_2HPO_4
KH_2HPO_4
Glucose
HEPES
Distilled water
Bleach

Equipment

Light microscope.
Water bath (37°C).
Bench-top centrifuge.
Incubator at 37°C gassed with 95% air / 5% CO_2
Cell counter chamber for microscope (haemocytometer)

Plasticware

Cell culture flasks (sterile) 50ml.
Disposable plastic pipettes (sterile) 5,10 and 20ml.
Disposable plastic syringes (sterile) 10 and 20 ml.
Disposable plastic tubes (sterile) 10 and 20ml.
0.2 mm syringe filters (sterile).
100mm dishes (sterile)
Glassware
50 and 200 cm^3 beakers
3 x 200 cm^3 bottles
1 x 1000 cm^3 bottle

Other equipment

Toothed forceps
Plain forceps
Dissecting scissors
Size 100 scalpel blades
100 mm nylon mesh filter
Rubber boots
White coat
Latex gloves

Hair net
Hard hat
Containers for ice and transport of adrenal glands

Procedures:

Time:
Preparative: 30mins
Abattoir: 2-3 Hours
Primary Cell Preparation: 2-3hrs.

Solutions

Locke's 10X stock solution

NaCl	1542 mM
KCl	26 mM
K_2HPO_4	22 mM
KH_2HPO_4	85 mM
Distilled water	Up to 1000 ml

Locke's solution

Locke’s 10X stock	100 ml
Glucose	10 mM, 1.8g
HEPES	20 mM, 4.766g
Pen/Strep 0.1%	2 ml
Distilled water	Up to 1000 ml
pH correct to:	7.4

Digesting solution

Collagenase and DNAse are added at 0.25mg/ml and 0.18mg/ml to a measured amount of Locke's solution.

Culture medium

DMEM no NaPYR, no HEPES	98 ml
ITSX	1 ml
Na Pyruvate 1%	1ml
Pen/Strep 0.1%	0.1ml

Protocols:

A) Preparation for adrenal gland collection
[1] All the glassware and instruments were autoclaved before use.
[2] The Locke's solution (for storage and washing of adrenal glands) was prepared in advance and filtered through a 200nm sterile filter and then stored for use in 2 X 100ml and 1 X 250ml sterile jars..
[3] All the solutions were placed on ice in an appropriate container.
B) Abattoir
[1] Dress was appropriate according to the health and safety guidance given by the meat inspector. (White coat, hair net, hardhat and appropriate footwear (rubber boots) were required.)
[2] The adrenal glands were collected after the meat inspector had completed the health inspection of the offal.
[3] Excess connective tissue and fat was trimmed with dissecting scissors, taking care to protect the adrenal artery and vein.
[4] The cleaned gland was placed in ice-cold Locke's solution

[5] Once enough glands had been collected work was continued outside the cattle line of the abattoir. 4-6 glands of reasonable quality were usually sufficient. Occasionally a larger number were required.
[5] The adrenal glands were perfused with iced Locke's solution using a syringe.
[6] The adrenal glands were stored in clean sterile Locke's solution on ice.
[7] The glands were transported on ice to the laboratory.

C) Primary Cell Preparation

[1] All media, sera, antibiotics and any supplements needed from storage were placed in a 37°C water bath.
[2] The laminar flow hood was opened and the working area was cleaned with 70% ethanol.
[3] The media for primary cell culture were then made up, along with digesting solution and culture medium. Antibiotics and supplements were filter-sterilised before use. All media were placed in the 37°C water bath.
[4] The glands were removed from the storage jar and perfused with Locke's solution until no blood returned from the artery.
[5] Further perfusion with the warmed digesting solution was then performed. The gland was filled with digesting solution until the gland was swollen.
[6] The gland was then placed in a sterile beaker in the 37°C water bath for 5 minutes.
[7] The perfusion step was repeated with digesting solution a total of 4 times (steps 5 and 6).
[8] The gland was bisected by careful dissection to remove the medullary portion and the removed medulla was placed in a petri dish containing a few millilitres of the digesting solution.
[9] Mechanical dispersion of the adrenal medulla was performed using scalpel blades and the dispersed tissue was placed in a sterile jar containing a stir bar. The jar was then placed in the 37°C water bath and stirred gently for 20 minutes.
[10] The larger remains of the dispersed and digested medullary tissue were removed from the solution using forceps. The remaining solution was aspirated into a syringe and then filtered through a moistened (with digesting solution) 100 μm filter into a 20 ml sterile centrifuge tube.
[11] The centrifuge tube was placed in the bench-top centrifuge and spun at 700 rpm for 5 minutes.
[12] The supernatant was removed using the aspirator pipette.
[13] The cell pellet was resuspended gently using 5 ml of culture medium, then adding a further 15 ml of culture medium to bring the volume up to 20ml.
[14] Steps 11 to 13 were repeated for a second time.
[15] At this point, a cell count was carried out using a haemocytometer.
[16] Calculations of cell numbers were then performed to allow an appropriate cell concentration for the planned experiment. The cells were then reconstituted in culture medium.
[17] The cells were plated onto the appropriate glass coverslips in wells or in the bespoke dishes for the chosen experiments.
[18] More culture medium was used to top up the cell suspension volume per container to 1.5 ml.
[19] Covers were then placed over the cells and the containers placed in the appropriate cell culture incubator with 95% / 5% CO_2 at 37°C.

D) Transfection protocol.

Extra precautions must be taken when working with the viral agent. All of these procedures must take place in the level 2 cell culture room following standard procedure and the universal precautions mentioned above must be adhered to.
[1] All media, sera, antibiotics and any supplements needed from storage were placed in a 37°C water bath.
[2] The laminar flow hood was opened and the working area was cleaned with 70% ethanol.
[3] The made up media, antibiotics and supplements were filter-sterilised before use.
[4] The required viral stock (200 μl) was defrosted.
[5] Chymotrypsin 10μl (250μg/ml) was added to the virus containing medium and left on ice for 10 minutes allowing the virus to become activated by digestion, then 2 μl aprotonin (0.67μg/ml) was added to halt the proteolysis.

[6] 2ml suspension cells were removed from the concentrated cell solution after resuspension and the activated virus was added. Alternatively 20ml of the activated viral stock was added to the cells plated on the bespoke microscope dishes.
[7] The mixture of cells and viral stock was stirred gently for 5 minutes.
[8] The cells were resuspended to the required volume for plating onto glass cover-slips or the bespoke microscope dishes.
[7] The covers were then placed over the cells and the containers then placed in the appropriate cell culture incubator with 95% air / 5% CO_2 at 37°C.

3.3s BESPOKE DISHES FOR MICROSCOPY

Standard operating procedure

Purpose:

Preparation of dishes used for cell culture and experiments on living cells with microscopy.

COSHH Status:

There was a moderate degree of risk when these dishes were being prepared. This related to the use of acid and alkali and in some instances the silane (medium risk) treatment.

General Comments

- Good laboratory practice was required for all handling of reagents and animal tissues.
- It was recommended that gloves and a laboratory coat were worn throughout procedure.
- All disposable contaminated items and spent media were autoclaved following use.
- Any contaminated sharps were disposed of in a sharps bin.
- Care must be taken when using the acid and alkali and particular care must be taken when preparing the acid and alkali solutions from concentrated stock. Appropriate safety equipment must be used during these steps.
- Any waste solution must be disposed of properly with adequate volumes of water.
- Working area must be cleaned before the procedure is started and sterile areas must be maintained accordingly using 70% ethanol.
- When work was finished, uncontaminated and autoclaved waste was disposed of through the appropriate waste management system.

References:

Nobles, M and Abbott, NJ. Endothelium. 4, 297-307. (1996)
Aplin, JD and Hughs RC. Anal Biochem. 113, 144-8. (1981)
Macklis, JD. Sidman RL, *et al*. In Vitro Cell Dev Biol . 21, 189-94. (1985)
Saltzman, WM. Parsons-Wingerter, P. *et al*. J Biomed Mater Res. 25, 741-59 (1991)

Reagents:

0.1N sulphuric acid
0.1N NaOH
3-aminopropyltriethoxysilane (APTS), Sigma-Aldrich
Distilled water
Sterile filtered distilled water
Glutaraldeyhde (approx.50%w/v))
Hanks Balanced Salt Solution (HBSS), Gibco BRL Life Technologies
Collagen type I, 0.4mg/ml, Sigma-Aldrich
Collagen type IV, 0.4mg/ml, Sigma-Aldrich
Poly-L-lysine, 0.1mg/ml, Sigma-Aldrich
Fibronectin, 0.01mg/ml, Sigma-Aldrich
70% ethanol
Ammonia (~14.8M)

Equipment:

Cover-slips 16mm / 19mm
Gauze
Orange sticks
Silgard
35 mm dishes, Nunc/ white Teflon‘ / black vinyl/ aluminium coated with Teflon‘
100 mm sterile dishes with lids
12 well cell culture plates with lids
Incubator: 80^{o}C oven
Fume hood
Level 1 hood
Incubator at 37°C in presence of 95% air and 5% CO_2
Glassware
50, 200, 1000 cm^3 beakers

Procedures:

Time:
Preparative: 30mins
Basic Procedure: 5 hours, and then overnight to dry
Protein treatment: 2-3 hours, and then overnight to dry

Protocol:

A) **Preparation of bespoke dishes**
[1] The dishes were placed on a metal sheet for use in the oven.
[2] The edge of the hole in the dish was lined with a thin layer of Silgard using an orange stick as the applicator.
[3] A coverslip was placed evenly over the hole
[4] The Silgard was allowed to cure overnight or cured at 60^{o}C in the oven for 1 hour. CAUTION: do not use oven for white dishes.

B**) Glass cover-slip cleaning**
Two methods of cleaning the glass were used depending on the planned experiment.
a)
[1] The bespoke dishes were placed in 0.1N sulphuric acid for 1 hour.
[2] These dishes were then removed from the sulphuric acid and placed in 0.1N sodium hydroxide for 10 minutes.
[3] The dishes were removed from the sodium hydroxide and rinsed 3 times with distilled water.
[4] Sterilization procedure follows in section D.
b)
[1] The laminar flow hood was opened and the working area cleaned with 70% ethanol.
[2] Each coverslip was picked up with forceps, dipped into 70% alcohol and then passed through a flame from bunsen burner.
[3] The coverslips were then placed in the cell culture wells (12 well plate) and then sterilised by UV light.

C) **Silane treatment**
Extra precaution was taken when working with silane and glutaraldehyde. All these procedures took place in the fume hood and the universal precautions mentioned above were adhered to.
[1] 3-aminopropyltriethoxysilane (APTS) was placed on the cover-slips (one side) and then left for 4mins.

[2] The APTS was then removed and disposed of with copious water down the drain in fume hood.
[3] The coverslips were then washed carefully with distilled water.
[4] The coverslips then had 1% w/v glutaraldehyde (diluted in HBSS) placed on them to cover the area treated with APTS and then they were incubated at room temp for 30 minutes.
[5] A further washing step was then carried by rinsing 3 times with HBSS.

D) **Sterilisation protocol**
[1] The bespoke dishes with coverslips in place and cleaned as described above were placed in 70% ethanol for 1 hour.
[2] The laminar flow hood was opened and the working area cleaned with 70% ethanol.
[3] The dishes were removed from the 70% ethanol inside the laminar flow hood and rinsed with sterile filtered distilled water.
[4] 3 bespoke dishes were placed in a 100mm dish.
[5] The aspirator pipette was used to rinse each bespoke dish 3 times with sterile filtered distilled water.
[6] The 100mm dishes were covered with their lids and placed in the drying oven upside down and left until the liquid had evaporated.

E) **Protein treatment**
[1] The laminar flow hood was opened and the working area cleaned with 70% ethanol.
[2] The 100mm dishes with 3 bespoke dishes that had been prepared and sterilised as described above were placed inside the laminar hood and had the lids removed.
[3] 0.3 ml of protein solution was applied at required concentration to centre of each glass coverslip.
[4] The dishes were covered and placed in the appropriate incubator at 37°C in presence of 95% air and 5% CO_2 at 37°C.
[5] They were then removed from incubator and placed back in the laminar flow hood.
[6] The remaining fluid was aspirated and the covers were placed over the dishes again.
[7] The 100mm dishes were then transferred to fume cupboard and fumigated with ammonia fumes for 10 minutes.
[8] These dishes were then placed in storage cupboard overnight to allow drying.

3.4.3sA TOTAL INTERNAL REFLECTANCE FLUORESCENCE MICROSCOPY (TIRFM)

Standard operating procedure

Purpose:

To describe the practical use of the TIRFM equipment.

COSHH Status:

This microscope was a class 2 laser and any person who used it had undergone appropriate laser safety training. All users had signed the appropriate COSHH forms. With the appropriate training and use of the correct guidelines the risk of injury was minimal.

General Comments

- Good laboratory practice was required for all handling of reagents and animal tissues.
- A laboratory coat was worn throughout procedure and eye protection was used whenever the laser beam was exposed.
- When work was finished, uncontaminated and autoclaved waste was disposed of through the appropriate waste management system.

References:

Bodammer, G. The TIRF Setup - a guide (1998) (Modified Don-Wauchope, AC (1999)), see appendix A.
Oheim, M. Loerke, D. *et al.* Philosophical Transactions of the Royal Society of London. Series B: Biological Sciences. 354, 307-318 (1999)
Duncan, R.R.. Greaves, J. *et al.* Nature. 422, 176-80 (2003)

Equipment:

415V power supply, Leeds Transformer Co
Coherent INOVA 90 argon ion laser
Fibre optic cable and coupling device
Olympus upright microscope with purpose engineered stage
Princeton instruments digital camera
Uniblitz shutter driver
Image intensifier, Princeton instruments
PC to run controlling software
Glass prism (70^{o})
200nm fluorescent beads, Molecular Probes
Bespoke dish
Lens cleaning paper
Isopropanol
Acetone
LENS CLENS“ kit
Sonicator
Drying oven

The instructions for switching on and maintaining the equipment can be found in the document: The TIRF setup (appendix A). The important procedures for experiments are described here.

Protocols

(A) **Centring the laser spot for TIRFM**
To optimise TIRFM illumination, the laser beam was aimed at a central spot on the top surface of the trapezoidal prism. To arrange this, there were two basic steps:
(i) Arranging Kohler illumination of the transillumination system and stopping down the field diaphragm, so that the transilluminated light is confined to an easily visible spot, centred in the objective field.
(ii) Securing the fiber-optic light guide to the microscope bench system, stopping down the iris diaphragm to the smallest diameter, and adjusting the X-Y translational stage to position the laser spot at the same place as the transillumination spot.

[1] The trapezoidal prism was placed in its cradle on the microscope stage. It fell into a stable, non-mobile position.
[2] A drop of immersion oil was placed on top of the prism and then the glass-bottomed chamber with 200-nm fluorescent beads dried on the chamber bottom was placed on the oil drop. (The 200 nm fluorescent bead cover-slip was prepared previously by applying a small drop of bead suspension in distilled water and allowing the water to evaporate)
[3] The 40X dry objective Focus was focussed on to the chamber bottom.
[4] The condenser front lens was rotated into position above the condenser assembly and the entire assembly was advanced upwards until it just touched the prism, then it was slightly lowered, so that it was no longer in contact with the prism.
[5] The condenser field diaphragm (located below the condenser assembly, on the microscope base) was closed down to a tiny spot.
[6] While looking through the microscope, the transillumination spot in the microscope's objective field was centred, using the two knurled knobs attached at the sides of the condenser assembly. When positioned correctly, the spot was in the centre of the microscope field, and it was possible to see the spot when looking into the chamber from the side. If it was not possible to see the spot from the side of the chamber, the light intensity was increased or the diameter of the field diaphragm aperture was increased. The spot was then located in the midpoint of the prism. If this did not line up then the prism cradle was moved until the spot appeared at the midpoint of the prism's top face.
[7] Adjustments of the laser beam position were then made. To allow the laser light to enter the microscope stage the Uniblitz shutter was switched to open, and the diaphragm in the laser beam pathway was stopped down to its smallest diameter.
[8] Then by using the X-Y translational stage, the laser beam spot was positioned at the same point as the transillumination spot.

When these steps have been completed, the transillumination spot and the laser spot should coincide in the centre of the microscope's objective field. This was confirmed by looking through the microscope at the coverslip. Total internal reflection illumination was then visualised.

To demonstrate that TIR illumination, a drop of bead suspension was added on top of the beads that had been previously dried onto the bottom of the glass chamber. When using TIR illumination, only the beads attached to the glass bottom were seen. When the epi-illumination system with a filter set that selected the 488 nm light was activated, not only the stationary beads on the bottom of the chamber were observed, but also beads dancing above the bottom of the chamber.

The transmitted light was set-up for Kohler illumination. Once in position the fine adjustment of the laser position was left untouched. If TIRF was not seen on cells then it was often a biological problem, rather than a problem with the physics. Fine adjustments were often made to optimise the fluorescence, particularly during the learning phase, but fine adjustments were not made once experiments were being underway.

(B) **Cleaning the prism**
This was a regular procedure carried out after every occasion that a dish had been coupled to the prism with immersion oil.
[1] A sheet of lens paper was cut into strips
[2] A strip of lens paper was placed on the prism.
[3] A drop of acetone was placed onto the paper and then the paper was dragged over the prism surface.
[4] After the acetone had evaporated a drop of isopropanol was placed onto the paper and then dragged over the surface again.
[5] This was repeated for all surfaces of the prism.
The acetone was to remove the oil from the surface. The procedure often required repeating with isopropanol a number of times to clean the lens.
[6] On one occasion monthly, or at any other time that this was required, the general lens cleaning solution (LENS CLENS“) was used to give the prism a thorough clean.

(C) **Cleaning a spillage of liquid onto the condenser**
The design of the dishes meant that spills of culture medium could not always be prevented. The position of the lens was also important because if it was pushed onto the glass surface it was likely to cause a flood of fluid from the dish.
[1] The condenser was removed and any excess liquid was dried up.
[2] The liquid usually got into the iris section and this needed to be dried and cleaned.
[3] The iris was cleaned in the sonicator.
[4] The iris was dried in a drying oven.
[5] All the lens surfaces were cleaned with the appropriate cleaning agent LENS CLENS“ for plastic, coated optics etc. available.
[6] All the parts were reassembled once clean and dry.

3.4.3sB USING METAMORPH‰

Standard operating procedure

Purpose:

To describe the practical use of Metamorph‰software.

COSHH Status:

Standard PC operating procedures must be followed, with correct seating and positioning of the computer components

References:

Metamorph‰help files on CD-ROM.

Equipment:

Windows 95‘ PC to run software.
Serial port dongle.
Software package from Universal Imaging Corporation.
The software was designed to work in Windows 95‰and the basic operation of the software was similar to other Windows 95‰software. Important procedures for experiments are described here.

Protocols

(A) **Define acquisitions**
[1] The define acquisitions window was selected from the toolbar in Metamorph‘ .
[2] The exposure time was defined, usually 25 milliseconds.
[3] The gain was then set to allow enough light to be detected for recording purposes. The gain was adjusted on the image intensifier with TIRF (too much light would saturate the recording chip).

(B) **Journal set up**: to enable software to run imaging sequences during procedures.
[1] The journal window was selected from the toolbar in Metamorph‘ .
[2] The journals were either recorded by using the record facility or written following the instructions in the required text format. See figure 3.4.3sB for an example of a journal.
[3] The timing of each phase was set correctly for the experiment.
[4] Settings for focal plane steps were made if required.
[5] The settings for exposure were dependent on the settings chosen in the define acquisitions window.

(C) **Focus controller**
[1] The focus window was selected from the toolbar in Metamorph‘ .
[2] The piezo focus device was switched on.
[3] The microscope was focussed manually.
[4] The focus controller was set to zero.
[5] The expected movement range required (-50 to 50 nm) was checked by running the piezo focus device with the software.

```
VERSION 2.3
Application stream
Function jnlAcqStream
        Image 59      imNew                m       Acquire Stream
End
Application mmproc
Function stackOpsJNL
        Integer       3       iOperation
        Image 4       imStack              m       Stream
        Image 5       imResult             m       Average
End
Application mmproc
Function uniqueSaveJNL
        Image 33      imSave               m       Untitled
End
Application mmproc
Function jnlCloseImage
        Image 34      im              m     Stream
        Logical       35      bSaveIt             FALSE
End
```

Note:

- These journals are set to do 4 or 8 images in a stream. This takes as long as the exposure time is set for.
- If the stream function is open either journal will run for the number given to the stream function.
- The stream is averaged, the stream saved with the sequential file function, the next stream will be stacked onto the average stack.
- It is important to set up the sequential file information prior to running this journal.
- It is useful for TIRF image collection once the focal plane is established.

Figure 343sB Example of a journal for Metamorph™

(D) **File naming**
[1] A directory was created for each experiment.
[2] The sequential file name function was used to allow the software to automatically generate and save files created from the imaging device.

(E) **Region selection**
[1] The region window was selected from the toolbar in Metamorph‘ .
[2] The marker was placed over the area of interest for imaging.

(F) **Image analysis**
[1] Metamorph‰has built-in de-convolution processes based on the Fourier theory. By using known objects (fluorescent latex beads of 200nm, molecular probes) we were able to define a suitable de-

convolution algorithm for use on individual vesicles. This enabled images of the object to be viewed with less background haze and hence more could be determined about the functions being investigated. (Figure 3.5.1)
[2] The image analysis window was selected from the toolbar in Metamorph‘ .
[3] An appropriate algorithm was selected.
[4] The algorithm was applied to image.
[5] The modified image was saved as a file.
[6] Data generated in Metamorph‘ were exported directly to Microsoft Excel by using the export data function.
[7] A variety of measurements could be applied to areas of interest. For example fluorescence intensity measurements were performed through a stack of images representing a time course experiment.
[8] Further data analysis could be undertaken in Microsoft Excel or Igor pro.

(G) **Vesicle exocytosis**
[1] A stack of images from an experiment were opened in Metamorph‘ .
[2] Single vesicles were selected by using the region tools function and placing a 7 X 7 pixel region over the vesicle. (Figure 3.5.2)
[3] The image stack was played to check that the vesicle was covered by the chosen region throughout the image stack, or until the vesicle had disappeared.
[4] A second, larger, region of 16 X 16 pixels was placed over the first region. (Figure 3.5.2)
[5] Steps 2-4 were repeated for all single vesicles visible in the stack of images.
[6] A data transfer file for Microsoft Excel was opened using the image analysis window in Metamorph‘ .
[7] Measurements for the regions, including time and average intensity, were then recorded.
[8] Once recorded the Microsoft Excel file was opened, a decimal time column was inserted and decimal time calculated (1024 X time field), an intensity difference column was inserted and the average intensity difference between the paired regions calculated.
[9] The Intensity difference was plotted against decimal time to look for vesicles that undergo sudden disappearance (exocytosis).

3.6.2s EXCITATION OF BOVINE ADRENAL CHROMAFFIN CELLS

Standard operating procedure

Purpose

Stimulation of exocytosis from cultured bovine adrenal chromaffin cells allowing measurement of episodes of exocytosis by TIRFM.

COSHH Status

Risks were low when experiments involved cells derived from pathogen-free animals or cell lines which were known to be free of adventitious agents. Cells transfected by Semliki Forest Virus were of medium risk, as the virus was not known to be a pathogen in humans.

General Comments

- Good laboratory practice was required for all handling of reagents and animal tissues.
- All work involving the handling of potential pathogens should be performed in a Class II laminar flow hood or other microbiological safety cabinet appropriate to the organism involved.
- Working area must be cleaned before use and maintained accordingly using 70% ethanol.
- It was recommended that gloves and a laboratory coat were worn throughout procedure.
- All disposable contaminated items and spent media were autoclaved following use.
- Any contaminated sharps must be disposed of in a sharps bin.
- Cultures that harboured pathogens were clearly labelled. A separate incubator was used for such specimens.
- When work was finished, uncontaminated and autoclaved waste was disposed of through the appropriate waste management system.

Reagents

Fluorescent Dyes for vesicles
Acridine orange, 2.5 mM,Sigma
LysoSensor Green, 40 nM, Molecular Probes
LysoTracker Red, 40 nM, Molecular Probes

Standard reagents
NaCl
KCl
$CaCl_2$
$MgCl_2$
HEPES
Glucose
NaOH
Distilled water

Equipment

Glass beakers 50ml
Glass bottles 250ml

Syringes 1/2.5/10/20 ml
Adjustable micro-pipettes and tips for 20 µl/ 100 µl / 1000 µl
Stir bars and plate
Level 1/2 laminar flow hood
Incubator at 37°C gassed with 95% air/5% CO_2

Procedures

Time:
Preparative: 1 hour
Experimental Procedure: 30 minutes to 1 hour per cell

Solutions

External solution

NaCl	140	mM
KCl	2.8	mM
$CaCl_2$	2.0	mM
$MgCl_2$	0.2	mM
HEPES NaOH (titrated to pH7.2)	10	mM
Glucose	10	mM

Excitation solution

NaCl (this varied from 82.8-22.8mM)	82.8	mM
KCl (this varied from 60-120mM)	60	mM
$CaCl_2$	2.0	mM
$MgCl_2$	0.2	mM
HEPES NaOH (titrated to pH7.2)	10	mM
Glucose	10	mM

Protocol

A) **Basic stimulation experiment**
[1] The laser, microscope, computer and stage-heating device (this required 2 hours to warm the microscope to 30^{o}C) were switched on.
[2] The laminar flow hood was opened and the working area was cleaned with 70% ethanol.
[3] A 100mm dish with cultured cells in 3 bespoke dishes was removed from the incubator.
[4] The dye (usually acridine orange, see staining procedure below) was added to the culture medium in which the cells were cultured. If the cells had a transduced GFP tagged protein this step was not performed unless dual staining with Lysotracker Red was required.
[5] The 100mm dish was placed back into the appropriate incubator for 20 minutes.
[6] During the 20 minutes the computer was set and the microscope stage was prepared for the experiment.
[7] The excitation fluid was prepared and the micro-pipettes checked.
[8] The 100mm dish was removed from incubator and the culture medium with dye was aspirated from the bespoke dish, the cells were washed twice with HBSS warmed to 37 ^{o}C and the culture medium was replaced with 500 µl external solution warmed to 37 ^{o}C.
[9] The bespoke dish was carefully transported to the TIRFM laboratory.
[10] The dish was placed in the holder on the microscope stage.
[11] A cell was selected under transmitted light.

[12] The selected cell was imaged with TIRFM, and if the cell was suitable then the experiment began, otherwise repeat step 11.
[13] The imaging sequence was selected and preparations to stimulate cell the cell were made.
[14] 500 ml of excitation solution was added with a micro-pipette at correct time in sequence.
[15] Images were collected for the required period of time for the experiment. Exocytosis was expected to occur within 2 minutes of the addition of the excitation medium.
[16] The data stack was saved.
[17] All used items were disposed of in the appropriate manner.
[18] The prism was cleaned for next experiment.

B) **Staining of Vesicles**
Large dense core vesicles in bovine adrenal chromaffin cells are acidophilic and take up dyes that concentrate and fluoresce in an acid environment. We used a number of such dyes for their different characteristics. Acridine Orange was used most often and was used for all of the experiments analysed in the methods section.
[1] Steps from procedure A 1- 3 were followed.
[2] The dye of choice was selected and applied according to following:
Acridine Orange (2 mmol/L) use 10ml per 2ml of culture medium.
LysoTracker Red“ (40 nM) use 20ml per 2ml of culture medium.
LysoSensor Green“ (40 nM) use 20ml per 2ml of culture medium.
[3] The incubation period was 20 minutes. The recommended period for the Molecular probes products was 30 minutes but we found that we had suitable uptake of dye after 20 minutes.
[4] Step 8 from procedure A was then followed.

3.6.3s MEMBRANE PATCH

Standard operating procedure

Purpose

Preparation of a membrane patch for use in other experiments.

COSHH Status

Risks were low when experiments involved cells derived from pathogen-free animals or cell lines which were known to be free of adventitious agents. Cells transfected by Semliki Forest Virus were of medium risk, as the virus was not known to be a pathogen in humans.

General Comments

- Good laboratory practice was required for all handling of reagents and animal tissues.
- All work involving the handling of potential pathogens should be performed in a Class II laminar flow hood or other microbiological safety cabinet appropriate to the organism involved.
- Working area must be cleaned before use and maintained accordingly using 70% ethanol.
- It was recommended that gloves and a laboratory coat were worn throughout procedure.
- All disposable contaminated items and spent media were autoclaved following use.
- Any contaminated sharps must be disposed of in a sharps bin.
- Cultures that harboured pathogens were clearly labelled. A separate incubator was used for such specimens.
- When work was finished, uncontaminated and autoclaved waste was disposed of through the appropriate waste management system.

Reagents

Fluorescent Dyes for vesicles
Acridine Orange, 2.5 mM,Sigma
LysoSensor Green, 40 nM, Molecular Probes
LysoTracker Red, 40 nM, Molecular Probes

Standard reagents
NaCl
L-Glutamic acid
$CaCl_2$
$MgCl_2$
MgATP
GTP
HEPES
Glucose
KOH
Distilled water

Equipment

Glass beakers 50ml
Glass bottles 250ml

Syringes 1/2.5/10/20 ml
Adjustable pipettes and tips for 20 µl/ 100 µl / 1000 µl
Stir bars and plate
Level 1/2 laminar flow hood
Incubator at 37°C in presence of 95% air and 5% CO_2
Glass 1mm diameter micropipettes
Pipette puller
Rack for storage of pulled pipettes

Procedure

Time:
Preparative: 1 hour
Experimental Procedure: 30 minutes to 1 hour per cell

Protocol

Solutions
Internal solution

L-Glutamic acid (monopotassium salt)	145	mM
NaCl	8	mM
$MgCl_2$	1	mM
MgATP	4	mM
HEPES (KOH titrated to pH 7,2)	10	mM
EGTA	1	mM
GTP	0.3	mM
Glucose	10	mM

NB. Ca^{2+}-free solution with Ca^{2+} chelator

A) **Preparation of rupturing pipette**
This technique produced a pipette with an opening about half the diameter of a chromaffin cell (~10µm) and was suitable for applying a jet of fluid over the cell allowing rupture of the cell membrane and washing out of the cell contents.
[1] The pipette puller was switched on.
[2] A pipette was placed in the puller with 5mm of the pipette protruding above the top clamp. The top heater filament was set to 2mm and the base clamp to 3.5mm.
[3] The first heat setting was set at 100%
[4] The second heat setting was set at 4.0
[5] The heater on the pipette puller was activated
[6] The position of the pipette was not adjusted after the first pull
[7] The second heater on the pipette puller was activated
[8] The pipette was removed and checked under microscope that there was an open tip.

B) **Basic membrane patch preparation**
[1] The laser, microscope, computer and stage-heating device (this required 2 hours to warm the microscope to 30°C) were switched on.
[2] The rupturing pipette was prepared, placed in the holder and flushed through with internal solution without MgATP or GTP.
[3] The laminar flow hood was opened and the working area was cleaned with 70% ethanol.
[4] A 100mm dish with cultured cells in 3 bespoke dishes was removed from the incubator.

[5] The dye (usually Acridine Orange) was added to the culture medium in which the cells were cultured. If the cells had a transduced GFP tagged protein this step was not performed.
[6] The 100mm dish was placed back into the appropriate incubator for 20 minutes.
[7] During the 20 minutes the computer was set and the microscope stage was prepared for the experiment.
[8] Thawed MgATP and GTP (from frozen stock) were added to the pre-prepared internal solution.
[9] The 100mm dish was removed from incubator and the culture medium with dye was aspirated from the bespoke dish, the cells were washed twice with HBSS warmed to 37 ^{o}C and the culture medium was replaced with 500 ml external solution with MgATP and GTP warmed to 37 ^{o}C.
[10] The bespoke dish was carefully transported to the TIRFM laboratory.
[11] The dish was placed in the holder on the microscope stage.
[12] A cell was selected under transmitted light.
[13] The selected cell was imaged with TIRFM, if the cell was suitable then the experiment began, otherwise repeat step 12.
[14] The rupturing pipette was placed over the cell.
[15] By using the jet of internal fluid the cell was broken open and the cell contents were washed away as far as possible, leaving behind some membrane tethered to the glass surface.
[16] A 10 minutes imaging sequence was started, unless another length of time was preferred.
[17] 10 ml 1M Ca^{2+} Chloride was added to overcome EGTA 1mM at the chosen time point if required to stimulate exocytosis.
[18] The data stack was saved.
[19] All used items were disposed of in the appropriate manner.
[20] The prism was cleaned for next experiment.

Appendix C

Published papers. Permission to place copies of these papers has been given by the respective editors.

RESEARCH COMMUNICATION

High-efficiency Semliki Forest virus-mediated transduction in bovine adrenal chromaffin cells

Rory R. DUNCAN, Andrew C. DON-WAUCHOPE, Sompol TAPECHUM, Michael J. SHIPSTON, Robert H. CHOW and Peter ESTIBEIRO[1]

Membrane Biology Group, Biomedical Sciences, University of Edinburgh Medical School, Teviot Place, Edinburgh, EH8 9XD, U.K.

Adrenal chromaffin cells are commonly used in studies of exocytosis. Progress in characterizing the molecular mechanisms has been slow, because no simple, high-efficiency technique is available for introducing and expressing heterologous cDNA in chromaffin cells. Here we demonstrate that Semliki Forest virus (SFV) vectors allow high-efficiency expression of heterologous protein in chromaffin cells.

Key words: acidic vesicle, confocal, double C2 protein β-isoform, exocytosis, SFV.

INTRODUCTION

Adrenal chromaffin cells have long been a model system of choice for studies of exocytosis. These neuroendocrine cells, like neurons, fire action potentials, exhibit calcium-dependent exocytosis, and express many proteins closely related to synaptic proteins.

An important barrier to the advance in understanding of the molecular mechanisms underlying exocytosis is the lack of a high-efficiency technique for introducing heterologous DNA or RNA into chromaffin cells. 'Traditional' methods for mammalian cell transfection, such as calcium phosphate precipitation, lipid-mediated transfection and electroporation have met with limited success and have variable efficiencies [1–4].

A number of viral transduction systems have been developed to permit the efficient transduction of cDNA into eukaryotic cells. The ideal viral-vector system would be easy to use, have a broad host range but low human pathogenicity, and permit efficient infection of target cells with high-level protein expression and low cytotoxicity. Of the existing expression systems for higher eukaryotic cells, perhaps the most efficient in terms of protein production is the baculovirus system for insect cell hosts [5]. Efficient viral transduction systems for mammalian cells based on a recombinant vaccinia virus, adenovirus or defective herpes simplex virus-1 have been developed (for a review, see [6]), but these require considerable expertise for use and can be time-consuming and expensive. In addition, adequate containment facilities may not be available.

The recently introduced Semliki Forest virus (SFV) transduction system [7,8] has several potential benefits over other viral transduction systems, in particular, minimal containment requirements and ease of use. The gene of interest may be ligated directly to a DNA cloning vector encoding non-structural SFV genes for replicase, reverse transcriptase and helicase. After *in vitro* transcription, resultant capped RNA is co-electroporated alongside structural gene RNA into a permissive host cell line, commonly baby-hamster kidney (BHK)-21 cells. Attenuated, non-infectious packaged viral particles are assembled in the host cells, secreted into the extracellular medium and can be stored for future use. Treatment of these viral particles with a protease renders them infectious [7–8].

The SFV transduction system has already been used to express a number of proteins in a broad range of mammalian cells, including cultured rat hippocampal neurons, BHK-21, HeLa, and Madin–Darby canine kidney cells [7–10,11]. This broad host cell range, the ability to sub-clone directly into the expression vector without the need for *in vivo* recombination steps, and the excellent attenuation of recombinant SFV together make this system a particularly attractive candidate for transducing cDNA into chromaffin cells. In the present study, we examine the efficacy of SFV transduction of green fluorescent protein (GFP) mut3 and double C2 protein β-isoform-enhanced GFP (DOC2β-EGFP) in chromaffin cells. DOC2β is a protein that has been shown to associate with secretory vesicles previously [12], and which may play a role in exocytosis [13]. Efficient SFV transduction of chromaffin cells is obtained with the modification of previously published procedures.

MATERIALS AND METHODS

Isolation of a cDNA encoding mouse brain DOC2β

A reverse-transcription PCR strategy was used to amplify a cDNA encoding the open reading frame of mouse brain DOC2β. mRNA (1 μg) was used as a template in a first-strand cDNA synthesis directed from an anchored deoxyoligo d(T) (5′-TTCTAGAATTCAGCGGCCGC$(T)_{30}N_1N_2$) primer, using Superscript II reverse transcriptase (Gibco BRL Life Technologies). The resultant cDNA was diluted and used in a PCR reaction between forward (5′-CTGCCTGCATGACCCTCCGGC) and reverse (5′-TCAGTCGCTGAGYACAGCCCCTG-

Abbreviations used: BHK, baby-hamster kidney; DOC2β, double C2 protein β-isoform; GFP, green fluorescent protein; EGFP, enhanced GFP; SFV, Semliki Forest virus.

[1] To whom correspondence should be addressed (e-mail Peter.Estibeiro@ed.ac.uk).

GG) deoxyoligonucleotides, using Expand polymerase cocktail (Boehringer Mannheim). The PCR product(s) were ligated to a T/A vector (pCR2.1, Invitrogen) and completely sequenced on both strands (Oswel DNA Services, Southampton, U.K.).

Cell culture

Bovine adrenal chromaffin cells were prepared from adrenal glands freshly obtained from an abattoir. The standard approach [14] involved collagenase digestion and mechanical dispersion. The dispersed cells were maintained in culture for up to 5 days in 30-mm diameter plastic culture chambers and on glass coverslips in Dulbecco's modified Eagle's medium supplemented with 1% (v/v) 1× insulin/transferrin/selenium supplement (ITS-X), 0.1% penicillin/streptomycin and 1% (w/v) sodium pyruvate (all from Gibco BRL Life Technologies) at 37 °C in 95% air, 5% CO_2. BHK-21 cells were cultured in Glasgow Modified Eagle's medium supplemented with 10% (v/v) tryptose phosphate broth, 10% (v/v) foetal bovine serum, 2 mM glutamine and 100 units/ml of penicillin/streptomycin (all from Gibco BRL Life Technologies) at 37 °C in 95% air, 5% CO_2, and used between passage numbers 5 and 15.

Generation of recombinant SFV particles

PCR was used to generate an *Eco*RI-*Bam*HI flanked DOC2β fragment for ligation to pEGFPN1 (Clontech). DOC2β-EGFP cDNA was sub-cloned into the *Sma*I site of pSFV1 expression vector (Life Technologies) as a T4 DNA polymerase blunt-ended *Eco*RI-*Not*I fragment from pEGFPN1. A GFPmut3 insert was amplified by PCR using forward (5′-CGGAGATCTATGAGT-AAAGGAGAAGAACTTTTCACT) and reverse (5′-GCCGG-ATCCCATATGTTTGTATAGTTCATCCATGCCATGTGT-AAT) deoxyoligonucleotides, and a GFPmut3 plasmid as a template. The PCR product was treated with Klenow enzyme and ligated to the *Eco*RV site of pBluescript II KS (Stratagene). The insert was subcloned as a *Bam*HI-*Bgl*II fragment into pSFV1. The orientation and integrity of the cDNA inserts were confirmed by DNA sequencing. Capped mRNA was generated from these constructs and pSFV2 helper vector (Gibco BRL Life Technologies) by linearizing both vectors with *Spe*I and transcribing *in vitro* using SP6 RNA polymerase according to the manufacturer's instructions. Five to ten micrograms of each *in vitro*-transcribed mRNA were electroporated into approx. 1×10^7 BHK-21 cells in Glasgow modified Eagle's medium supplemented with 2 mM glutamine at 2125 V/cm, 25 μF and pulsed twice using a Bio-Rad GenePulser apparatus. Cells were allowed to recover for 5 min, resuspended in 24 ml of complete medium and plated for culture for a further 48 h. Medium was recovered from these plates, and filtered through a 0.25 μm-pore-size filter before storage at −20 °C.

Infection of chromaffin cells with recombinant SFV particles

Approx. 1×10^6 freshly prepared chromaffin cells were plated in 90-mm diameter tissue-culture plates containing sterile glass coverslips. After 24 h of culture at 37 °C, the conditioned culture medium was removed and stored for later use. Virus stock was activated by the addition of chymotrypsin A4 (250 μg/ml; Sigma–Aldrich) and digestion for 10 min on ice. Proteolysis was halted by the addition of aprotinin (0.67 mg/ml; Sigma–Aldrich). A 1:10 dilution of the virus stock was made in conditioned chromaffin cell medium, and approx. 1 ml of this was overlaid on to the cells. The cells were incubated with the virus for 2 h, then the medium was removed and replaced again with conditioned chromaffin cell medium. The infected cells were cultured for specific times post-infection before harvesting for immunoblot analysis and confocal fluorescence microscopy.

Immunoblotting

Cells were removed from culture at appropriate time points after infection and washed three times with ice-cold PBS, pH 7.4 (Gibco BRL Life Technologies). Cells were homogenized in the plate by the addition of 500 μl of lysis buffer [10 mM Tris/HCl, 0.1% (w/v) SDS, 1μg/ml leupeptin, 1 μg/ml aprotinin, 0.2 mM 4-(2-aminoethyl)benzenesulphonyl fluoride, pH 7.4] and scraping into a fresh tube. The protein concentration was determined by assaying a 1 in10 dilution of the mixture using the Bradford method according to the manufacturer's instructions (Bio-Rad). Approx. 10 μg of protein per sample were electrophoresed in an SDS/10% polyacrylamide gel using the method of Laemmli [15]. Proteins were transferred to poly(vinylidene difluoride) (Bio-Rad) using a Trans-Blot SD (Bio-Rad) semi-dry electroblotter at 20 V for 30 min. Following transfer, excess binding sites on the membrane were blocked by incubating in blotting buffer (PBS, 5% (w/v) non-fat skimmed milk) for 1 h. Monoclonal anti-synaptotagmin, anti-rSEC8, anti-rabphilin-3A, anti-munc-18 (Transduction Laboratories), monoclonal anti-GFP (Clontech) or polyclonal anti-dopamine-β-hydroxylase (D-β-H) were diluted in blocking buffer and incubated with the membranes for 1 h. Membranes were washed extensively with PBS before incubation with horseradish peroxidase-conjugated anti-mouse IgG (Transduction Laboratories, for monoclonals) or horseradish-peroxidase conjugated anti-rabbit IgG (Amersham–Pharmacia Biotech, for polyclonal), diluted in blocking buffer as before. Decorated proteins were revealed by ECL® (Amersham–Pharmacia Biotech) according to the manufacturer's instructions.

Single-cell fluorescence and electrophysiology

Cells expressing GFP or EGFP fusion proteins were identified by their green fluorescence. The cells attached to glass coverslips were mounted in a perfusion chamber located on the stage of an inverted microscope (Zeiss Axiovert 100), and illuminated via the epi-illumination pathway by a monochromated light source (TILL Photonics, Planegg, Germany). Excitation was at 488 nm for EGFP and 395 nm for the mut3.1GFP. The filter combination was a dichroic mirror Q500L and the emission filter HQ500LP (Chroma Technology, Brattleboro, VT, U.S.A.).

Fluorescent cells were subjected to perforated-patch recording with an EPC-9 patch clamp system (HEKA Elektronik, Germany); a system which performs automated on-line measurements of ionic currents, membrane capacitance, membrane conductance and series conductance. Membrane capacitance is proportional to cell-membrane-surface area and serves as a measure of secretion, since the surface area increases upon exocytotic addition of vesicular membrane and decreases upon endocytosis [14]. The patch pipette solution contained 135 mM caesium glutamate, 9 mM NaCl, 1 mM triethylammonium chloride, 10 mM Hepes (pH 7.3, titrated with CsOH). For perforation of the membrane patch, standard protocols were followed [16] and the amphotericin (Sigma–Aldrich) concentration was 200 μg/ml. After seal formation, the series resistance was measured continuously and recordings were started when the series resistance dropped below 20 MΩ. The external bath solution contained 145 mM NaCl, 2.8 mM KCl, 5 mM $CaCl_2$, 1 mM $MgCl_2$, 10 mM Hepes (pH 7.3, titrated with NaOH) and 10 mM glucose. The external bath solution was constantly perfused at 0.5–1 ml/min. Recordings were made at room

temperature (approx. 20 °C). The values of membrane current and capacitance responses are reported as the mean ± S.E.M. in the text.

Confocal microscopy

Cells cultured on glass coverslips were washed twice with PBS supplemented with Ca^{2+} and Mg^{2+} before fixation for 5 min with ice-cold 4% (w/v) buffered paraformaldehyde, or living cells were imaged using a Leica TCS NT Confocal System (Leica Lasertechnik GmbH, Heidelberg, Germany) with a PL APO 63 × /1.32–0.6 oil immersion lens, also made by Leica. If required, cells were counter-stained using the acidotropic dye LysoTracker Red according to the manufacturer's instructions (Molecular Probes).

RESULTS

Highly efficient SFV infection of adrenal chromaffin cells

Previously published procedures for SFV transduction yielded low efficiencies of infection/expression (10–20%) in chromaffin cells. Adding the step of inactivating the chymotrypsin A (used to activate the viral particles) increased the number of cells that survived viral incubation, but the numbers of cells expressing GFP still remained low (< 30%). The further modification using conditioned chromaffin cell medium rather than PBS or BHK-21 medium for both the virus incubation and recovery stages dramatically improved the final percentage of cells observed to have a fluorescent phenotype 48–72 h post-infection. Approx. 90–100% of all cells were observed to fluoresce, estimated by directly counting the fluorescent cells compared with the total number of cells counted under visible light (Figure 1B). Immunoblot studies of viral-infected chromaffin cells demonstrated that DOC2β-EGFP could be detected using a monoclonal anti-GFP antibody between 16–19 h post-infection. These observations were supported by the development of a fluorescent-chromaffin-cell phenotype in infected cells between these time-points. The levels of detectable decorated DOC2β-EGFP increased steadily up to 72 h post-infection, with no apparent change in cellular morphology (Figures 1A and 1B).

In this study, we used a 1:10 dilution of one-sixtieth of the virus stock (approx. 8×10^6 infectious units) to infect approx. 1×10^5 cells. This provided a multiplicity of infection of approx. 8, assuming that all the viral particles were competent to infect chromaffin cells. In practice, the dilution of the viral stock could have been greater.

Chromaffin cell biology after SFV infection

Immunoblot studies of the endogenous chromaffin cell proteins synaptotagmin, D-β-H, rSEC8, rabphilin-3A and munc-18 demonstrated that the steady-state levels of these proteins did not decrease throughout this time course (Figure 1A). The stabilities of synaptic proteins are variable [11], although no data is available relating to these proteins in bovine adrenal chromaffin

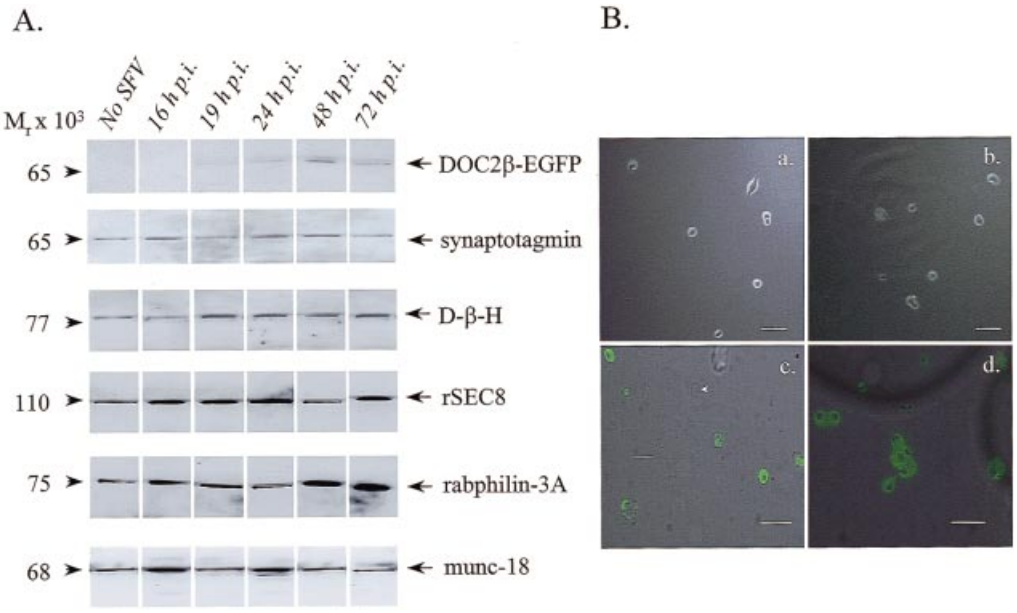

Figure 1 (A) Immunoblot analysis of DOC2β-EGFP fusion protein expression in SFV-infected bovine adrenal chromaffin cells, and (B) low-power confocal images superimposed on bright-field images of SFV-infected bovine adrenal chromaffin cells

(**A**) DOC2β-EGFP fusion protein was first detected between 16 h and 19 h post-infection (p.i.), with the level of detectable protein increasing with time up to 72 h post-infection. The levels of synaptotagmin, dopamine-β-hydroxylase (D-β-H), rSEC8, rabphilin-3A and munc-18 did not decrease over the time of the study. The time course of expression is in contrast with the time course of SFV-transduced expression, reported previously, where host-cell protein synthesis was sequestered as early as 9 h post-infection (see text for references). (**B**) Cells grown on sterile glass coverslips were removed from the same cultures used for immunoblot analysis and examined under 488 nm illumination as described in Materials and methods section. DOC2β-EGFP could be seen from 19 h post-infection, and increased in intensity up to 72 h post-infection. No EGFP fluorescence could be detected in non-infected cells. (a) At 16 h post-infection, no fluorescence is visible. (b) At 19 h post-infection, some EGFP fluorescence is just visible. This correlates with immunoblot analyses, which first detected decorated DOC2β-EGFP between 16 h and 19 h. (c) and (d) The intensity of the EGFP-fluorescence appeared to increase between 24 h and 72 h post-infection. The relative percentage of cells with the green fluorescent phenotype can be judged by comparing fluorescent cells with non-infected cells, revealed by the superimposition of the bright-field image. At 24 h post-infection, a single cell (arrow) that is not expressing DOC2β-EGFP can be seen in this field. In these experiments, we judged the efficiency of infection and expression to be 90–100% by 48–72 h post-infection. These images are representative of several independent experiments, where the observed transduction efficiencies were comparable ($n > 25$ experiments). Scale bars: 10 μm.

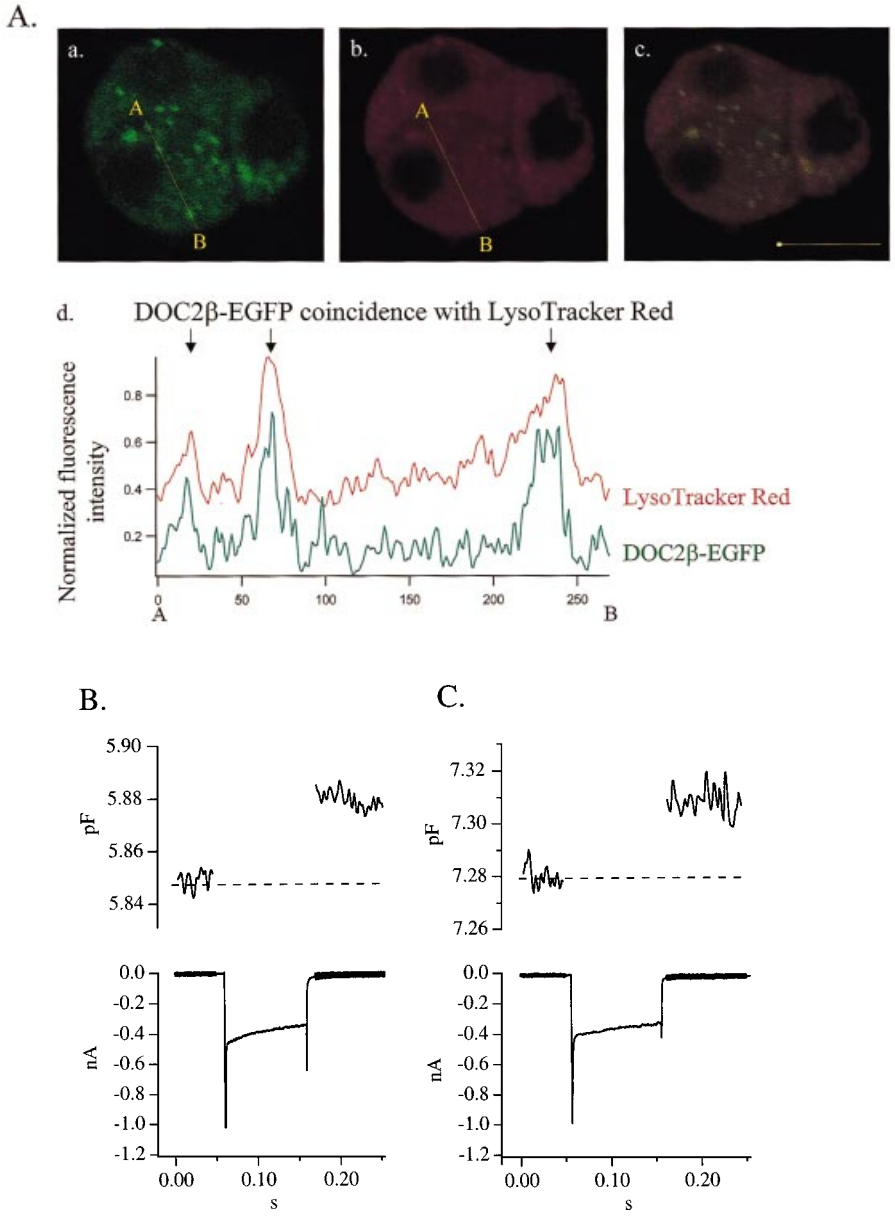

Figure 2 Confocal microscopy and electrophysiology of DOC2β-EGFP-expressing chromaffin cells

(**A**) High-power confocal images of a group of three DOC2β-EGFP-expressing chromaffin cells 48 h post-infection. A single 1 μm-thick confocal optical section, illuminated at 488 nm and 577 nm, was used to produce these images. (a) The EGFP fluorescence is seen distributed throughout the chromaffin cell in a punctate distribution with nuclear sparing, reminiscent of a vesicular localization. This coincides with the distribution of LysoTracker Red in the same cell (b), which also shows a punctate distribution with nuclear sparing. (c) Superimposition of the two images revealed the fluorescent spots to be overlapping, as indicated by yellow. A yellow line AB shown on (a) and (b), was measured for fluorescence intensity. (d) Shows the normalized intensity under the line proceeding in arbitrary distance units from point A to point B. Similar vertical lines were drawn through 55 vesicular areas in 5 cells. DOC2β-EGFP peaks were coincident with LysoTracker Red peaks in 98% of cells. Conversely LysoTracker Red peaks were coincident with DOC2β-EGFP peaks in 76% of cells. The arrows mark peaks that are representative of vesicular fluorescence. Scale bar: 10 μm with bold inset (yellow square on left hand end of scale bar in panel c; 0.39 μm) representing the approximate size of a large dense core vesicle. Membrane currents and capacitance responses in response to depolarizations of 100-ms duration to $+10$ mV, from a holding potential of -70 mV for (**B**) non-infected cells and (**C**) infected cells. The solutions have been designed to isolate the inward currents – an initial rapidly inactivating sodium current, followed by a maintained calcium current. The membrane capacitance increases in response to the injections of calcium due to the depolarizations. There is a gap during the depolarizations, during which the capacitance measurements are not calculated.

cells. Interestingly, the half-life of synaptotagmin I in neurons has recently been shown to be within 8–22 h during 1–3 days of culture [11]. The stable synaptotagmin level in our experiments suggest that the ability of SFV-infected cells to synthesize new proteins remains unaffected over the course of this experiment. Biophysical studies of cells expressing GFP and DOC2-EGFP constructs 48 h after SFV infection revealed that the cell membranes were intact, with no significant increase in the leak current [2.8 ± 0.4 pA ($n = 18$) compared with 3.2 ± 0.5 pA ($n = 18$) in non-infected cells], and the cells displayed significant calcium currents and capacitance increases, indicative of exocytosis (Figures 2B and 2C). When subjected to 100-ms depolarizations to $+10$ mV, the chromaffin cells displayed a mean calcium current amplitude of 297 ± 23 pA ($n = 18$), which is approx.

25% less than the current measured in non-infected chromaffin cells at 407 ± 37 pA ($n = 18$). In response to the injection of calcium current, the transduced cells responded with an increase in membrane capacitance of 14 ± 2 fF ($n = 18$), compared with 31 ± 4 ($n = 18$) in non-infected cells. Thus, 48 h after viral infection, all the infected cells are expressing heterologous protein, and they continue to carry out normal physiological processes of calcium current conduction and exocytosis.

DOC2β is localized to an acidic, vesicular compartment in chromaffin cells

Confocal microscopy revealed that DOC2β-EGFP fluorescence was distributed throughout the cell in a characteristic punctate pattern with nuclear sparing, reminiscent of a vesicular localization. Cells that were loaded with the acidic compartment probe LysoTracker Red showed a similar fluorescence distribution. The vesicular distribution of DOC2β-EGFP shows 98% coincidence with LysoTracker Red in double-labelled cells, suggesting that the DOC2β-EGFP fusion protein was directed to an acidic compartment in these cells (Figure 2A). In contrast, transduced GFPmut3 displayed a homogeneous cytoplasmic distribution (results not shown).

DISCUSSION

We have developed a modification of the SFV transduction approach that efficiently introduces heterologous cDNA into bovine adrenal chromaffin cells. The steady-state levels of several endogenous chromaffin cell proteins remain unaffected up to 72 h post-infection. This result is surprising because SFV has been shown to sequester host-cell protein-synthesis machinery after infection, effectively halting endogenous protein synthesis in favour of viral protein production; however, the observation suggests that there may be a time window over which meaningful biophysical studies of exocytosis can be carried out. Indeed, our preliminary results with patch-clamp measurements have demonstrated that the cells still have significant calcium currents and secretion, though somewhat depressed compared with non-infected cells. These data are in agreement with a recent paper describing the use of SFV vectors to express synaptic proteins in cultured neurons without cytotoxic effects [11].

The time course of heterologous protein expression in chromaffin cells appeared to be slower than in cultured cell-lines such as BHK-21 cells, COS-7 cells and Chinese hamster ovary cells (e.g. [17]), where it has been reported that expressed protein can be detected as early as 9 h post-infection, at which point host endogenous protein synthesis is already depressed. Furthermore, the levels of heterologous protein expression, judged by immunoblotting and GFP fluorescence intensity, are relatively low compared with those in other cell types reported previously [8–10].

The observation here that DOC2β-EGFP is directed to an intracellular acidic compartment, in support of earlier work on DOC2 intracellular localization (e.g. [12]), provides evidence that proteins expressed from SFV-based vector systems in chromaffin cells can be correctly processed and targeted. Furthermore, this is the first direct visualization of DOC2-EGFP *in vivo*. Additional experiments using SFV-GFPmut3 alone confirmed the high-efficiency of transduction using these conditions, and the ability of SFV-expressed proteins to be directed to the appropriate intracellular localization.

SFV transduction systems have, until now, been used for large-scale, high-efficiency protein production in mammalian cells. The slow time course, high-efficiency of infection and expression, and reduced expression levels seen in bovine chromaffin cells should make the SFV transduction system a valuable tool in the study of chromaffin cell biology.

We thank Dr. David Apps for his gift of the rabbit polyclonal anti-bovine dopamine-β-hydroxylase antibody. We also thank Ms. Linda Sharp for her expert assistance with the confocal microscopy. This work was funded by a Wellcome Trust Project grant to R.H.C and M.J.S.

REFERENCES

1 Ma, W. J., Holz, R. W. and Uhler, M. D. (1992) J. Biol. Chem. **267**, 22728–22732
2 Liu, F., Housley, P. R. and Wilson, S. P. (1996) J. Neurochem. **67**, 1457–1462
3 Wick, P. F., Senter, R. A., Parsels, L. A., Uhler, M. D. and Holz, R. W. (1993) J. Biol. Chem. **268**, 10983–10989
4 Wilson, S. P., Liu, F., Wilson, R. E. and Housley, P. R. (1995) Anal. Biochem. **226**, 212–220
5 Moss, B., Elroystein, O., Mizukami, T., Alexander, W. A. and Fuerst, T. R. (1990) Nature (London) **348**, 91–92
6 Moss, B. and Flexner, C. (1989) Annals N.Y. Acad. Sci. **569**, 86–103
7 Berglund, P., Sjoberg, M., Garoff, H., Atkins, G. J., Sheahan, B. J. and Liljestrom, P. (1993) Bio/Technology **11**, 916–920
8 Liljestrom, P. and Garoff, H. (1991) Bio/Technology **9**, 1356–1361
9 Olkkonen, V. M., Liljestron, P., Garoff, H., Simons, K. and Dotti, C. G. (1993) J. Neuroscience Res. **35**, 445–451
10 Olkkonen, V. M., Dupree, P., Killisch, I., Zerial, M. and Simons, K. (1993) J. Cell Sci. **106**, 1249–1261
11 Daly, C. and Ziff, E. B. (1997) J. Neurosci. **17**, 2365–2755
12 Verhage, M., deVries, K. J., Roshol, H., Burbach, J. P. H., Gispen, W. H. and Sudhof, T. C. (1997) Neuron **18**, 453–461
13 Orita, S., Naito, A., Sakaguchi, G., Maeda, M., Igarashi, H., Sasaki, T. and Takai, Y. (1997) J. Biol. Chem. **272**, 16081–16084
14 Lindau, M. and Neher, E. (1988) Pfluegers Arch. **411**, 137–146
15 Laemmli, U. K. (1970) Nature (London) **277**, 680–668
16 Zhou, Z. and Neher, E. (1993) J. Physiol. (London) **469**, 245–273
17 Cicciarone, V., Anderson, D. and Jesse, J. (1997) Focus **16**, 94–98

Received 7 May 1999/30 June 1999; accepted 16 July 1999

Exocytosis Studies in a Chromaffin Cell–Free System

Imaging of Single-Vesicle Exocytosis in a Chromaffin Cell–Free System Using Total Internal Reflection Fluorescence Microscopy

ULRICH K. WIEGAND,[a] ANDREW DON-WAUCHOPE,[a] IOULIA MATSKEVICH,[a] RORY R. DUNCAN,[a] JENNIFER GREAVES,[a] MICHAEL J. SHIPSTON,[a] DAVID K. APPS,[a] AND ROBERT H. CHOW[b]

[a]*Membrane Biology Group, University of Edinburgh, Edinburgh EH8 9XD, United Kingdom*

[b]*Department of Physiology and Biophysics, Keck USC School of Medicine, Los Angeles, California 90089-9142, USA*

ABSTRACT: We have developed a system for the real-time study of regulated exocytosis in living, cultured bovine adrenal chromaffin cells (BCCs). Exocytosis was monitored by the use of total internal reflection fluorescence (TIRF) microscopy to image single large dense-core secretory vesicles (LDCVs). Fluorescent labeling of LDCVs was achieved either with the membrane-permeant weak base, acridine orange (AO), or by transduction of BCCs so as to express a fluorescent chimeric "cargo" protein that is targeted to LDCVs. In either case, exocytosis is visible by the disappearance of a vesicle accompanied by a bright flash as the fluorescent contents leave the acidic LDCV lumen, move towards the source of the evanescent wave, and disperse into the extracellular medium. Furthermore, for the first time, we have developed a broken-cell system for real-time imaging in BCCs, in which individual plated cells are mechanically "unroofed" with a jet of intracellular medium, leaving a membrane patch with docked vesicles on the coverslip. In this cell-free system, a subpopulation of docked granules undergoes exocytosis in response to calcium. This approach allows us direct experimental access to membrane-docked LDCVs in order to investigate the dependence of exocytosis on defined protein components and intracellular conditions at the single-vesicle level. In addition, this system can be used for a reconstitution analysis of the exocytosis machinery. Finally, we demonstrate the use of 2D+1 image analysis for visualizing single-vesicle exocytosis. We use this approach for a rapid analysis of larger numbers of imaged vesicles.

KEYWORDS: single-vesicle exocytosis; chromaffin cell–free system; total internal reflection fluorescence microscopy; EGFP; acridine orange; 2D+1 image analysis

Address for correspondence: U.K. Wiegand, Membrane Biology Group, Hugh Robson Building, George Square, University of Edinburgh, Edinburgh EH8 9XD, UK. Voice: +44-131-650-2864; fax: +44-131-650-6527.
u.wiegand@ed.ac.uk

Ann. N.Y. Acad. Sci. 971: 257–261 (2002).

INTRODUCTION

Secretion of peptide hormones or neurotransmitters from neuroendocrine cells occurs by regulated exocytosis. Large dense-core secretory vesicles (LDCVs) derived from the trans-Golgi and filled with secretory polypeptides undergo a cycle, which includes their maturation, translocation, membrane docking, priming, and the highly regulated fusion of a subpopulation of vesicles with the cell membrane. Although a growing amount of data implicates the involvement of a multitude of cytoplasmic and membrane proteins, the exact temporal and spatial pattern of molecular interactions during this process needs to be analyzed.

For better experimental access and manipulation and for reconstitution studies of the exocytic machinery, cell-free systems for investigating regulated exocytosis are very desirable. Although permeabilized cells have proved to yield a great amount of information, these systems have some limitations;[1] for example, cell-free systems using cell homogenates in solution[1] have been used successfully for biochemical studies, but are not suitable for imaging techniques. More recently, a cell-free system has been reported using membrane sheets from PC12 cells after sonication for cell disruption.[2,3]

Here, we report a cell-free system using the mechanical disruption of single cells in cultured bovine adrenal chromaffin cells (BCCs), the first in primary mammalian cells. This technique allows us to study LDCV behavior at the single-vesicle level with an improved experimental access to the machinery involved in vesicle release.

RESULTS

Total Internal Reflection Fluorescence (TIRF) Microscopy of Fluorescently Labeled Vesicles

In order to analyze fluorescently labeled vesicles, we use real-time imaging with TIRF microscopy.[4] In this technique, the evanescent wave produced by total internal reflection of a laser beam near the underside of cells growing on glass coverslips excites fluorescence-labeled LDCVs that are within 100–200 nm of the plasma membrane. Vesicles were labeled with acridine orange (AO), a cell-permeant, weak base, which accumulates within acidic intracellular compartments and becomes trapped in the vesicles upon protonation. Alternatively, enhanced green fluorescent protein (EGFP) fused to prepro-atrial natriuretic factor (ANF) was targeted to the lumen of BCCs using Semliki Forest virus as a vector.[5]

For TIRF time-lapse microscopy, we used a Zeiss Axioskop FS, equipped with a 63× water immersion lens (NA = 0.9; working distance: 2 mm), a 2× Optovar, and an intensified Pentamax CCD camera (Princeton Instruments). TIR was generated using a prism-based setup. A laser beam from a Coherent Innova 90-4 argon-ion laser was targeted at the top surface of a glass prism (n = 1.52) at an incident angle of 61°, which totally reflected the beam into the prism. Coverslips with cells attached were optically coupled to an underlying prism via a thin layer of immersion oil. The totally reflected laser beam produced an evanescent wave (wavelength: 488 nm) at the interface between glass and culture medium (n = 1.37). The intensity of this electromagnetic field decreased exponentially with distance and was half-

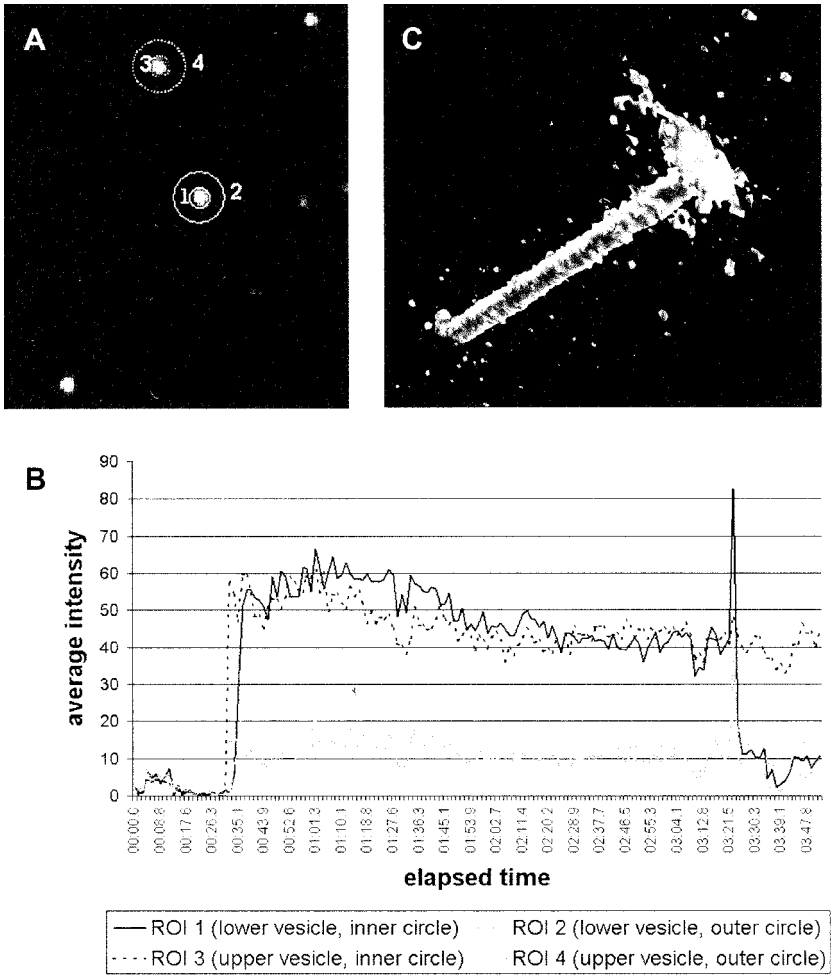

FIGURE 1. Quantitative analysis of two AO-labeled LDCVs imaged by time-lapse TIRF microscopy. A time-lapse image stack was analyzed using *MetaMorph 4.5*. **(A)** Regions of interest (ROI) were defined in order to allow intensity measurements of two areas surrounding each LDCV: an inner area of ~200 nm diameter, defining the actual vesicle, and an outer ROI (~800 nm diameter), which covers the area, briefly illuminated after vesicle release, as the fluorescent label dissipates. **(B)** Intensity curves of the ROI given in panel A of two LDCVs. Here, 100 μM free calcium was added 25 s after the start of the experiment. Whereas the upper vesicle in panel A remains stable over the length of the experiment, the lower vesicle fuses after 3 min with the membrane patch, visible as an intensity peak in both measured areas (ROI 1 and 2). **(C)** 2D + 1 image analysis. An ROI of the lower vesicle in panel A was defined, and a pseudo-3D image was generated with time as the third dimension (z-axis; for more details, see below). The LDCV is stable for 3 min before it fuses with a "flash," dissipating its fluorescent contents into the surrounding medium. This is visible as a mushroom-like cap.

maximal at approximately 80–100 nm from the interface. A UniBlitz D122 shutter at the output of the laser was used to avoid overexposure of the samples. A typical imaging frequency was 4.5 Hz.

After release of AO or ANF-EGFP from the vesicle upon stimulation, the consequent dequenching and the dissipation of the fluorophores towards the TIRF light source lead to an increase of fluorescence intensity, which is visible as a "flash" (FIG. 1).

Generation of Membrane Patches from Cultivated BCCs

BCCs were grown on collagen-coated coverslips glued to customized cell culture dishes. Firmly attached cells were labeled with AO and then "unroofed" using a glass micropipette connected to an injector, which we used to generate a "liquid jet" for disruption or microperfusion of the resulting membrane patch. Flat membrane patches were perfused in order to remove unwanted components of the cell. All manipulations were carried out at a constant ambient temperature of 30°C and monitored using transmitted light. In order to image the membrane relative to attached vesicles, all samples were counterstained with the membrane dye FM1-43 and imaged after each experiment.

LDCVs Attached to BCC Membrane Patches Fuse in Response to Elevating Ca^{2+} Concentrations

Experiments to study fusion of LDCVs with the attached membrane patches were carried out in intracellular medium with a free calcium concentration of 100 nM. All analyzed vesicles were located on areas of cell membrane and were immobile. When membrane patches were subjected to a higher concentration of free calcium (100 μM), fusion of a subpopulation of the attached vesicles could be observed after adding the calcium, visible as a number of "flashes." In order to rule out that vesicles burst in response to the laser irradiation, controls without adding calcium were included in the experiments. Vesicles of these untreated membrane patches showed no changes in the appearances of attached vesicles for imaging periods of 10 min and longer.

For quantitation, intensities of imaged vesicles and their surrounding areas were measured using *MetaMorph 4.5* (Universal Imaging Corp.) (FIG. 1A). FIGURE 1B shows fluorescence intensity curves of a stationary versus fusing vesicle.

2D+1 Image Analysis of Time-Lapse Image Recordings

Finally, we demonstrate 2D+1 image analysis as a quick and very graphic method of studying resulting image stacks with multiple vesicles.

Time-lapse imaging at high speed generates large 2D image stacks, which are sometimes difficult to analyze on a 2D screen, in particular when a large number of moving, appearing, or disappearing objects have to be tracked. We have developed a graphic method to quickly process and study such files using *Bitplane* software on an *SGI Octane 2* workstation. The 2D time-lapse stacks were loaded into *Imaris 3.0* in order to produce 3D images with the elapsed time as the third dimension (z-axis). This 3D image was then surface-rendered using *Isosurface 2.0*. Single vesicles appear in these 3D images as tubular objects, which are easy to track and study. FIG-

URE 1C shows one extracted AO-labeled LDCV from a membrane patch (see above). The vesicle is stable for about 3 min before it fuses with the plasma membrane, releasing its fluorescent contents into the surrounding medium. The dispersing AO is visible as a mushroom-shaped cap.

ACKNOWLEDGMENTS

This work was supported by Wellcome Trust Grant No. 060034 (Sir Henry Wellcome Commemorative Award).

REFERENCES

1. AVERY, J. *et al.* 1999. Reconstitution of regulated exocytosis in cell-free systems: a critical appraisal. Annu. Rev. Physiol. **61:** 777–807.
2. AVERY, J. *et al.* 2000. A cell-free system for regulated exocytosis in PC 12 cells. J. Cell Biol. **148:** 317–324.
3. LANG, T. *et al.* 2001. SNAREs are concentrated in cholesterol-dependent clusters that define docking and fusion sites for exocytosis. EMBO J. **20:** 2202–2213.
4. AXELROD, D. *et al.* 1989. Total internal reflection fluorescence microscopy. Methods Cell Biol. **30:** 245–270.
5. DUNCAN, R.R. *et al.* 1999. High-efficiency Semliki Forest virus–mediated transduction in bovine adrenal chromaffin cells. Biochem. J. **342:** 497–501.